

WATER INGRESSION INTO POLY(IMIDE-SILOXANE)S

by

Joyce Marie Kaltenecker-Commerçon


Dissertation submitted to the Faculty of the
Virginia Polytechnic Institute and State University
in partial fulfillment of the requirements for the degree of

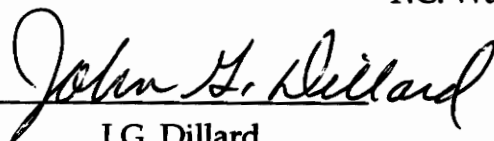
DOCTOR OF PHILOSOPHY


in

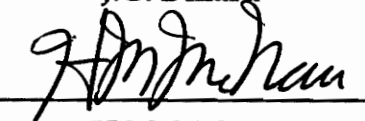
Chemistry


APPROVED:


T.C. Ward, Chairman


J.G. Dillard


J.E. McGrath


H.M. McNair


J.P. Wightman

December, 1992
Blacksburg, Virginia

C.2

LD
5655
V856
1992

K358

C.2

WATER INGRESSION INTO POLY(IMIDE-SILOXANE)S

by

Joyce Marie Kaltenecker-Commerçon

Committee Chairman: T.C. Ward

Chemistry

(Abstract)

The interaction of water vapor with the surface and bulk of poly(imide-siloxane) copolymers has been characterized in an attempt to determine the important factors in the copolymer's resistance to water ingress. The multi-block copolymers were synthesized from benzophenone tetracarboxylic dianhydride, bisaniline P and pre-formed amine-terminated poly(dimethylsiloxane) oligomers, with phthalic anhydride as an end-capping agent. Similar copolymers had been previously shown to have reduced water sorption, increased surface hydrophobicity, and increased adhesive durability in hot/wet environments.

Inverse gas chromatography was used to conduct surface energetics studies on copolymers of different siloxane concentration and a polyimide homopolymer. Free energies of specific interaction of water vapor, ΔG_{sp}° , with the polymer surfaces were found to decrease with the incorporation of siloxane into the polyimide. The dispersive components of the solid surface free energy of the siloxane-containing copolymers were equal within error to that of pure poly(dimethylsiloxane), indicating a PDMS-rich, hydrophobic surface. The ΔG_{sp}° of the copolymers were not significantly different, suggesting that the

copolymer surfaces were very similar. This indicated a minimum weight percent of siloxane incorporation required to maximize the copolymer's surface water resistance. The minimum amount for the studied system was at most ten percent.

Diffusion coefficients of water vapor in the polyimide and copolymers were determined from gravimetric sorption experiments. Higher levels of siloxane incorporation caused a definite increase in the diffusion coefficient, indicating a decreased resistance to water ingress. The increase in diffusion was found to be influenced by siloxane block length and was interpreted in terms of morphological and free volume theories. The diffusion coefficient of a 10 weight percent PDMS copolymer, however, was found to be the same within error as the polyimide diffusion coefficient.

The incorporation of siloxane into polyimides has been shown to increase water resistance due to the hydrophobicity of the siloxane-rich surface. However, high siloxane contents also increased the rate of water ingress in the bulk of the polymer. Increased water resistance of the surface may be achieved at lower siloxane concentrations without increasing diffusive (or decreasing mechanical) properties to undesirable levels.

ACKNOWLEDGEMENTS

I would like to thank Dr. T.C. Ward not only for being my committee chairman but also for being the dedicated teacher that first introduced me to the wonderful and strange world of physical chemistry and thermodynamics as an undergraduate. As a graduate student in his research group, I have greatly appreciated his words of encouragement as well as being allowed a large amount of freedom in the direction of my own research.

I would also like to thank the other members that served on my committee: Dr. J.G. Dillard, Dr. J.E. McGrath, Dr. H.M. McNair, and Dr. J.P. Wightman. I also thank Dr. D.A. Dillard for serving on my committee at the time of my proposal defense.

The Adhesive and Sealant Council, Inc. provided me with ASC Fellowships throughout most of my graduate years for which I am very grateful. Dr. Wightman and the Center for Adhesive and Sealant Science were also very helpful during my graduate time at VPI & SU. I thank Dr. Wightman and the invaluable CASS secretaries: Virginia Keller, Katie Hatfield and Kim Linkous.

I thank the NSF Science and Technology Center for High Performance Polymeric Adhesives and Composites, which provided some funding for required equipment. I thank all the secretaries associated with the center and its principle professors: In particular, I thank Joyce Moser, Esther Brann, Millie Ryan and Bonnie Johnson.

I thank Dr. J.E. McGrath and several members of his research group for the polymers used in this research. In particular I thank Dr. Attila Gungor and Tim Flynn for synthesizing the polymers. I would also like to thank Laura Kiefer, for

providing the functionalized poly(dimethylsiloxane) oligomers for a copolymer, and also Greg Lyle and Martin Rogers.

I thank the members of Dr. Wightman's group for allowing me to work in their laboratories. I thank Joannie Chin for teaching me how to use the goniometer. I am very grateful to Francis Webster for the many times he has helped me; I thank him for the odd research discussion and for setting up the sorption apparatus data collection system. I also thank Janet Webster for endeavoring to obtain good TEM pictures of my uncooperative polymer films.

I thank Dr. McNair and his group for allowing me to borrow the Hewlett-Packard headspace sampler for use in the IGC experiments. I thank Vince, Bob, Laura, Dorothea, Greg and Maha for their occasional help.

I thank Mr. Frank Cromer of the Surface Analysis Lab for teaching me how to use the SEM. I thank Mr. Dave Miller, Mr. Fred Blair and especially Mr. Bob Ross of the machine shop for making various items, including a very nice humidity cabinet, that I needed for one phase of my research. I thank Mr. Jim Coulter, Mr. Larry Jackson and Mr. Jim Hall of the electronics shop and Mr. Van Damme and Mr. Mollick from the glass shop.

I thank all my past and present colleagues in my research group. In particular, I am grateful to Mia Siochi for her advice and guidance during my early years in the group. I thank Randy Minton for teaching me the "nuts and ferrules" of gas chromatography so that I could begin my IGC research in earnest. I thank Paul Vail and Taigyoo Park for teaching me how to use the Dupont and Perkin-Elmer Thermal Analysis Systems, respectively. I must also thank Taigyoo Park, Saikat Joardar, Button Lents and George Dallas for a number of interesting discussions, which were mostly related to research. I thank Steve Wilkinson and

Yan Yang (and Gil Garnier) for the IGC-related discussions. I am grateful to Saikat for the dynamic mechanical analyses of the polymer films. I thank Martin Konas for characterizing all the polymers by GPC at short notice.

Finally I would like to thank my family. I thank my parents and my sister for being supportive of my endeavors. I am also deeply grateful to my husband, Pascal, for his great moral support during my past few years as a graduate student and also during the writing of the dissertation. The road would have been much rougher without him. In particular, I thank Pascal for writing the algorithm that generated the "sign" array used in my error calculation program, for performing the XPS experiments and for proof-reading the dissertation draft.

TABLE OF CONTENTS

LIST OF FIGURES	x
LIST OF TABLES	xii
1. INTRODUCTION	1
2. BACKGROUND	8
2.1 IGC Theory	8
2.1.1 Introduction.....	8
2.1.2 Basic Theory.....	10
2.1.3 Surface Energetics Study.....	14
2.2 IGC Literature Review	16
2.2.1 Introduction.....	16
2.2.1 IGC Technique.....	17
2.2.3 IGC Surface Studies of Polymers and Other Solids.....	18
2.3 Diffusion Theory	21
2.3.1 Introduction.....	21
2.3.2 Fickian Diffusion.....	21
2.3.3 Experimental Approach.....	23
2.3.4 Free Volume Diffusion Theories.....	26
2.4 Diffusion Literature Review	33
2.3.1 Introduction.....	33
2.3.2 Polyimides.....	34
2.3.3 Blends.....	37
2.3.4 Copolymers.....	39

3. EXPERIMENTAL.....	42
3.1 Polymers.....	42
3.2 Sample Preparation.....	43
3.2.1 Capillary Column Preparation.....	43
3.2.1.1 Coating Apparatus.....	43
3.2.1.2 Coating Materials.....	48
3.2.1.3 Coating Procedure.....	48
3.2.2 Sorption Film Preparation.....	52
3.2.2.1 Casting Materials.....	52
3.2.2.2 Casting Procedure.....	53
3.3 Instrumental.....	57
3.3.1 General Polymer Characterization.....	57
3.3.1.1 Surface Characterization.....	57
3.3.1.2 Gel Permeation Chromatography.....	58
3.3.1.3 Bulk Characterization.....	58
3.3.2 Inverse Gas Chromatography.....	59
3.3.3 Gravimetric Sorption.....	59
4. GENERAL POLYMER CHARACTERIZATION:	
Results and Discussion.....	65
4.1 Surface Characterization.....	65
4.1.1 x-ray Photoelectron Spectroscopy.....	65
4.1.2 Contact Angle Measurements and Calculations.....	65
4.2 Gel Permeation Chromatography.....	69
4.3 Bulk Characterization.....	71
4.3.1 Thermal Gravimetric Analysis.....	71
4.3.2 Dynamic Mechanical Thermal Analysis.....	74
4.3.3 Differential Scanning Calorimetry.....	78

5. INVERSE GAS CHROMATOGRAPHY SURFACE ENERGETICS.....	81
5.1 Comments.....	81
5.2 IGC Results and Discussion.....	81
5.2.1 Capillary Columns.....	81
5.2.2 Surface Energetics Study.....	84
5.3 IGC Surface Summary.....	94
6. GRAVIMETRIC SORPTION BULK DIFFUSION.....	96
6.1 Comments.....	96
6.2 Diffusion Results and Discussion.....	96
6.2.1 Sorption Films.....	96
6.2.2 Bulk Sorption Study.....	97
6.2.2.1 Introduction.....	97
6.2.2.2 Data Collection and Correction.....	98
6.2.2.3 Corrected Results and Discussion.....	101
6.2.2.4 Free Volume Interpretations.....	113
6.3 Sorption Bulk Diffusion Summary.....	116
7. CONCLUSION.....	118
8. SUGGESTED FUTURE WORK.....	120
9. REFERENCES.....	122
APPENDICES.....	131
Appendix A: Capillary Column Non-uniformity Discussion.....	131
Appendix B: Thermodynamic and Experimental Diffusion Coefficient Relation.....	133
Appendix C: Error Propagation.....	135
VITAE.....	143

LIST OF FIGURES

Figure 1. Water sorption of immersed BTDA-DDS-based polyimide and poly(imide-siloxane) copolymers. ⁷	5
Figure 2. Schematic of gas chromatograph and sample column.....	11
Figure 3. Generalized retention diagram for semi-crystalline polymer. ¹⁸	12
Figure 4. Structures 1 and 2 represent the blocks of the multi-block poly(imide-siloxane) copolymers.....	44
Figure 5. Schematic of the Capillary Column Coating Apparatus.....	45
Figure 6. Detailed schematic of heavy-walled \approx 10 milliliter pressurizable glass vial and modified vial cap.....	47
Figure 7. Schematic cut view from the side of the epoxy end-cap with water as the intervening liquid.....	51
Figure 8. Schematic of arrangement of glass petri-dish and ferrotype plate, cut to size and used in casting of siloxane-containing copolymer films.....	54
Figure 9. Schematic of the apparatus used in sorption experiments.....	61
Figure 10. GPC elution traces for polyimide and the siloxane-containing copolymers.....	70
Figure 11. TGA weight percent loss in air of polyimide and poly(imide-siloxane) copolymers.....	72
Figure 12. 30 wt% (3.6 K) PDMS TGA in air, run twice with intermediate ambient humidity exposure.....	73
Figure 13. Log $\tan \delta$ and log storage modulus vs. temperature for 10 wt% (3.6 K) PDMS copolymer.....	75
Figure 14. Log $\tan \delta$ and log storage modulus vs. temperature for 30 wt% (3.6 K) PDMS copolymer.....	76

Figure 15. Log tan δ and log storage modulus vs. temperature for 30 wt% (1.5 K) PDMS copolymer.....	77
Figure 16. SEM pictures of the polyimide control capillary column.....	82
Figure 17. SEM pictures of the copolymer capillary columns.....	83
Figure 18. Extrapolation of corrected retention times to infinite dilution.....	86
Figure 19. Polynomial extrapolation of n-alkane molecular probe surface areas from literature data.....	88
Figure 20. IGC Surface Energetics Plot for polyimide control at 50°C.....	90
Figure 21. IGC Surface Energetics Plot for 30 wt% (3.6 K) PDMS copolymer at 40°C.....	91
Figure 22. Plot of raw data of mass uptake of water vapor in micrograms and relative humidity for polyimide control sorption experiment.....	100
Figure 23. Curve fitting of blank sorption run in order to obtain a smooth curve for subtraction.....	102
Figure 24. Final smoothed curve of blank sorption run in comparison with the raw blank uptake data.....	103
Figure 25. Example of subtraction of the blank run sorption curve from the raw uptake data of the first sorption cycle of the aged polyimide control film.....	104
Figure 26. Reduced sorption plot for quenched polyimide film.....	105
Figure 27. Compilation of reduced sorption plots for first sorption cycle of quenched films.....	106
Figure 28. Compilation of reduced sorption plots for first sorption cycle of T_g-5°C aged films.....	107
Figure 29. Reduced sorption plot for quenched polyimide film with regression line representing the initial 60% of uptake, excluding initial deviation.....	110

LIST OF TABLES

Table 1. Weight percent PDMS at copolymer surfaces of BTDA-DDS-based poly(imidesiloxane)s determined from x-ray photoelectron spectroscopy. ⁵	3
Table 2. Time to failure in hot/ wet environments for lap shear specimens of bulk and solution imidized BTDA-DDS-based polyimide control and ten weight percent siloxane containing copolymers. ⁶	6
Table 3. Weight percent PDMS at and near copolymer surfaces as determined from x-ray photoelectron spectroscopy.....	66
Table 4. Measured and calculated contact angles.....	66
Table 5. Listing of surface tensions and dispersive and polar components of the surface tensions for the liquids used to determine contact angles against sample polymer films. ^{128,130}	68
Table 6. Listing of the dispersive components of the solid surface free energy of the polyimide control as determined from the different pairs of liquids.....	68
Table 7. Upper glass transition temperatures (in °C) determined by DSC of polymer films cast from chloroform and methylene chloride.....	79
Table 8. Comparison of literature ²⁵ and polynomially-extrapolated molecular surface areas, a , (in Å ²) of n-alkane probes.....	89
Table 9. Free energies of specific surface interaction of water vapor with the polymer surfaces at various experimental temperatures.....	93
Table 10. Dispersive component of the solid surface free energy of polymer surfaces as determined from slope of IGC dispersive reference line at 50°C.....	93
Table 11. Average and standard deviation of thickness of films used in sorption experiments.....	99
Table 12. Diffusion coefficients determined from the first and second sorption cycles of the gravimetric sorption experiments.....	111

1. INTRODUCTION

The durability of many adhesive-adherend systems is decreased by the ingress of water. High humidity environments are considered aggressive environments for adhesive joints because the presence of water in the adhesive can influence overall bulk polymer properties and, most importantly, can cause interfacial failure due to the displacement of the adhesive from the adherend by the polar water molecules. The decrease in adhesive strength in hot/ wet environments also tends to be accelerated by the application of stress.¹ Increasing the water resistance and durability of an adhesive joint is therefore of great interest. During the past few years, it has been shown that the incorporation of poly(dimethylsiloxane) segments into polyimides increases the possible-adhesive polymer's resistance to water ingression.^{2,3} It is important to understand the mechanism of water ingression (or indeed the tendency of water resistance) in order to be able to predict and characterize the copolymer adhesive durability effectively.

Aromatic polyimides are heterocyclic polymers which generally have thermal and mechanical properties suitable for high-performance, high-temperature applications. Some polyimides have been found to exhibit good properties as structural adhesives and also as coatings, for example in circuit board applications.⁴ One of the limitations to the utilization of polyimides in many possible applications has been the poor solubility and processability of the polymers. Attempts to decrease polyimide intractability have included the

incorporation in the chemical structure of aromatic diamines that are meta-substituted (kinked) or have bulky side groups. These modifications increase the solubility and processability of the polyimides by making the overall structure more flexible. Incorporating a short, highly flexible structural segment, such as poly(dimethylsiloxane) by copolymerization has a similar effect on solubility. However, while incorporation of very short segments of siloxane increases processability it also undesirably decreases high temperature properties and lowers the glass transition temperature. The use of higher molecular weight blocks of siloxane in the copolymers results in microphase separation, which allows the upper glass transition temperature and overall bulk polymer properties of the copolymer to be similar to those of the homopolymer, for low weight percents of incorporated siloxane.⁵

In the course of a number of synthesis and characterization studies of structural, solubility, dielectric and durability studies of these poly(imide-siloxane) copolymers^{5,6,7} it was revealed that the copolymers had an increased resistance to water compared to the polyimide homopolymer. It is considered that both the bulk and the surface characteristics of the microphase separated copolymer may contribute to this water resistance. ESCA (or XPS) surface characterization studies revealed that the concentration of hydrophobic siloxane at the surface was greater than the proportional amount incorporated into the copolymer.² The weight percents of the siloxane segment at the surface of various diaminodiphenylsulfone-based polyimidesiloxane copolymers are listed in Table 1.² The high concentration of the hydrophobic poly(dimethylsiloxane) segment at the surface is suggestive of a barrier to the initial entry of water into the bulk. The resistance to water may also be related to morphological bulk

Table 1. Weight percent PDMS at copolymer surfaces of BTDA-DDS-based poly(imidesiloxane)s as determined from x-ray photoelectron spectroscopy.⁵

Wt% PDMS	PDMS M _n	Take-off angle	
		<u>15°</u>	<u>90°</u>
5	950	85	34
10	950	77	35
10	10,000	87	39
20	950	87	53
40	950	86	63

properties. Sorption studies involving the immersion of poly(imidesiloxane) copolymers into water have shown that water mass uptake is decreased by an increasing concentration of siloxane.⁷ Sorption to equilibrium for copolymers of several amounts of incorporated siloxane is shown in Figure 1. The equilibrium mass uptake was dependent not only on weight percent incorporated siloxane but also on the molecular weight of the siloxane segment for a given weight-percent siloxane incorporated into the copolymer.² This indicated that the water resistance was influenced by morphology. It has been suggested that the microphase separation could act in a manner to limit diffusive entry,⁵ although equilibrium results are more often related to overall solubility. Perhaps the most important revelation was that siloxane-containing polyimides were found to have increased durability in hot/wet environments compared to homopolymer polyimides.^{6,8} The time to failure for single lap shear specimens tested at 80°C and 100% relative humidity was determined for polyimide homopolymers and poly(imide-siloxane) copolymers containing 10 weight percent siloxane. The results, shown in Table 2, are for bulk thermally imidized and solution imidized polymers. The incorporation of siloxane increased the durability by a factor of three. The lap shear strength of the siloxane-containing copolymer was also not greatly reduced from that of the homopolymer.

The purpose of the present research was to examine the possible surface and morphological bulk factors involved in the increased water resistance of the copolymers. Once the relative importance of a factor's contribution to water resistance is ascertained, the siloxane-containing copolymers can be synthetically tailored to maximize the water resistant qualities. The influence of siloxane incorporation on water ingress was investigated by studying the bulk and

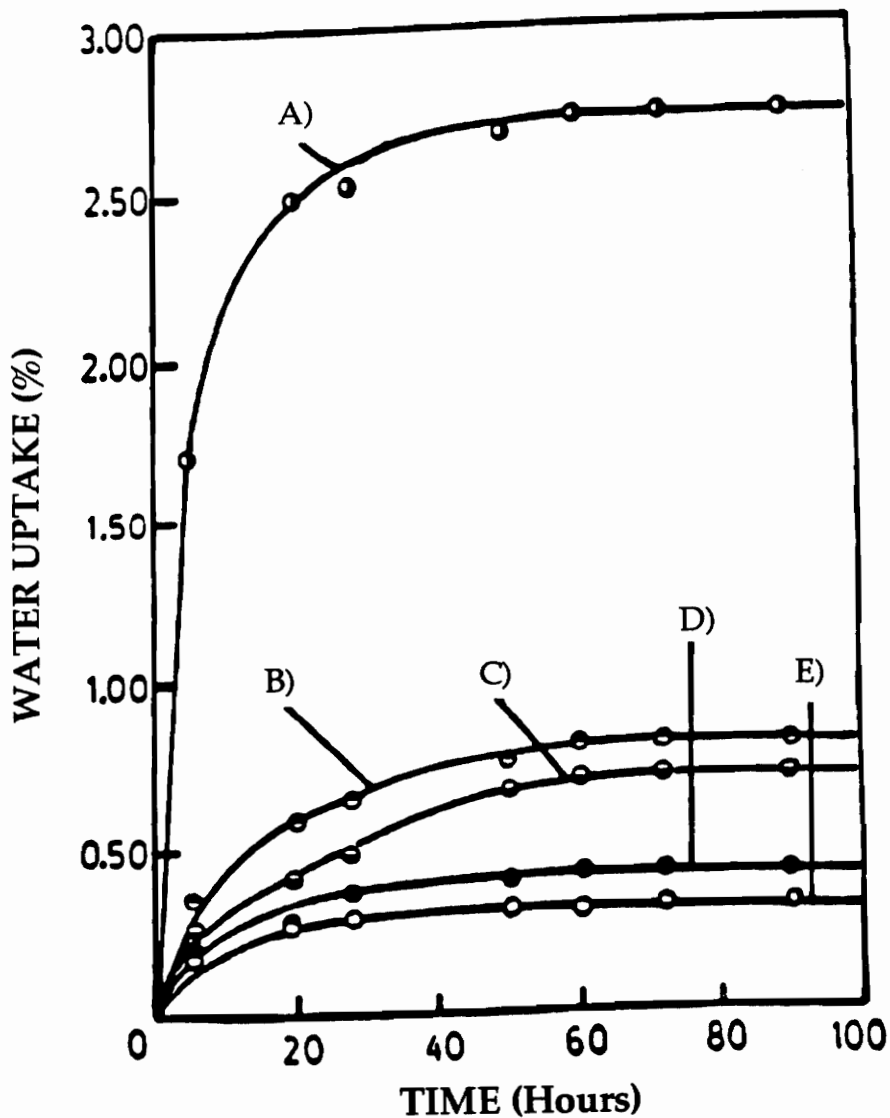


Figure 1. Water sorption of immersed BTDA-DDS-based polyimide and poly(imide-siloxane) copolymers.⁷ A) Polyimide control; B) 30 wt% PDMS 2500 g/mol; C) 30 wt% PDMS 910 g/mol; D) 50 wt% PDMS 2500 g/mol; E) 50 wt% PDMS 910 g/mol.

Table 2 Time to failure in hot/wet environments for lap shear specimens of bulk and solution imidized BTDA-DDS-based polyimide control homopolymer and ten weight percent siloxane containing copolymers.⁶

<u>Preparation (composition)</u>	<u>Time to Failure</u>
Bulk (control)	2.7 days
Solution (control)	2.4 days
Bulk (10 wt%, 950 M _n)	9.7 days
Solution (10 wt%, 800 M _n)	8.9 days

All bonds contained scrim cloth.

Test conditions: 8.3 MPa (1200 psi) load, 80°C, 100% R.H.

surface interactions of water vapor with a series of poly(imide-siloxane) copolymers of different siloxane concentration. Inverse Gas Chromatography (IGC) was used to examine the interaction of water vapor with the various polymer surfaces. Free energies of specific interaction of water vapor with the surface were determined as well as the dispersive components of the solid surface free energies. Diffusion coefficients were determined by gravimetric sorption experiments of free-standing thin films as a measure of the interaction of water vapor with the bulk polymer. The speed with which water was able to move through the bulk of the polymer and perhaps toward a bonded interface was of interest, since interfacial water is considered to be the most detrimental to adhesive properties.^{1,9}

2. BACKGROUND

2.1 IGC THEORY

2.1.1 Introduction

Inverse gas chromatography (IGC) is very similar to and is based on the same theoretical foundations as conventional gas chromatography. It is substantially different in that the object of study is the stationary phase not the volatile injected matter carried by the mobile phase. The stationary phase is contained in a column through which a mobile phase of carrier gas constantly flows. A single volatile molecular probe of known physical properties is injected as a vapor pulse into the mobile phase which carries it through the column. As it travels down the column the probe is distributed between the mobile and stationary phases according to its partition coefficient. (The partition coefficient is the ratio of the amount of probe per unit volume in the stationary phase to the amount of probe per unit volume in the mobile phase.¹⁰) These are the same partition coefficients that conventional gas chromatography relies on to separate components in mixtures of injected compounds. A suitable detector is placed at the end of the column to determine the time at which the probe exits as well as the final peak shape of the "pulse." The time that the probe remains in the column, its retention time, is a measure of its interaction with the stationary phase. The retention time is the major piece of information obtained from an IGC experiment.

In order for different IGC studies to be comparable, the experimentally obtained retention time data must be corrected for conditions which change from

column to column and experiment to experiment. The specific retention volume is the volume of carrier gas required to elute a probe per gram of stationary phase at a temperature of 0°C:

$$V_g^{\circ} = (273.16 \cdot V_n) / (T_{col} \cdot w) \quad (1)$$

where T_{col} is the column temperature, and w is the weight of polymer in the column. V_n is the net retention volume, which is given by:

$$V_n = J F_{corr} (t_r - t_o) \quad (2)$$

where " t_r " is the retention time of the probe and " t_o " is the retention time of a non-interacting marker (nitrogen or methane). The subtraction of the marker effectively subtracts the dead volume in the system. "J" is the James and Martin correction factor for gas compressibility, which is expressed:

$$J = \frac{3}{2} \frac{\left[\left(\frac{P_i}{P_o} \right)^2 - 1 \right]}{\left[\left(\frac{P_i}{P_o} \right)^3 - 1 \right]} \quad (3)$$

where P_i and P_o are the pressures at the column inlet and outlet, respectively. While important for packed columns, this correction factor is less important for capillary columns due to the low pressure drop. " F_{corr} " is the column flow rate corrected for the water-vapor saturation of the carrier gas. This is necessary if the flow measurement was made using a soap-film flowmeter.

$$F_{\text{corr}} = (F/P_o)(P_o - P_{\text{H}_2\text{O}}) \quad (4)$$

"F" is the measured flow rate. " $P_{\text{H}_2\text{O}}$ " is the vapor pressure of water at the temperature of the flowmeter.

A schematic representation of a gas chromatograph is given in Figure 2. The instrumentation used is the same as that used in conventional gas chromatography. The column containing the stationary phase becomes the experimental sample. It can be a capillary column or a packed column filled with coated chromatographic support, or various fibers or fillers, for example.

2.1.2 Basic Theory

One of the earliest applications of the inverse gas chromatographic technique was accomplished by Smidsrød and Guillet.¹¹ By utilizing poly(N-isopropylacrylamide) as the stationary phase and a series of weakly interacting solutes, they were able to detect the glass transition temperature, T_g , of the polymer. Several studies followed which reaffirmed this discovery and examined a number of polymer stationary phases.¹²⁻¹⁴ Figure 3 is a generalized retention diagram which is based on these studies. It shows the variation of the natural logarithm of the specific retention volume against the inverse of absolute temperature. The deviations from linearity in the diagram correspond to transitions in the polymer stationary phase. In the linear region from A to B, the polymer is below its glass transition temperature and the retention mechanism of the probe is predominantly surface adsorption. In this temperature range, surface studies can be done. The first deviation from linearity corresponds to the

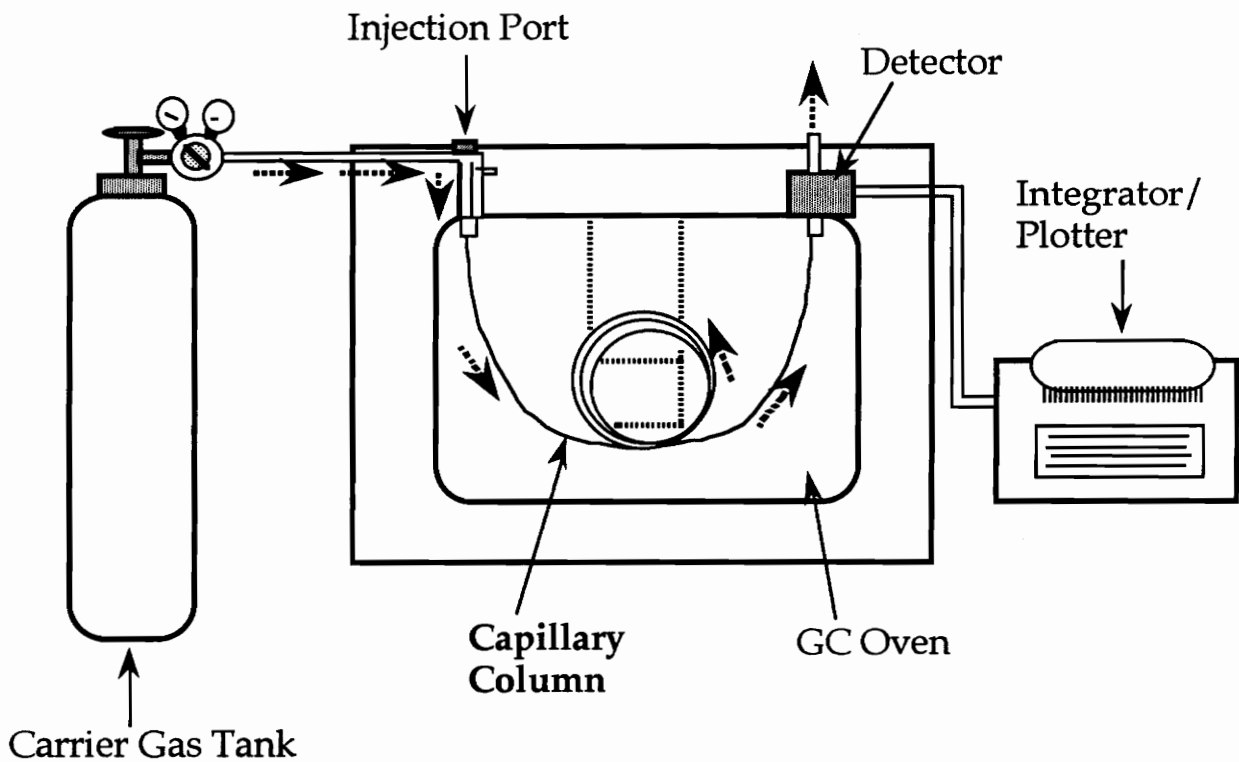


Figure 2. Schematic of a gas chromatograph and sample column. Thick dotted arrows trace helium carrier gas flow through the column.

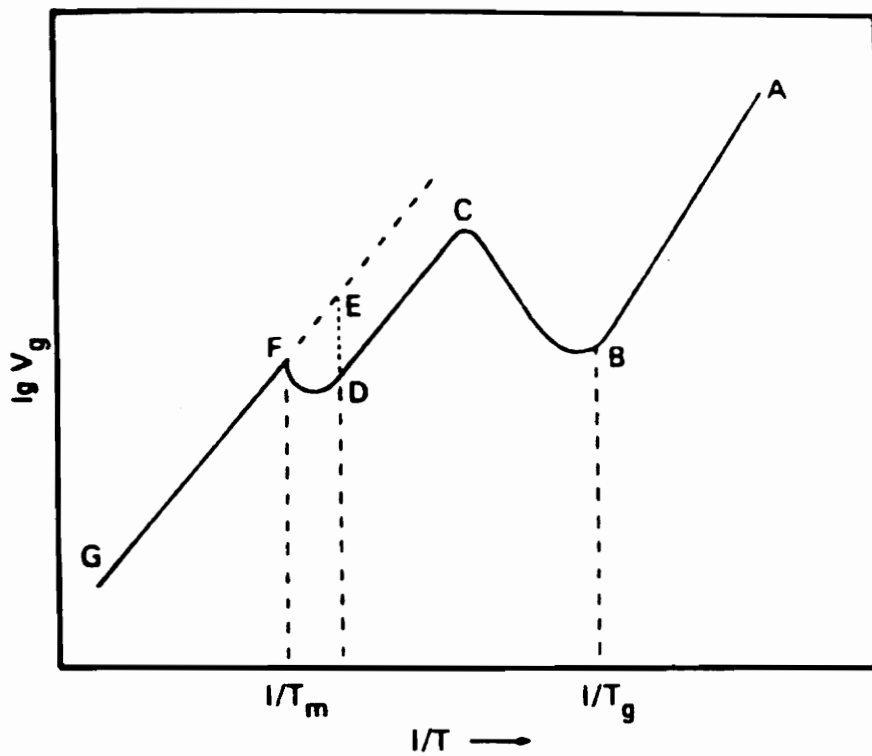


Figure 3. Generalized retention diagram for semi-crystalline polymer.
 (From reference 18)

glass transition temperature. The region B to C is a non-equilibrium region; the probe begins to be able to penetrate into the bulk polymer but diffusion is slow. From C to D, equilibrium conditions prevail and studies of the bulk polymer can proceed. Studies in this temperature range include determinations of heats of solution, diffusion coefficients, and polymer-solvent and polymer-polymer interaction parameters.¹⁵⁻¹⁷ This equilibrium region has been said to be approximately 50°C above T_g .¹⁸ If the polymer is amorphous, there are no further deviations. If it is crystalline, a melting point is detected at point F. At temperatures below T_m , the probe cannot penetrate the crystallites. Retention increases above T_m since there is an increased amount of polymer for the probe to access. This has been used to determine percent crystallinity.^{19,20}

The initial studies found the trends in the above described general retention diagram to be true for the probes that were nonsolvents for the polymer. A probe that could solvate the polymer was found to be likely to be able to penetrate into the bulk of the polymer below T_g , and the detection of the T_g by IGC depended on the change in retention mechanism from surface adsorption to bulk sorption. One study, however, found that a solvating probe was actually required to detect the glass transition of atactic polypropylene, but the temperature range involved was much lower (below 0°C) than those normally studied.²¹ Studies such as that prompted Braun and Guillet²² to investigate further. It was found that surface adsorption was the predominant retention mechanism below T_g . Failures to detect T_g could be attributed to various factors. One factor was the influence of polymer film thickness. Thinner films had lower volume to surface ratios and gave less noticeable deviations at T_g due to a decreased effect of the bulk sorption mechanism. Another factor was

due to an inability of hydrocarbon non-solvents to enter the bulk of a polar polymer even above T_g . Surface adsorption can be a predominant retention mechanism even above T_g for some systems.

2.1.3 Surface Energetics Study

IGC studies using non-solvating probes and conducted at temperatures well below the glass transition temperature of a given polymer reveal characteristics of that polymer's surface, since adsorption is the predominant retention mechanism. The following theory was perhaps developed initially for acid-base studies of carbon fiber surfaces, for which adsorption can be the only retention mechanism, but it has also been successfully used with polymer surfaces.²³⁻²⁶ Specific or non-dispersive polar free energies of surface interaction between polar probes and the polymer surface are obtained by the subtraction of a dispersive reference term. The corresponding subtracted dispersive reference term is determined from a dispersive reference line obtained experimentally by the injection of a homologous series of normal alkanes. This dispersive reference line is described by the following equations.²³

✧ The free energy of adsorption or desorption, ΔG° , of a mole of probe from a reference adsorption state can be written:

$$\Delta G^\circ = RT \ln V_n + K \quad (5)$$

where "R" is the universal gas constant, "T" is the temperature and "K" is a sum of constants. This union of surface thermodynamics and chromatography assumes the probe interacts with the surface at infinite dilution so that equilibrium is

achieved. Equilibrium is ideally indicated by gaussian elution peaks. The work of adhesion, w_A , per unit surface area, between a probe and a solid surface can be related to the free energy by:

$$\Delta G^\circ = N_A a w_A \quad (6)$$

where " N_A " is Avogadro's number and " a " is the probe molecule surface area. This equation can be viewed as a mathematical description of the verbal definition of the work of adhesion. In the case of dispersive or Van der Waals type interactions, w_A can be written in this form:²⁷

$$w_A = 2(\gamma_s^d \gamma_l^d)^{1/2} \quad (7)$$

where γ_s^d and γ_l^d are respectively the dispersive components of the solid and liquid surface free energies. By substitution one obtains:

$$RT \ln V_n = 2 N_A (\gamma_s^d)^{1/2} a (\gamma_l^d)^{1/2} + K \quad (8)$$

A plot of " $a (\gamma_l^d)^{1/2}$ " versus the left-hand-side of the equation gives a straight line for a homologous series of normal alkanes. The dispersive component of the solid surface free energy, γ_s^d , of the polymer stationary phase can be determined from the slope of this reference line.

$$\gamma_s^d = (\text{slope} / 2N_A)^2 \quad (9)$$

A polar probe is capable of having both dispersive and non-dispersive interactions with a polar stationary phase surface. Data corresponding to the injection of a polar probe will therefore fall above the dispersive reference line due to an increase in retention caused by increased interactions. The free energy of specific surface interaction is obtained by subtracting the corresponding dispersive interaction obtained from the reference line from the total interaction of the polar probe. The mathematical expression is the following:

$$\Delta G_{sp}^{\circ} = RT \ln (V_n/V_{nR}) \quad (10)$$

where V_n is the net retention volume of the polar probe and V_{nR} is the value from the dispersive reference line.

2.2 IGC LITERATURE REVIEW

2.2.1 Introduction

Since the beginnings of inverse gas chromatography studies in the late 1960's, numerous papers have been published on applications to theory and technique improvement and many different stationary phases have been studied for a variety of purposes. This literature review will attempt to point out some of the more important and recent contributions involving IGC technique and surface studies. General theory behind IGC and applications have already been well discussed and reviewed by several authors.^{18,28-32} A compilation of papers, which exhibits the wide range of applications of IGC has also been published.³³

A review of recent papers by Voekel³⁴ contains 145 references for IGC studies of polymers, fibers, silicas and surfactants.

2.2.2 IGC Technique

There have been a number of papers which have pointed out the various contributions to error involved in IGC experiments. Early studies by Courval and Gray examined the importance of injected probe size, flow rate and distribution of stationary phase loading in packed columns.³⁵ They also indicated the importance of correcting for the effects of surface adsorption in experiments conducted near melting transitions on polar polymers with polar probes such as water or ethanol.³⁶ More recently, Munk and colleagues have published a series of papers dedicated in part to increasing the precision of IGC. In order to reduce the error associated with the determination of the weight of polymer (for V_g°) in a packed column, a new "soaking" method for coating chromatographic support was developed.³⁷ The role of "inert" dimethylchlorosilane-treated Chromosorb W support in probe retention,³⁸ the dependence of retention on the amount of probe injected,³⁹ and errors in soap bubble flowmeter measurements⁴⁰ were also examined. The minimization of errors associated with IGC experiments has also been addressed by Koning.⁴¹ Moment analysis of peak shape has been proposed as a more appropriate determination of peak retention time.⁴² This analysis suggested that deviations from linearity in plots of $\ln V_g^\circ$ versus reciprocal temperature which had been attributed to polymer transitions were simply artifacts of inappropriate determination of retention times from peak maximum. However, the authors themselves attributed deviations from linearity of the reciprocal theoretical plates

at increasing temperatures to a polymer glass transition and a change in retention mechanism.

2.2.3 IGC Surface Studies of Polymers and Other Solids

Gray and Guillet⁴³ determined adsorption isotherms of n-decane and n-hexanol onto poly(methyl methacrylate) (PMMA) and polystyrene (PS) surfaces. For high concentrations of injected sorbate (probe), the isotherms were non-linear. For low injected amounts of probe onto PMMA, retention times were independent of injected amount and isotherms were considered linear. Studies of PS surfaces were complicated by a slow diffusion into the bulk. It was suggested that non-swelling or non-solvating probes be used and that studies be conducted well below T_g .

The influence of the solvent, used to cast polymer onto chromatographic support, on the polymer surface properties has been examined by Schreiber and Croucher.^{44,45} Although no simple correlation was found between casting-solvent properties and resulting polymer surface characteristics, it was found that polymers with polar groups showed differences in surface retention. Non-polar polystyrene surfaces were not dependent on casting solvent.⁴⁵ Casting PMMA from a poor solvent such as toluene was considered to give a more "porous" coating than that obtained from a good solvent, chloroform. Increased probe retention in the toluene-cast column was attributed to an increased surface area.⁴⁴

The acid/base nature of polymer as well as other solid surfaces have been investigated--often in relation to the elucidation of composite and filled material adhesive properties. Although specific techniques vary, the general approach

always involves the use of probes defined as being acidic or basic. IGC polymer-solute interaction studies of poly(ethyl hexyl methacrylate) have shown it to be a basic polymer.⁴⁶ Schreiber and colleagues⁴⁷ used an arbitrary acid/base parameter, defined as the ratio of the specific retentions of the acidic (t-butanol) probe and the basic (butylamine) probe, to examine polyethylene (PE), polyvinylchloride (PVC) and treated fillers. PE had no acid/base character, as expected, and PVC was acidic. The acid/base characteristics of carbon fibers as well as possible composite matrix polymers have been studied by determining and comparing free energies of specific interaction for acidic and basic probes.^{23-26,47-50} The probes were chosen using Gutmann's⁵¹ acceptor-donor numbers. Carbon fibers were found to be predominantly acidic in nature while the polymers studied exhibited basic surface characteristics. It was also found that fiber/matrix adhesion could be correlated to the acid/base interactions determined by IGC. Lewis acid/base acceptor-donor interactions at polymer interfaces has been recently studied by Chen.⁵² An acid/base interaction heat was related to IGC-determined heats of adsorption. Literature data was utilized to show that the calculated acid/base interaction heats could be put in terms of Drago's four parameter equation⁵³ and that parameters could be assigned to polymers as well as probes. Due to a lack of numerous completely-acceptable studies on polymer surfaces, the assumption was made that IGC-determined heats of solution could approximate heats of adsorption.

Panzer and Schreiber⁵⁴ have evaluated the use of inverse gas chromatography to study acid/base surface characteristics of polymers, specifically polycarbonate. Three different methods of determining specific free energies and enthalpies of interaction of polar probes with the surface were

compared and found to be equivalent. Additional work using one of the methods and a corrected version of Gutmann's acceptor-donor numbers for polar probes indicated that the polycarbonate surface was amphoteric but predominantly basic. This was in good agreement with the work of Bolvari and Ward.²⁶

Early work on gas chromatographic studies of solid surfaces was reviewed by Kiselev.⁵⁵ These studies involved GC applications to the investigation of silica surfaces. Recent work on non-polymer surfaces includes the determination of adsorption isotherm data on fine ceramic particles coated along the inner wall of a capillary column.⁵⁶ The acid/base surface characteristics of untreated and aminopropyltriethoxysilane-treated glass beads were studied as model fillers.⁵⁷ Using infinite dilution IGC, heats of adsorption were determined using n-alkanes, acidic and basic probes. N-alkane heats of adsorption were confirmed to involve dispersive interactions. Polar probe acid/base interaction heats were obtained from the adsorption heats by subtracting a heat of probe vaporization as an estimate of the dispersive component. (A corrected dispersive term was assumed to be required for self-interacting probes.) The IGC technique was found to be quantitative. The untreated glass beads were predominantly acidic, while the treated beads were found to be more basic than the untreated beads.

A new IGC method of estimating specific surface areas of solids has recently been developed by Jagiello and Papirer.⁵⁸ In studies at infinite dilution, the specific retention volume, V_g° , is expected to be related to the specific surface area by a Henry's law constant, k . Surface areas can be determined from V_g° if k has been determined from a separate experiment on a surface of known area. The new method avoids this by determining surface area from a series of

injections of n-alkanes and assuming retention increases in constant increments with each additional $-\text{CH}_2-$ group. A plot of the logarithm of n-alkane specific retention volume versus n-alkane carbon number gives an intercept term that contains the specific surface area and a constant, k_{α} , for a hypothetical zero-carbon n-alkane.

2.3 DIFFUSION THEORY

2.3.1 Introduction

The diffusion of penetrants into polymers can follow either Fickian or anomalous kinetics. Fickian diffusion is discussed in detail below. An example of anomalous diffusion is Case II transport, which exhibits a linear relation for fractional uptake against time. Such non-Fickian kinetics are considered to be due to the effects of the superimposition of relaxational phenomena over the diffusion process. A good introduction to Case II diffusion is given by Windle.⁵⁹ Phenomenological theories of diffusion are often based in part on descriptions of the free volume. Some free volume related theories are reviewed later in this section.

2.3.2 Fickian Diffusion

Diffusion can be described as the movement of matter within a system due to random molecular motions within that system. Fick's⁶⁰ first law of diffusion was drawn by analogy from Fourier's⁶¹ derived equation of the conductance of heat, which results from random molecular motions. For uni-directional diffusion:

$$J = -D \left(\frac{\delta c}{\delta x} \right) \quad (11)$$

This law states that the flux, J , (or the amount of matter transferred) in the x -direction through a plane of unit area during a unit time is proportional to the concentration gradient of the diffusing species in that direction. The negative sign means that the diffusive flux moves toward areas of lower concentration by diffusing in the direction of decreasing concentration. Concentration, c , refers to the concentration of penetrant in the matrix.

Vieth⁶² gives a short summary of the application of Fourier's theory to mass transfer in which the proportionality matrix elements become thermodynamic diffusion coefficients, \mathcal{D} , and the gradients become chemical potential gradients. For a system of two components influenced only by chemical potential gradients, each component's flux can be represented:

$$J_1 = -\mathcal{D}_{11} \left(\frac{\delta \mu}{\delta x} \right)_1 - \mathcal{D}_{12} \left(\frac{\delta \mu}{\delta x} \right)_2$$

$$J_2 = -\mathcal{D}_{21} \left(\frac{\delta \mu}{\delta x} \right)_1 - \mathcal{D}_{22} \left(\frac{\delta \mu}{\delta x} \right)_2 \quad (12)$$

For systems in which one component is very dilute and the other component is significantly less mobile compared to its companion component, the above equations reduce to:

$$J_1 = -\mathcal{D}_{11} \left(\frac{\delta \mu}{\delta x} \right)_1 \quad (13)$$

This is the assumed case for many low-molecular-weight gas and non-solvating vapor penetrants into polymers, the long chain molecules of which act as a "fixed" reference frame. The change of polymer (component 2) concentration with distance (x) is therefore considered to be very small. The flux, J_2 , of the polymer is also considered negligible under these conditions. The relation between the thermodynamic and experimental diffusion coefficients is derived in Appendix B.

2.3.3 Experimental Approach

Experimental approaches to obtaining diffusion coefficients are based on various solutions to Fick's second law. This second law describes the increase (or decrease) in concentration with respect to time of penetrant within a volume element, for example a unit cube in Cartesian coordinates.

$$\frac{\delta c}{\delta t} = D \left(\frac{\delta^2 c}{\delta x^2} + \frac{\delta^2 c}{\delta y^2} + \frac{\delta^2 c}{\delta z^2} \right) \quad (14)$$

It is derived from the first law by taking into account the fluxes entering and exiting the plane faces of the unit volume cube.⁶³ For diffusion limited to only one direction, the equation simplifies to

$$\frac{\delta c}{\delta t} = D \left(\frac{\delta^2 c}{\delta x^2} \right) \quad (15)$$

which gives the change of concentration with time at any plane in the matrix. The form of the second law will differ for other coordinate systems such as cylindrical and spherical. These forms are listed by Comyn.⁶⁴

Solutions to this basic differential equation depend on the the matrix sample geometry and also on the chosen boundary conditions. Crank⁶⁵ solves the second law, assuming constant D , for planar, cylindrical and spherical geometries for various boundary conditions. Several solutions can also be obtained from the heat conduction treatise by Carslaw and Jaeger,⁶⁶ if concentration and diffusion coefficient terms replace temperature and thermal diffusivity terms.⁶⁷ Evaluation of solutions for which D is a function of concentration is possible if the function $D(c)$ is known ahead of time, but this can be extremely difficult.^{62,67} Determining $D(c)$ often involves utilizing equations which assume D is constant.

The simplest solution to the differential equation is the case of constant or steady state flux. The change in concentration with time is zero. The diffusion coefficient can be determined if the constant flux and concentration gradient are known.⁶² Two common approaches to the determination of the diffusion coefficient which are based on planar solutions are the time lag method and the mass uptake or sorption method. The time lag method is a permeation approach which takes into account initial non-steady state and final steady state permeation while relating the diffusion coefficient to the lag in the approach to the final steady state permeation.^{62,64,68} Good discussion of the various techniques are given by Vieth⁶² and Felder and Huvard.⁶⁸

The sorption method is based on the solution for diffusion into a semi-infinite film exposed to an infinite bath of the penetrant:⁶⁴

$$\frac{C}{C_1} = 1 - \frac{4}{\pi} \sum_{n=0}^{\infty} \frac{(-1)^n}{2n+1} \exp\left(\frac{-D(2n+1)^2\pi^2t}{4l^2}\right) \cos\left(\frac{(2n+1)\pi x}{2l}\right) \quad (16)$$

where l is one-half the film thickness and x is set equal to zero at the middle of the film. The concentration, C_1 , at the faces of the film reach equilibrium immediately. Diffusion into the edges of the film are ignored. This equation can be integrated⁶⁹ to give the following equation:

$$\frac{M_t}{M_\infty} = 1 - \sum_{n=0}^{\infty} \frac{8}{(2n+1)^2\pi^2} \exp\left(\frac{-D(2n+1)^2\pi^2t}{l^2}\right) \quad (17)$$

M_t is the mass uptake of penetrant into the film at time, t , and M_∞ is the equilibrium uptake at long times. In this equation, unlike the previous equation, the film thickness equals l . The fractional uptake is given by M_t/M_∞ and D is the diffusion coefficient. For short times, this can be approximated by:

$$\frac{M_t}{M_\infty} = \frac{4}{\pi^{1/2}} \left(\frac{Dt}{l^2}\right)^{1/2} \quad (18)$$

which is a linear function for a plot of the fractional uptake against " $t^{1/2}/l$ ". The diffusion coefficient is obtained from the slope of this plot.

Fickian diffusion is the common type associated with penetrant diffusion into a rubbery polymer or, in other words, a polymer that is above its glass transition temperature. Diffusion of penetrants into glassy polymers is often

non-Fickian, but there are cases in which diffusion with Fickian characteristics have been reported.⁶³

Some important characteristics of Fickian diffusion are the following:⁷⁰ 1) Plots of fractional uptake versus the square root of time are initially linear for both sorption and desorption studies. For sorption, the plot must be linear up to at least 0.6 of the fractional uptake. 2) The sorption curves must be concave to the "x-axis" after the initial linear region. 3) Reduced sorption plots (given by fractional uptake against square root of time divided by film thickness) are the same for films of different thicknesses. 4) Sorption and desorption plots coincide when the diffusion coefficient is not a function of concentration but is a constant. In general, it has been found that if the diffusion coefficient is an increasing function of concentration, then the desorption curve will fall below the sorption curve, i.e. the diffusion coefficient will be smaller upon desorption than sorption. If the diffusion coefficient is a decreasing function of concentration as is the case of water in hydrophobic polymers, then the desorption curve will be above the sorption curve.⁶⁸

2.3.4 Free Volume Diffusion Theories

Fick's law describes entropic diffusion driven by random responses to a concentration gradient. There have been many approaches and developments in theories of diffusion, which have been reviewed.^{62,67,68,71-73} Many of these theories share a similar basic phenomenological assumption that the diffusion of a penetrant is the rate of movement of that penetrant into and out of a series of vacancies or "holes" (equal to or larger than the penetrant size) in its random

walk in the direction of the concentration gradient. A simple equation which expresses this was derived by Bueche:⁷⁴

$$D = \frac{\phi \lambda^2}{6} \quad (19)$$

where D is the diffusion coefficient, ϕ is the average number of "jumps" of the penetrant in a unit time, and λ is the jump distance. For the case of small penetrant molecules in a polymer matrix, the maximum possible jump rate of the small molecules is much greater than the rate of formation of vacancies for the small molecules to jump into. Therefore the diffusion coefficient becomes proportional to a limiting rate of adjacent critical size hole formation which is influenced largely by the mobility of segments of the polymer chains.⁷⁵ The probability of hole formation is considered to increase with increased segmental mobility. This visualization involving "holes" has led many theories of diffusion to include various free-volume relations.

Many theories, starting with Fujita's⁷⁶ have involved the WLF equation⁷⁷ which can be derived from the Doolittle equation that describes the mobility of polymer segments in the form of a viscosity:

$$\eta = A \exp\left(-\frac{B}{f}\right) \quad (20)$$

where A and B are constants. The fractional free volume, f , is the free volume divided by the total volume. Using the glass transition temperature, T_g , as a reference temperature, one obtains

$$\ln\left(\frac{\eta}{\eta_g}\right) = B \left(\frac{1}{f} - \frac{1}{f_g} \right) \quad (21)$$

Assuming a linear increase in fractional free volume above T_g described by the following equation,

$$f = f_g + \alpha_f(T - T_g) \quad (22)$$

one can by substitution obtain

$$\log\left(\frac{\eta}{\eta_g}\right) = \frac{\frac{-B}{2.303 f_g}(T - T_g)}{\frac{f_g}{\alpha_f} + (T - T_g)} \quad (23)$$

where the subscript, g , refers to values at the reference temperature, T_g . This is the WLF equation, in which "universal" constants C_1 and C_2 are given as

$$C_1 = \frac{B}{2.303 f_g} \quad (24)$$

$$C_2 = \frac{f_g}{\alpha_f} \quad (25)$$

If B is approximated equal to one, then α_f , the difference between the thermal expansion coefficients of the rubbery and glassy states, is calculated to be $4.8 \times 10^{-4} \text{ deg}^{-1}$ and f_g , the fractional free volume at T_g , is 0.025.⁷⁸ This approach

reveals a similar free volume state for all polymers at the glass transition temperature.

The above equation is often used to describe the temperature dependence of the relaxation time shift factor, $\ln a_T$, where⁷⁸

$$\log a_T = \log \left(\frac{\tau}{\tau_g} \right) \approx \log \left(\frac{\eta}{\eta_g} \right) \quad (26)$$

and τ represents polymer relaxation time(s). (Strictly speaking, for polymers there is a distribution or spectrum of relaxation times, not a single time.) The shorter or smaller the relaxation time, the greater the segmental mobility of the polymer. The relaxation time can be considered the inverse of the mobility such that the above equations can be rewritten in the following fashion:

$$\frac{\tau}{\tau_g} = \frac{\left(\frac{1}{\phi} \right)}{\left(\frac{1}{\phi_g} \right)} \quad (27)$$

$$\phi = \phi_g \exp \left(\frac{2.303 C_1 (T - T_g)}{C_2 + (T - T_g)} \right) \quad (28)$$

An equation extremely similar to the one above is given by Stuk⁷⁹ with the addition of a temperature shift term, ΔT , added to T in order to account for the plasticizing effect of the solute molecule. The substitution of this mobility, ϕ , into Bueche's equation in the place of the jump frequency provides an equation for the diffusion coefficient. Stuk fitted this equation to the diffusion data of

several gases in natural and butyl rubber assuming that the jump distance and the ΔT were constant for a given polymer and gas, respectively. It was concluded that diffusion of gases may be described by the same segmental diffusive processes associated with polymer relaxation as related to mechanical properties. This approach, like all approaches based on the WLF equation, is truly valid only for diffusion in rubbery polymers--above the glass transition temperature.

Vrentas and Duda and colleagues have authored numerous papers⁸⁰⁻⁸⁸ focussed on the many aspects of diffusion theory. A diffusion theory applicable to rubbery polymers was developed which incorporates aspects of several earlier diffusion theories as well as some Flory-Huggins polymer solution theory. The major equations of this theory have been derived and well explained in the references cited above. Volume is considered to consist of an occupied volume, an interstitial free volume and a hole free volume, which is the free volume available to a diffusing penetrant. This theory includes an adaptation of Fujita's WLF free volume-temperature relation, which is contained in the following equation:⁸¹

$$\ln\left(\frac{D}{D_g}\right) = \frac{\gamma V_2^* \xi}{K_{12}} \frac{T - T_g}{K_{22}(K_{22} + T - T_g)} \quad (29)$$

where $K_{22} = C_2$, and $\gamma V_2^*/K_{12} = 2.303C_1C_2$. "C₁" and "C₂" are the WLF constants. The term, ξ , is designed to remove Fujita's assumption that the molecular weight of the penetrant equals the molecular weight of the polymer jumping unit. The minimum critical hole free volume per gram of polymer required for a jump is given by V_2^* . An overlap factor is described by γ . The

theory has been found to fit experimental data over a wide range of temperatures and concentrations, but it has so many parameters that even the authors have admitted it can be difficult to implement.⁸³

Vrentas and Duda have also attempted to modify the above theory to make it applicable to diffusion in glassy polymers at temperatures below the glass transition. The non-equilibrium structure is assumed to be constant during a diffusion process so that the hole free volume is fixed. For diffusion in a glassy polymer for extremely small concentrations of penetrant:⁸⁷

$$D = D_0 \exp\left[-\frac{E}{RT}\right] \exp\left[-\frac{\gamma\xi V_2^*}{V_{FH}(0)}\right] \quad (30)$$

$$\frac{V_{FH}(0)}{\gamma} = \frac{K_{12}}{\gamma} [K_{22} + \lambda(T - T_g)] \quad (31)$$

where E is the molar energy needed to overcome attractive forces prior to a jump and V_{FH} is average hole free volume per gram. The temperature dependence of the diffusion coefficient is derived from a modified WLF equation,⁸¹

$$\ln\left(\frac{D}{D_g}\right) = \frac{\gamma V_2^* \xi}{K_{12}} \frac{T - T_g}{K_{22} \left(\frac{K_{22}}{\lambda} + T - T_g\right)} \quad (32)$$

or in more familiar terms

$$\ln \frac{D}{D_g} = \frac{2.303 C_1 \xi (T - T_g)}{\frac{C_2}{\gamma} + T - T_g} \quad (33)$$

The modifier, γ , addresses the volume contraction change with the glass transition. For $\gamma = 1$, the original WLF equation applies and there is equilibrium contraction below T_g . If $\gamma = 0$, then the specific hole free volume equals a constant value equal to the value at the T_g . Aging phenomena is not incorporated here. A theory has also been derived for diffusion a finite concentration of penetrant in a glassy polymer.^{84,85,88} A predictive approach to sorption as well as an application to water in glassy poly(methyl methacrylate) has been published.^{85,86,88}

Lefebvre, et.al.,^{89,90} developed constitutive equations for the diffusion of a small penetrant under the influence of temperature, stress and concentration. The WLF equation was also incorporated into this theory to describe the influence of temperature on free volume above the glass transition temperature. The above theory was applied to the diffusion in the glassy state by assuming that any invalidity stemmed from the expression for temperature dependence. It was assumed that some small scale local motions continue to exist below T_g . The temperature dependence below T_g was described by an Arrhenius-like expression containing an activation energy. An additional component of the theory was added specifically to address time-dependent physical aging below the glass transition temperature.

2.4 DIFFUSION LITERATURE REVIEW

2.4.1 Introduction

There are numerous studies of the sorption and diffusion of water and water vapor into various types of polymer systems. Many practical applications of polymers require an understanding of the interaction of water under given conditions. Such applications include adhesives, composites, separation membranes and hydrogel drug-delivery systems. Recent work includes studies of water sorption and mechanical properties of carbon fiber composites with epoxy,⁹¹ poly(ether ether ketone) (PEEK) and poly(phenylene sulfide) (PPS)⁹² matrices. In both studies, the diffusion was Fickian and the temperature dependence of the coefficient followed an Arrhenius relationship. Mechanical properties dropped with humidity, but the PEEK composites showed good properties even at relatively high humidity.⁹² Other studies have shown an Arrhenius temperature relationship holds as well for epoxy coatings exposed to water.⁹³ Fickian kinetics have been reported in other durability studies as well.^{63,94} Poly(ethylene terephthalate) (PET) and poly(butylene terephthalate) (PBT) and their glass fiber composites, however, have shown non-Fickian sorption kinetics, which are due to the occurrence of various structural changes in the semi-crystalline polymers during sorption.⁹⁵ Temperature dependence of apparent diffusion coefficients above and below the glass transition temperature were fitted to an Arrhenius relation; there was sharp increase in activation energy for diffusion below the glass transition. Of course, the sorptive interaction of water in non-composite, pure polymer systems is also an important area of study. With its ability to hydrogen bond, water can have a large influence

on the properties of polyamides. Some recent work includes studies of water diffusion into poly(isophthalamide)s⁹⁶ and several types of Kevlar^{97,98} and Nylon⁹⁸ fibers. Other more specific categories of recent diffusion-related work is discussed below.

2.4.2 Polyimides

The diffusion and distribution of water and deuterated water in Kapton (pyromellitic dianhydride oxydianiline or PMDA-ODA) polyimide films has been examined using sorption, nuclear magnetic resonance and dielectric relaxation among other techniques.⁹⁹ These studies revealed that bulk sorbed water existed in two types of site. One site was found to be distributed through the film whereas the other site, which appeared at higher relative humidities, was distributed more in the interior of the film and was found to have more localized motions. These second sites were thought to be clusters of two or three molecules. Although the diffusion coefficient was found to increase with increasing film thickness and depend somewhat on concentration, all sorption curves were found to be Fickian. Reported diffusion coefficients were of the magnitude of 10^{-9} cm²/sec. Other studies involving water include the sorption and diffusion of water from water/ethanol mixtures through aromatic poly(etherimide) membranes in terms of pervaporation separation techniques.¹⁰⁰ Water was sorbed preferentially over ethanol at all "feed" mixture compositions.

A bending beam technique has been utilized to determine diffusion coefficients of water into three polyimides and their blends and copolymers.¹⁰¹ The amic acids were cast on silicon wafers and then cured. Film thicknesses ranged from 3 to 25 μ m. The variation of curvature of the bi-layer was followed

during sorption to determine diffusion. The polymers studied were pyromellitic dianhydride-4,4'-oxydianiline (PMDA-ODA), pyromellitic dianhydride-*p*-phenylenediamine (PMDA-PDA) and 3,3',4,4'-benzophenone tetracarboxylic dianhydride-*p*-phenylenediamine (BPDA-PDA). Uptake was termed Fickian in all cases, although there were sometimes slight deviations from the theoretical curves just before equilibrium. Short "induction" periods were also observed in these curves. No dependence of diffusion coefficient on film thickness was found. PMDA-ODA samples had faster diffusion coefficients than PMDA-PDA samples. This was attributed to the ether linkage and the relatively amorphous nature of PMDA-ODA compared to the semi-crystallinity of PMDA-PDA. Diffusion coefficients of the blends and copolymers of these two polyimides fell between the homopolymer values for PMDA-ODA and PMDA-PDA. The BPDA-PDA samples had the smallest diffusion coefficients. Since it appeared that the BPDA-PDA and PMDA-PDA had similar levels of crystallinity and packing coefficients, it was considered that the decrease in diffusion coefficient¹⁰² was due to BPDA-PDA having a larger hydrophobic group in its structure. Blends and copolymers of these polyimides were found to be compatible and have reduced structural order. However, diffusion coefficients were only slightly higher than BPDA-PDA homopolymer values, indicating crystallinity was a secondary influence.

Recent work has also included the diffusion of various solvents into polyimides. A gravimetric study of the sorption of several solvents, including methylene chloride, into a number of polyimides produced non-Fickian sorption curves.¹⁰² Other investigations¹⁰³ include the diffusion of N-methylpyrrolidone (NMP) solvent vapor into pyromellitic dianhydride-4,4'-oxydianiline (PMDA-

ODA) and pyromellitic dianhydride-p-phenylenediamine (PMDA-PDA) polyimides via utilization of the bending beam technique. Diffusion into the amorphous relatively flexible PMDA-ODA was Case I or Fickian, which was considered to be due to flexibility and possible void formation. An "induction" period was observed in these curves. Diffusion into the highly crystalline PMDA-PDA was Case II anomalous. The NMP was apparently required to first solvate or relax the semi-crystalline structure before further diffusion could take place. The relaxation of the polymer was seen as a rate limiting step indicating a sharp diffusion front which is a characteristic of Case II. In both cases, diffusion was found to increase with increasing film thickness, apparently related to a decrease of ordering in the film coating with increasing thickness. Thicknesses ranged from 0.5 to 10 μm . Diffusion rate also decreased with increasing cure temperature.

Diffusion of permanent gases has also been studied for polyimides. The permeability of permanent gases in relation to the degree of methyl-group substitution on the phenylenediamine structural portion of some polyimides has been investigated with an emphasis on selectivity.¹⁰⁴ Diffusion constants of the chemically-imidized polymers were calculated from experimentally obtained permeability and solubility data. Fractional free volumes were estimated from specific molar volumes at temperature and absolute zero using density data and Van der Waals volume data. Methyl substitution was found to increase the fractional free volume and the diffusion coefficient. The increase in fractional free volume was attributed to steric hindrance leading to a loss of conformational freedom, which caused less dense packing. The permselectivity of the bulky, non-planar structure polymers was found to decrease for small-large

combination penetrant pairs such as hydrogen/ methane or carbon dioxide/ methane. The increased hole volume allowed for an increase in diffusion of the larger penetrant while the smaller penetrant diffusion would remain relatively unaffected. Sorption and diffusion studies of carbon dioxide, nitrogen and helium gases in a Dow commercial polyimide have shown that relaxation processes can influence the diffusion kinetics.¹⁰⁵ Nitrogen and helium, which had linear isotherms, were found to follow slightly non-Fickian sorption kinetic. This was attributed to a relaxational process occurring on the same time scale as the diffusion process. Carbon dioxide showed a dual-mode sorption isotherm, which indicated sorption into two types of site--dissolved and mobile or adsorbed in small voids and immobile. CO₂ appeared to have Fickian diffusion. The diffusion coefficients determined for CO₂ were of the magnitude 10⁻⁹ cm²/sec while those for N₂ and He were of the magnitude 10⁻⁸ cm²/sec. The diffusion process of CO₂ was considered to be on a different time scale than the relaxation and thus diffusion appeared non-anomalous or Fickian.

2.4.3 Blends

Moisture diffusion into polyimide blends have been investigated.¹⁰⁶ Incompatible blends of rigid PMDA-B (pyromellitic dianhydride-benzidine) and semi-flexible 6FDA-PDA (6F-dianhydride-phenylenediamine) polyimides were prepared by blending the amic acids at room temperature prior to thermal curing. Heating the amic acid blend to 50°C for 40 hours prior to curing produced compatible blends, as determined by X-ray diffractometry. Bending beam experiments were used to follow sorption of moisture. Diffusion followed Case I or Fickian kinetics and the diffusion coefficients were in the range of 10⁻¹⁰

cm²/sec. Pure PMDA-B had the slowest diffusion coefficient. Pure amorphous 6FDA-PDA had a coefficient of magnitude 10⁻⁹ cm²/sec, which was much faster than all the blends. A larger interchain spacing in the amorphous homopolymer compared to that in the blends and in the relatively crystalline PMDA-B was considered to be the reason. The diffusion constants of the blends increased with increasing content of 6FDA-PDA for all blends, but were higher for the series of compatible blends than for the the series of incompatible blends. This was attributed to the domains of crystallinity in the incompatible blends acting as impenetrable barriers to water.

Water has been used as a diffusional probe to examine segmental mobility in blends of poly(methyl methacrylate) (PMMA) and styrene-acrylonitrile (PSAN) copolymers with polystyrene (MPS) modified to contain hydroxy groups.¹⁰⁷ The hydrogen-bondable groups of the MPS provided blend miscibility. Blends with higher hydroxy contents, however, showed positive excess volumes, which were attributed to poor chain packing due to inherent immiscibility with non-modified styrene units and the break-up of what would otherwise be (in a MPS homopolymer) self-associated hydroxy groups. The activation energy for diffusion was correlated to the excess volume. Diffusion coefficients were in the range of 10⁻⁷ to 10⁻⁸ cm²/sec. Those determined for the blends were in many cases higher than the expected values, which were averaged from component volume fractions. This was perhaps due again to poor chain packing. The coefficients varied consistently with specific volume-- increasing with increasing specific volume.

Sorption of water into sulfur-containing polymer blends includes a study done on a series of polyethersulfone (PES)/ phenoxy polymer blends.¹⁰⁸

Diffusion coefficients for these miscible blends fell between those of the homopolymers: $3.2 \times 10^{-8} \text{ cm}^2/\text{sec}$ for PES and $6.5 \times 10^{-9} \text{ cm}^2/\text{sec}$ for the phenoxy polymer. Permeability was found to increase when phase separation was induced in the 67% PES blend. Immiscible blends of semi-crystalline poly(phenylene sulfide) (PPS) and amorphous, hydrolytically unstable poly(arylate) (PAR) have also been studied¹⁰⁹ via water immersion. Sorption curves for PPS showed Fickian-like behavior, while those for PAR revealed anomalous uptake due to hydrolytic degradation at long sorption times. Diffusivity of the blends was found to decrease with increasing PPS content until a point was reached at approximately 45% where the diffusivity became constant and equal to that of pure PPS. This was related to a morphological change in the blend in which PPS appears to become continuous at or near the surface.

2.4.4 Copolymers

Water vapor sorption of graft copolymers of polycaproamide (PCA) and poly-(N,N-dimethylaminoethyl methacrylate) (PDMAEMA) have been investigated using an interval sorption technique.¹¹⁰ Solubility was independent of the amount of PDMAEMA graft polymer. Diffusion coefficients were found to increase with increasing graft content--with the increase becoming less significant at higher vapor concentrations. This increase was related to a "loosening" of the structure and to a decrease in overall amide group concentration. High water contents in the polymers were found to cause plasticization and clustering, with the plasticization of the PCA being the greatest.

Sorption by water immersion studies have been done on hydrogel network copolymers of 2-hydroxyethyl methacrylate (HEMA) crosslinked with

various multi-ethylene glycol dimethacrylates.¹¹¹ These were prepared by either a bulk polymerization or a solution copolymerization in the presence water or ethanol. Special efforts were made to produce uniform copolymers that showed no visible signs of phase separation or cracking. It was generally found that the uptake of water into the crosslinked systems was relaxation dependant Case II transport. The solution polymerized copolymers sorbed to equilibrium at an increased rate, which was suggested to be due to a more open and relaxed structure attained during polymerization. Sorption of water vapor into the same types of copolymer networks has been studied with an emphasis on the effect of the degree and nature of the crosslinking.¹¹² Sorption was reduced by higher crosslinking and was again found to be generally non-Fickian Case II. However, at low relative humidities, sorption almost conformed to Fick's law for the copolymers. A homopolymer PHEMA network showed Fickian uptake, except at 100% RH.

The influence of the soft segment on water sorption into segmented polyurethanes has been examined in terms of cluster theory.¹¹³ Ethylene and propylene oxide soft segments as well as propylene-ethylene-propylene oxide (PEP) triblock soft segments were studied. Propoxamer units tended to increase clustering. Similar increases in clustering due to the more hydrophobic propylene oxide groups were found in sorption studies of the PEP copolymer in a previous paper.¹¹⁴ The interaction of water with polyurethanes containing soft segments composed of EPE triblock copolymers has also been investigated.¹¹⁵ The sorption of water and the small depression of the soft segment T_g by water were believed to be influenced by interactions between the copolymer components and possible restricted motion of the ethylene oxide.

The diffusion of CO₂, argon and methane in a glassy-polystyrene/rubbery-polybutadiene star-branched block copolymer exhibiting well-defined lamellar morphology has been recently reported.¹¹⁶ The diffusion coefficients of each gas in the copolymer fell between the values determined for the homopolymers, as was expected. However, a higher than normal temperature dependence was shown by the activation energies of diffusion. Theoretical diffusion coefficients, which were initially determined by a computer simulation of unsteady diffusion which utilized homopolymer properties, also did not match experimental coefficients. This led to the conclusion that the motion of the polybutadiene chains in the copolymer was more restricted than they would be in the homopolymer. A temperature dependent mobility factor pertaining to the proportional change in the polybutadiene diffusion coefficient was determined. As temperature approached the polystyrene T_g, the mobility factor was found to go to unity. The study also pointed out that the solubility of the gases in this glassy-rubbery phase-separated copolymer was equal to the sum of the volume fractions of each component multiplied by its respective homopolymer solubility.

3. EXPERIMENTAL

3.1 POLYMERS

The polyimide and poly(imidesiloxane) copolymers were synthesized by members of Dr. J.E. McGrath's research group at Virginia Tech. The specific details of the synthesis itself have been well described elsewhere^{7,117} and will only be briefly described here. Siloxane segments are pre-formed as α,ω -aminopropyl poly(dimethylsiloxane) oligomers, which are synthesized^{118,119} by a reaction involving the equilibration of D4, a cyclic siloxane tetramer. Oligomer number average molecular weights were determined using potentiometric titration of the amine end-groups. The synthesis of the polymers involves the use of a cosolvent system of N-methyl-2-pyrrolidinone (NMP) or N,N-dimethylacetamide (DMAC) with tetrahydrofuran (THF) in order to have a homogeneous solution of all the monomers; generally a greater proportion of THF is needed if a greater molecular weight or percentage of siloxane is in the reaction mixture. The amine-terminated siloxane is added to a solution of the given dianhydride so that the siloxane is capped with anhydride groups. The given diamine is then added slowly to the solution, producing a randomly segmented multi-block amic acid-siloxane copolymer. A monofunctional anhydride is added also as a molecular weight controlling end-cap. The amic acid portion of the copolymer is then imidized by a solution imidization process^{7,8} which occurs in a cosolvent system of NMP and cyclohexylpyrrolidinone (CHP) at temperatures near 160°C, much lower than in bulk imidization. The physical properties of such multi-block polyimidesiloxane

copolymers have been examined for a number of chemical structure variations.^{5,6,117}

The polymers used in this study were synthesized from benzophenone tetracarboxylic dianhydride (BTDA), bisaniline P (Bis P) and aminopropyl-terminated polydimethylsiloxane (PDMS) oligomers of two different number average molecular weights. The siloxane oligomers had approximate number average molecular weights of 3600 grams per mole and 1500 g/mol. Target molecular weight for the polymers was 25,000 g/mol. Phthalic anhydride (PA) was used as an end-capping agent. A BTDA-Bis P-PA polyimide homopolymer with no siloxane was synthesized as a control. The polyimide control and two BTDA-Bis P-PDMS copolymers containing approximately 10 and 30 weight percent of the "3.6 K" PDMS segments were provided by Dr. Attila Gungor. A BTDA-Bis P-PDMS polyimidesiloxane copolymer containing 30 weight percent of the "1.5 K" PDMS segments was also synthesized by Tim Flynn. Figure 4 gives the general polymer structure.

3.2 SAMPLE PREPARATION

3.2.1 Capillary Column Preparation

3.2.1.1 Coating Apparatus

The apparatus used to coat the capillary columns was built in the laboratory. A schematic of the coating apparatus is given in Figure 5. A double water bath was utilized to maintain the column at a constant temperature during the final evaporation stage of coating. The double water bath consisted of an Alltech heavy glass thin-layer-chromatography vapor developing chamber placed inside a common rectangular ten-gallon fish aquarium tank. Distilled

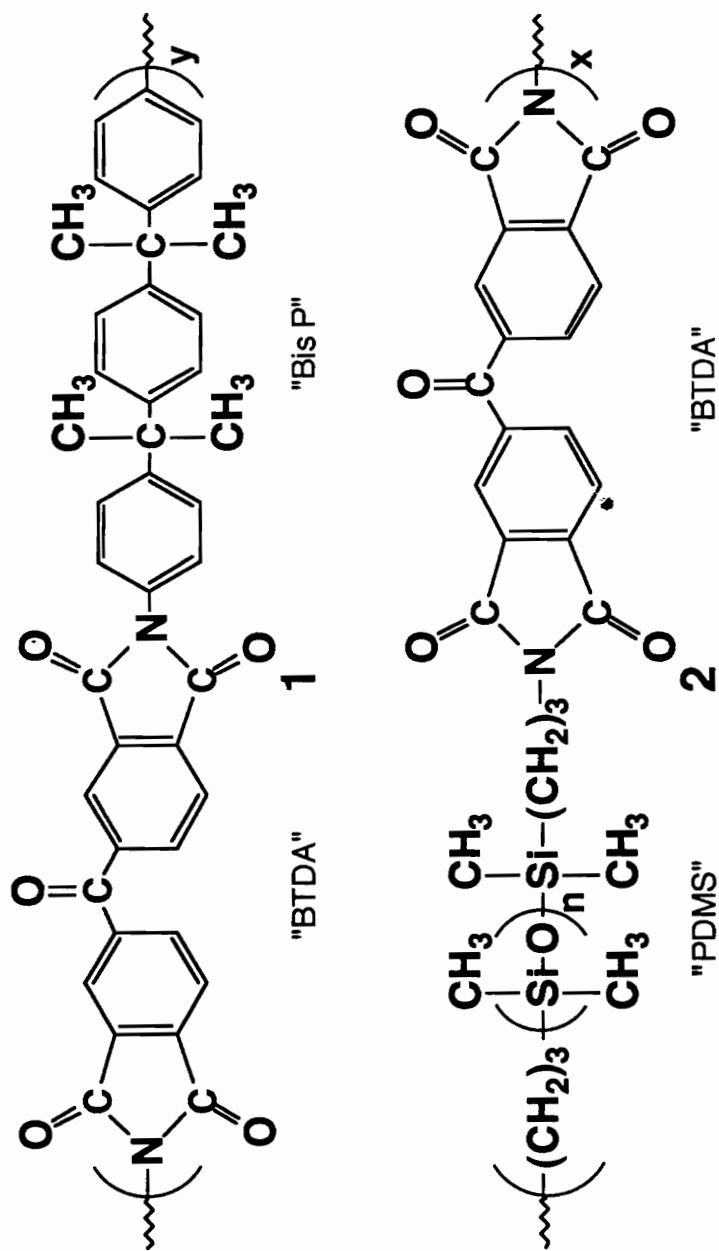


Figure 4. Structures 1 and 2 represent the blocks of the multi-block poly(imide-siloxane) copolymers. Benzophenone tetracarboxylic dianhydride (BTDA) and Bisphenol A (Bis P) form the polyimide block (1). Poly(dimethylsiloxane) preformed oligomers of given molecular weight constitute the other block (2).

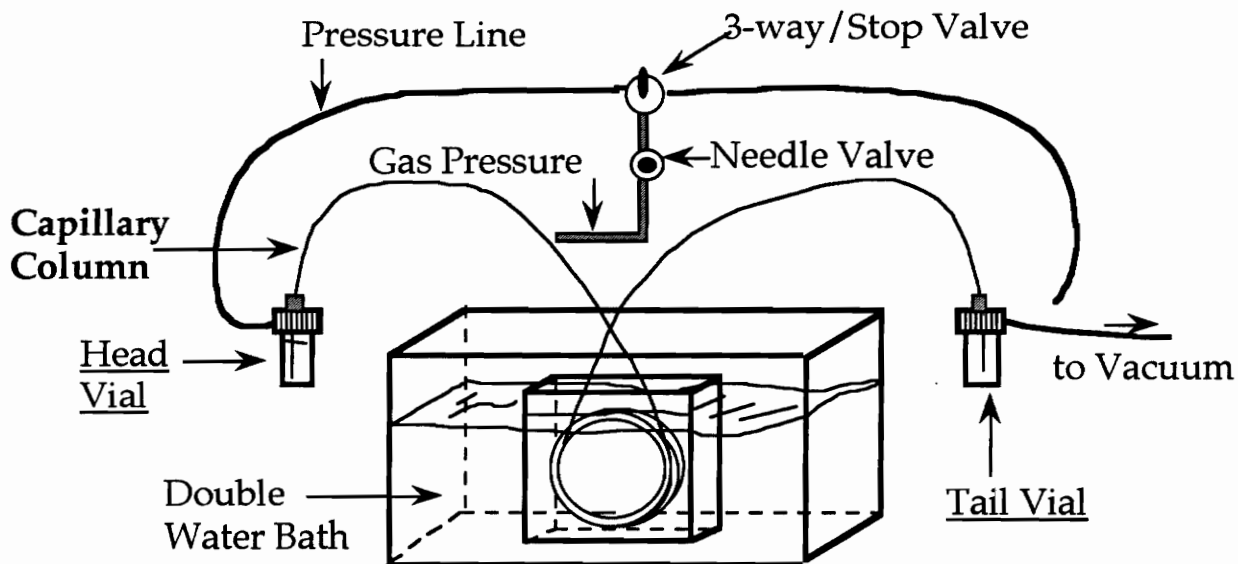


Figure 5. Schematic of the Capillary Column Coating Apparatus. Not shown in picture: mobile support system for the vials and vacuum line as well as a water bath heater with circulation pump and a copper-tubing cooling coil that were located in the outer portion of the double water bath.

water was used in the water bath. Temperature in the outer bath was controlled above ambient by a Fisher Scientific Isotemp Immersion Circulator heater Model 70. For temperatures not far below ambient, the bath temperature was controlled by a combination of the above circulating heater and a heat sink colder than the surrounding lab. The heat sink was provided by submerging into the outer bath a cooling element, which consisted of two meters of un-insulated, coiled 1/4" O.D. soft copper tubing attached by insulated tubing and the appropriate fittings to VPI&SU's pressurized Chilled Water Supply/Return. The temperature of this water supply is approximately 12°C.

Heavy-walled glass vials were obtained from Alltech and fitted with caps modified with the addition of Swagelok 1/16" stainless steel T-shaped union fittings (see Figure 6). Graphite ferrules were used against the capillary column in order to obtain a good seal. These pressurizable vials were placed at each end (head and tail) of the capillary column. Sealed vials could be pressurized by dried helium gas or depressurized by application of vacuum. Vial pressure could be made atmospheric by loosening or "opening" the cap. Pressure (or vacuum) could be applied or released as needed using the directional needle valve and tightening or loosening the appropriate caps. Pressure was utilized to push fluid located in the head vial through the column. A vacuum applied to the sealed tail vial was utilized to pull fluid located in the "open" head vial through the column. Vacuum was supplied by an ordinary vacuum pump that had a line fitted with a trap kept cold by isopropyl alcohol and dry ice.

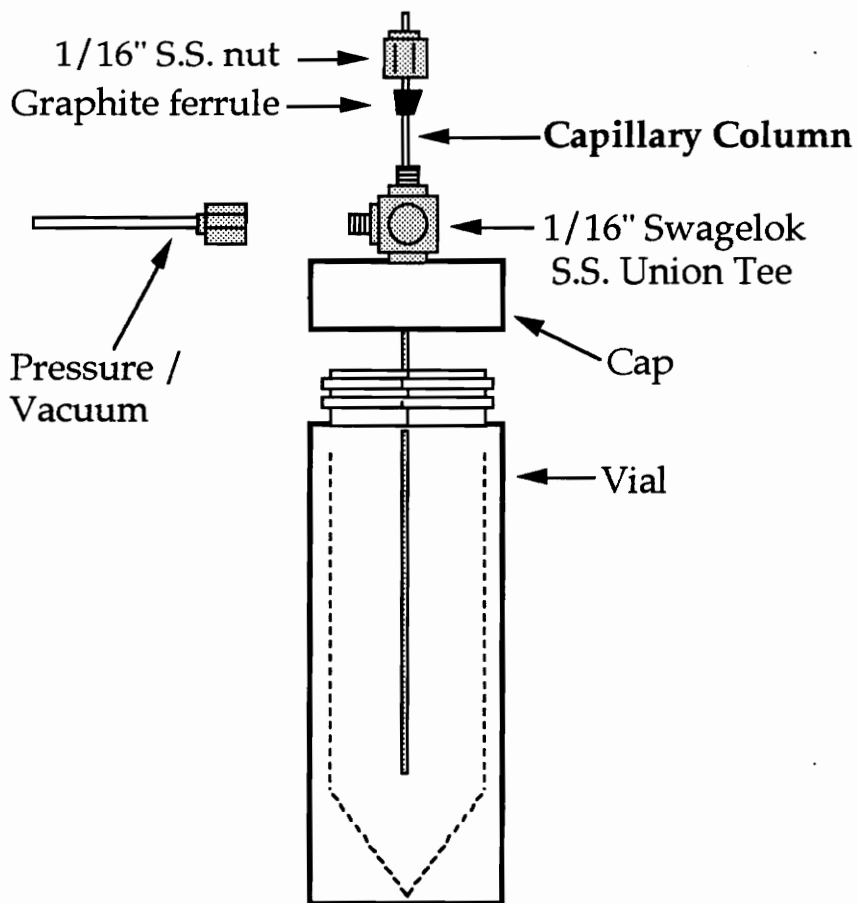


Figure 6. Detailed schematic of heavy-walled ≈ 10 milliliter pressurizable glass vial and modified vial cap. Stainless steel union tee fitting is put through a hole drilled in the cap and sealed in place with commercial epoxy.

3.2.1.2 *Coating Materials*

The polymers used to coat the columns were BTDA-BisP-PA polyimide and the two companion polyimidesiloxane copolymers containing 10 and 30 weight-percent of 3600 g/mol PDMS. Baker Analyzed Grade Methylene Chloride was the solvent used to dissolve the polymers. Tru-Value Two Ton (30-minute set) commercial epoxy and 1/50" I.D. silicone tubing obtained from Cole-Parmer were used in the end capping procedure. The columns used were 30-meter Hewlett-Packard empty, deactivated, mega-bore (0.53 mm I.D.) fused silica capillary columns that had an outer unknown-polyimide coating to increase toughness. Capillary columns were cut as necessary using the edge of an ordinary whetstone.

3.2.1.3 *Coating Procedure*

Capillary columns were successfully made using the static coating method. To summarize, this method involved filling the column with the polymer solution. One end was then sealed (capped) and the solvent was slowly removed by vacuum-aided evaporation from the open end. As the evaporation meniscus moved toward the capped end, the polymer was coated against the walls of the column in an annular film. The concentration of the polymer solution determined the final film thickness. The solvent chosen for the purpose was required to dissolve the polymer and not have a high boiling point. In order for the coating procedure to be successful, the incorporation of dissolved air or air bubbles in the polymer solution in the column or at the sealed column end was avoided. If an air bubble was present in the solution-filled column when

vacuum was applied to the open end, the bubble moved toward the vacuum and pushed the intervening polymer solution out of the column into the vacuum line.

Six columns, two of each polymer, were prepared; final experimental columns ranged in length from 45 to 60 meters and consisted of the two columns connected in series. The polymers were dissolved in methylene chloride to obtain solutions of approximately 7.5 ppt (0.75 % weight/ weight) concentration. One polyimide column was prepared using a 30 ppt solution.

Prior to beginning the coating procedure, the inside of the capillary column was washed with 5 to 7 column volumes of methylene chloride. Helium or nitrogen gas was then passed through the column until it was dry. Immediately before beginning the coating procedure, pure solvent and the polymer solution were separately filtered using a coarse glass frit and then degassed via sonication under vacuum. The solution, located in the head vial, was pulled into column under reduced pressure (low vacuum) to avoid the re-incorporation of air. This method necessarily involved the evaporation of some of the solution's solvent at the travelling meniscus where the solution was in contact with the vacuum. To minimize this evaporation at the travelling meniscus, a slug of pure solvent was pulled into the column ahead of the polymer solution so that it could protect the solution's travelling meniscus from the vacuum. Once the column was filled in this manner, however, extra solution was still pushed through the column in order to remove any possible axial concentration gradient formed at the tail end of the column by the solvent evaporation of the travelling meniscus.

Once filled, the column was sealed at the tail end using a technique adapted from C.A. Pawlisch, who gives an excellent description of capillary

column static-coating.¹²⁰ The column end-capping technique utilized the two-part room temperature epoxy mentioned above as the sealing agent. Distilled water was used as a buffer liquid between the polymer solution and the epoxy, since the methylene chloride used in the solution tended to prevent the epoxy from curing well. The distilled water was degassed prior to use by boiling it to one-fourth its volume, rapidly cooling the remainder in an ice-water bath and then sonicating it under reduced pressure. The degassed buffer water was kept cold and ready while the column was being filled with the polymer solution. As soon as the column was appropriately filled, the buffer water was then forced into the tail end of the column by means of pressurized helium. Approximately one meter in length of the column was filled with water. Care was taken not to introduce an air bubble between the polymer solution and water phases. The "30-minute-set epoxy" was mixed well and allowed to sit no more than 10 minutes from time of initial mixing. It was then drawn into one inch of a three inch length of 1/50".ID silicone tubing via an attached blunt-needled syringe. The tail end of the column was held in a downwards vertical position. A drop of the buffer water was then forced out the tail end of the column by means of a second syringe now attached to the head end of the column in place of the head vial. (This syringe provided better control than the pressurized helium in this instance.) The epoxy-filled tubing was then forced over the water droplet and the column tail end. The epoxy was pushed into the column tail end, which was then placed in a upwards vertical position. The seal was allowed to harden at least 8 hours. Please refer to Figure 7. This capping technique produced successful seals after only a few attempts.

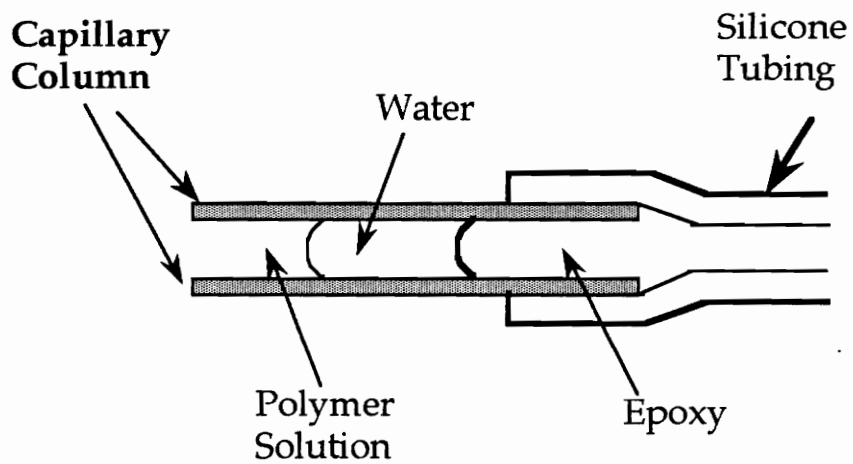


Figure 7. Schematic cut view from the side of the epoxy end-cap with water as the intervening liquid.

The capillary column, filled with the polymer solution and successfully capped, was placed in the equilibrated double water bath in order to shield it from temperature gradients during evaporation of the solvent. (Small temperature changes affect the polymer solution volume in the column and shift the position of the meniscus due to the smallness of the capillary bore which disrupts the coating process.) Vacuum was then applied to the open (head) end of the column and the meniscus moved slowly away from the vacuum and towards the capped tail end. The bath temperature for the polyimide columns was approximately 23°C. The initial coating rates for the 7.5 and 30 ppt polyimide solution columns were 2.4 and 0.1 meters per hour. The bath temperatures for the two siloxane-containing polymers were required to be slightly lower in order to proceed with coating. The 10wt%(3.6 K)PDMS copolymer columns were coated at 20°C at an initial coating rate of approximately 3.5 meter/hr. The 30wt%(3.6 K)PDMS copolymer columns were coated at 17°C at an initial coating rate of approximately 1.0 meter/hr. The copolymer columns would not coat at even slightly higher temperatures.

3.2.2 Sorption Film Preparation

3.2.2.1 Casting Materials

The polymers used were the BTDA-Bis P PA polyimide control and the 10- and 30-weight-percent (3.6 K) PDMS copolymers, mentioned previously, and a 30-weight-percent (1.5 K) PDMS copolymer, again provided by Dr. J.E. McGrath's research group. The solvents used were Fisher HPLC Grade Chloroform and Baker Analyzed Grade Methylene Chloride. The "10 X 90 mm"

Pyrex glass petri-dish bottoms were obtained from Fisher. Only the dishes that were the most flat on the bottom were used. Tests for flatness involved a general visual inspection and a counter-top spin test. Flat dishes did not spin well. Only one dish in approximately ten was acceptable enough to give good uniform thickness films. Apollo mirror-finish Chrome Ferrotypes (steel base) plates were cut to size prior to use.

3.2.2.2 *Casting Procedure*

All glassware involved in the following method were cleaned by means of solvent rinsing and a brief soak in a potassium hydroxide/isopropyl-alcohol base bath, followed by thorough rinsing with water. The glassware was then given a neutralizing rinse with nitric acid, followed again by a thorough water rinsing. Distilled water was used as a final rinse before drying. The ferrotypes plates were cleaned and degreased prior to use with a rinse of methylene chloride or chloroform.

The following procedure was used to cast films of the (3.6 K) segment siloxane-containing copolymers. Approximately one gram of copolymer was dissolved into 15 to 20 milliliters of chloroform. The polymer solution was then filtered through a coarse glass frit which had been previously "wet" with some chloroform. The solution was filtered directly into a flat glass petri-dish, in which a ferrotypes plate had been previously placed with the shiny chromium side facing upwards (see Figure 8). The petri-dish, filled with the solution, was carefully covered with a pre-formed aluminum foil cover which had numerous pin-hole size perforations. A crude cardboard enclosure was also placed around and over the petri-dish. These things were done in order to slow the rate of

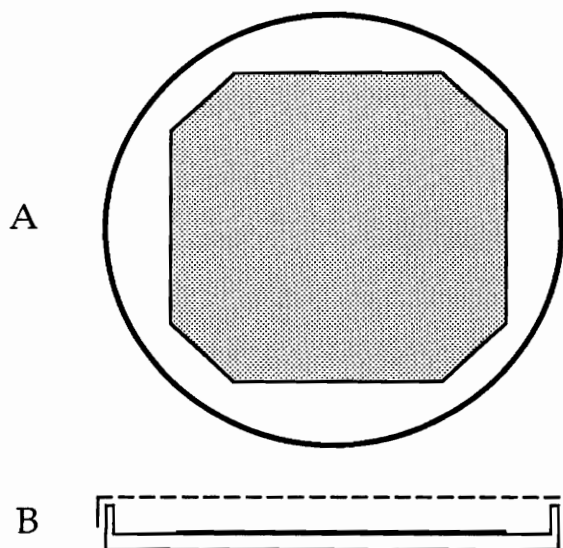


Figure 8. Schematic of arrangement of flat glass petri-dish and ferrotype plate cut to size and used in casting of siloxane-containing copolymer films. A) Top view. B) Side view of a cut through the middle, which shows also the placement of the perforated foil cover.

evaporation and also to protect the forming film from the air currents caused by the pull of the hood.

After 24 hours, the formed film was removed from the ferrotype plate. The free film was allowed to dry for 24 hours at ambient temperature. Further drying was accomplished by placing it into a Napco Model 5831 vacuum oven and heating by 30-40°C increments to approximately 215°C, the maximum oven temperature. After approximately six hours at 215°C, the heat was turned off and the oven allowed to cool to room temperature overnight. Each film was stored in separate polystyrene petri-dish with lid in a desiccator.

The same procedure was followed to cast the (1.5 K) segment siloxane-containing copolymer films as was used for the (3.6 K) segment siloxane-containing copolymers above except that methylene chloride was used as the solvent. This copolymer film was the most difficult to remove from the ferrotype plate and petri-dish; successful removal was accomplished only by shattering the bottom of the glass petri-dish. The film itself was protected from the shattering blow by the ferrotype plate.

Films of the polyimide homopolymer were cast and treated in exactly the same manner as the (3.6 K) PDMS copolymer films described above, except for one detail. It was found that casting the film against the glass of the flat petri-dish instead of the chromed surface of the ferrotype plate gave much less wrinkled films. Therefore the ferrotype plates were not employed. It was important however to remove the films from the glass surface promptly after 22-23 hours or the polyimide film would pull away fragments of the glass surface thus ruining the film and the petri-dish's flatness. The lower adhesion to the

glass at earlier times is thought to be the result of a small amount of solvent still remaining at the interface.

Prior to sorption, the cast films were given final heat treatments in order to try to remove remaining traces of solvent and also to fully relax any stresses in the films resulting from the solvent casting. The two treatments were quenching from well above the glass transition temperature and aging just below T_g . A Fisher Scientific Isotemp Programmable Model 838F forced air convection oven was utilized to accomplish the thermal treatments. The sample film was placed on a flat Teflon sheet at the bottom of a high-sided crystallizing dish, which was then placed in the ambient temperature oven. The oven was then ramped at $10^\circ\text{C}/\text{min}$ to either 275°C for the copolymers or 280°C for the polyimide homopolymer. This is 30°C above T_g for the (3.6 K) PDMS copolymers and 50°C above T_g of the (1.5 K) PDMS copolymer. Heating to approximately 30°C above T_g for the polyimide (to 295°C) tended to turn the film from yellow to brown, whereas the yellow color of the copolymer films did not change on heating. The polyimide film's maximum temperature was therefore lowered to 280°C . A given film was held at its maximum temperature for 2 to 2.5 hours. The quenching of the film involved quickly removing it from the oven at this time and placing it (and the Teflon sheet) on the counter top at room temperature--causing it to cool very rapidly. In the aging treatment, after the film had been held above its T_g for 2 to 2.5 hours, the oven temperature was ramped down at approximately $10^\circ\text{C}/\text{min}$ to a temperature 5°C below the T_g and then held constant for 24 hours. The film was then rapidly cooled from $T_g-5^\circ\text{C}$ to room temperature by removing it from the oven and placing it on the counter top. The

circular polyimide films showed noticeable radial shrinkage and an apparent increase in thickness upon thermal treatment.

3.3 INSTRUMENTAL

3.3.1 General Polymer Characterization

3.3.1.1 *Surface Characterization*

Scanning electron micrographs of the capillary column features were obtained using an ISI SX 40 scanning electron microscope with an acceleration voltage of 10 kV. Small sections of capillary column were attached to sample mounts by means of double stick tape. The samples were then sputter coated with gold for two minutes. Attempts to view inside the columns required an almost 90° rotation of the sample holder. Difficulties involving charging of the surface were occasionally encountered perhaps due to inadequate gold sputtering on the inside of the columns.

XPS data was obtained using a 5400 Perkin Elmer x-ray photoelectron spectrometer. It was operated in a fixed analyzer mode using Mg $K\alpha_{1,2}$ x-ray radiation (400 W, 15 kV, 1253.6 eV). Data was collected using three orientations of the sample holder: 15°, 45° and 90°. The collecting time for each element was five minutes. Samples consisted of copolymers spin-coated onto ferrotype plates. The copolymers had been cast from methylene chloride and dried under a flow of nitrogen.

Contact angle measurements were performing using a Ramé-Hart goniometer with a vapor chamber attachment. The small troughs inside the enclosed vapor chamber were filled with the liquid used for the contact angle measurements several minutes prior to the actual measurement. Liquids used

for contact angle measurements were distilled de-ionized water, formamide and diiodomethane. The formamide and diiodomethane were obtained from Aldrich and were 99% pure. The diiodomethane was stored in a manner to protect it from light. Polymer films were spin-cast from methylene chloride onto small ferrotype plates. Cast films were allowed to dry at ambient temperature for 2 hours and were then dried at 100°C in foil covered clean beakers inside the GC oven.

3.3.1.2 *Gel Permeation Chromatography*

Gel permeation chromatography was performed utilizing a Waters 150-C ALC/GPC fitted with a Chromatrix KMX-6 low angle laser light scatterer and a Viscotek differential viscometer. Universal calibration and polystyrene standards were used. The solvent was N-methylpyrrolidinone (NMP). It was necessary to filter some copolymer solution samples prior to the experiment.

3.3.1.3 *Bulk Characterization*

Thermal analysis was performed using a Perkin-Elmer TGA 7 Thermogravimetric Analyzer and a Perkin-Elmer DSC 7 Differential Scanning Calorimeter. A Digital DECstation 325c computer with Perkin-Elmer Thermal Analysis Version 2.00 software was used to control the instruments as well as to collect and analyze the data. All TGA experiments were performed in a flowing air environment at a heating rate of 10°C per minute from 30°C to 850-900°C. DSC experiments were performed using Polymer Laboratories aluminum DSC pans and at a heating rate of 10°C per minute from 30-50°C to 300°C. Baselines, automatically subtracted from sample runs, were performed the same day using the same type of PL pans.

Dynamic mechanical thermal analysis was accomplished using a Polymer Laboratories Dynamic Mechanical Thermal Analyzer DMTA. The automatic system was controlled by a Hewlett-Packard 9153C Computer with the appropriate Polymer Laboratories software. Subambient to above-ambient temperature scans were run at 2.5°C per minute at frequencies of 1, 5 and 10 Hz with a maximum displacement of 40 microns.

3.3.2 Inverse Gas Chromatography

The IGC surface studies were performed using a Hewlett-Packard 5890 Series II Gas Chromatograph, which was equipped with a Series II Thermal Conductivity Detector cell suitable for use with capillary columns. Prior to the collection of data, the columns were conditioned at 110°C under constant flow of helium gas. The conditioning lasted for at least 24 hours or until a stable baseline with a threshold of zero or below was obtained. The experimental data from the chromatographic analyses was plotted and analyzed by an HP 3396A Integrator linked to the gas chromatograph. Injections of probe vapor (with nitrogen as a non-adsorbing marker) into the columns were accomplished with an HP 19395A Headspace Sampler. The carrier gas and approximate column flow rate used in all analyses were, respectively, dry helium and 5 ml/min. The capillary split ratio was approximately 1/20. The probes used in this study were distilled water and the homologous series of n-alkanes from nonane to dodecane. All n-alkanes were from Aldrich Chemical Company, Inc. in the 99% or 99+% pure state.

3.3.3 Gravimetric Sorption

The sorption of water into the sample films upon exposure to water vapor was determined gravimetrically. The instrumentation utilized for this

experiment is shown schematically in Figure 9. A Perkin-Elmer TGS-2 Thermogravimetric System analyzer was fitted with a lengthened sample hook and a sample chamber through which either dry or humid air could be passed. The sample chamber was heated to just above room temperature by means of an exterior wrap of thermal tape regulated by a Variac resistor. The temperatures in the wrap insulation and inside the bottom of the sample chamber were monitored using an Omega 871 Digital Thermometer and Type K (NiCr-NiAl) thermocouples. The temperature inside the sample chamber was found to be about 2°C less than the outer wrap temperature. During the initial testing of the apparatus, it was also noted that the inner sample chamber temperature did not change significantly upon switching from a flow of dry air (0% humidity) to a flow of humidified air. The average inner sample chamber temperature over all runs was 32 ± 4 °C. The mouth of the sample chamber limited the maximum width of the thin rectangularly-cut sample films to approximately 2 centimeters. Lengths varied between 5 and 6 cm.

An air flow of controlled humidity was introduced into the sample chamber in the following manner. A cylinder of compressed breathing air was used as an "infinite" source of dry air flow through the tubing system and sample chamber, with the outlet of the tubing at atmospheric pressure. The air pressure was reduced to approximately 4 psi by means of the air tank pressure gauge. The air was passed through an Alltech Associates Gas Purifier containing indicating drierite and molecular sieves prior to entering a needle valve flowmeter with steel and glass floating balls. The flowmeter was adjusted so that the flowrate would approximately be 100 ml/min at the open system's outlet; the steel ball of the flowmeter would come to rest near 80 on the flowmeter scale for these

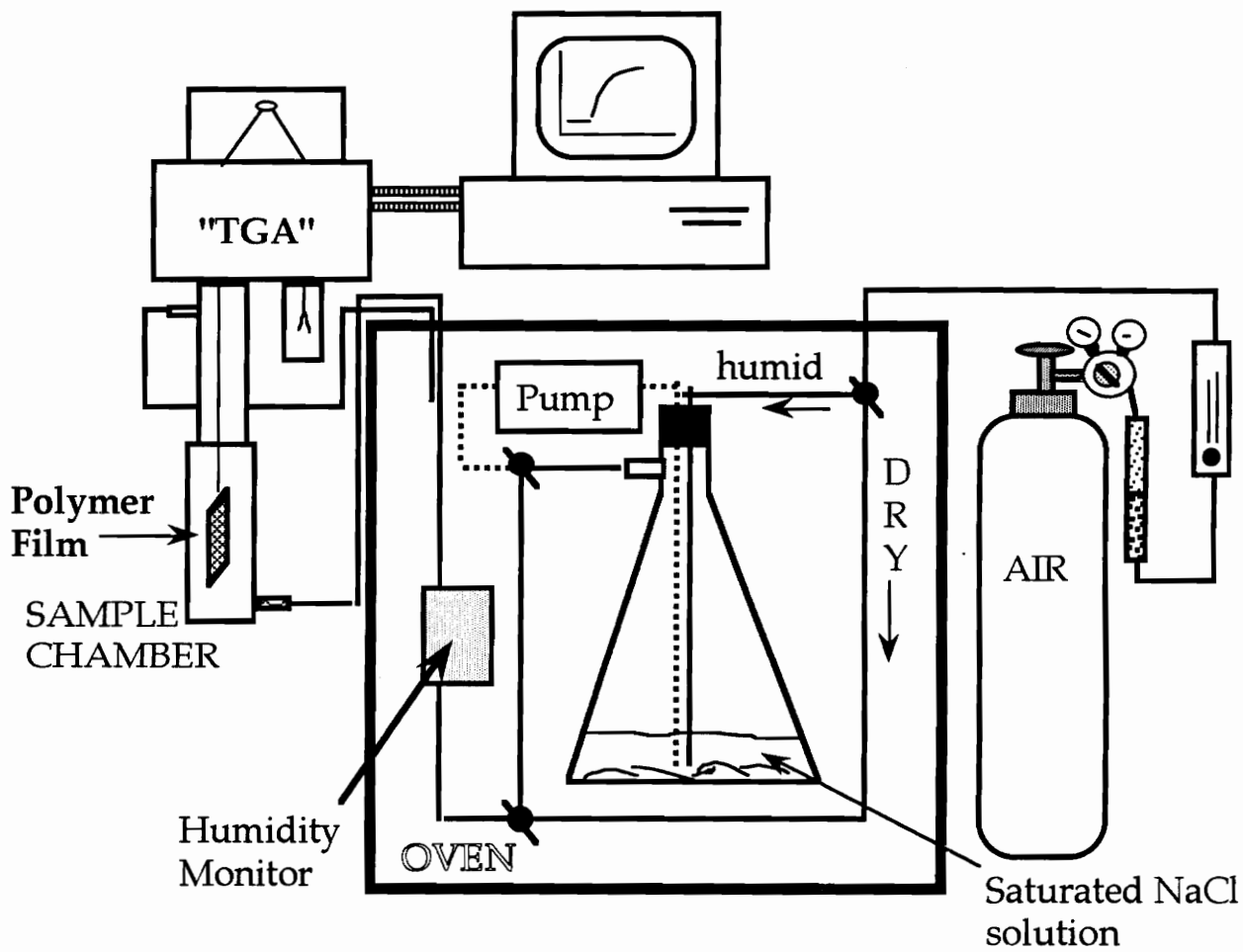


Figure 9. Schematic of the apparatus used in sorption experiments. Closed flow path used to equilibrate humidity inside salt solution chamber is indicated by the dotted line.

conditions. The average volumetric flow rate measured under these conditions was 100 ± 7 ml/min.

The air flow could be routed one of two directions. The dry air from the tank could be routed directly to the sample chamber or it could be diverted first into a humidifying chamber containing a saturated sodium chloride salt/distilled water solution. In order to have a properly controlled humidity, precautions were taken. The salt solution chamber was placed in an oven, whose temperature was controlled by means of a Variac. To insure that the salt solution was truly saturated it was stirred and heated to a temperature above its use temperature before it was allowed to cool to the oven temperature; it was found that the presence of undissolved salt was a necessary but not sufficient indicator of saturation. The dry air entering the salt solution chamber was passed through the liquid of the saturated solution in order to maximize the humidifying contact. The tubing which bridged the gap between the oven and the sample chamber was made as short as possible and was insulated using foam pipe insulation to prevent condensation due to temperature changes. Ideally, the entire sorption apparatus should have been placed inside a controlled temperature environment, but no available oven was large enough to house the thermal gravimetric analyzer.

Humidity was monitored by means of a Dickson Temperature/Humidity Meter. The humidity monitor probe was located in a small volume chamber immediately before the tubing exited the oven. The probe tip was placed in the chamber such that it was shielded from direct flow path of the air. In order to maximize the rate of initial increase in humidity, a large, 6 liter vacuum flask was utilized as the saturated salt solution chamber. The salt solution chamber was

connected in a separate closed loop to an aquarium air pump, so that the controlled humidity could be built up and equilibrated prior to the introduction of the dry air into the solution chamber. Using the large flask as a humidity reservoir was found to maximize the rate of humidity increase for this system. The jump in humidity was not instantaneous (as required by theory) but took a minimum of approximately two minutes to approach maximum.

The average temperature of the oven was 25 ± 3 °C and the average relative humidity provided by the NaCl salt solution at this temperature was 82 ± 2 percent. As a failsafe measure against possible condensation in the bridging tubing, the sample chamber temperature was kept at a slightly higher temperature of about 32°C. Relative humidity is defined as the ratio of the quantity of water vapor present in the air to the quantity that would saturate the air at the given temperature.¹²¹ The relative humidity inside the sample chamber was estimated using the known average humidity at 25°C and the definition of relative humidity by the following equation:

$$H_{\text{sample},32^{\circ}\text{C}} = \frac{X_{25^{\circ}\text{C}} * H_{\text{oven},25^{\circ}\text{C}}}{X_{32^{\circ}\text{C}}} \quad (34)$$

where X is the weight in grams of a cubic meter of saturated water vapor at the indicated temperature of the oven and the sample chamber. The calculation was also done with X as vapor pressures of water at the given temperatures. From both calculations, the relative humidity inside the sample chamber was approximately 55 percent. Literature values for X were obtained from tables in the CRC Chemistry and Physics Handbook.¹²¹ Data was collected using a

Gateway 2000 386/25 computer and a data collection program written by H. Francis Webster. Humidity and sample weight data were averaged and collected at a rate of one saved data point each minute.

4. GENERAL POLYMER CHARACTERIZATION: Results and Discussion

4.1 SURFACE CHARACTERIZATION

4.1.1 x-ray Photoelectron Spectroscopy

Atomic concentration XPS data was collected on the three siloxane-containing copolymers used in the present research. Data on silicon and nitrogen was used to distinguish between the siloxane and imide blocks. Weight percent siloxane present is listed as a function of sampling depth in Table 3, with the 15° take-off angle being the most shallow sampling depth ($\approx 10\text{-}20 \text{ \AA}$). The 90° take-off angle samples at depths of approximately 70 to 100 \AA . The results show a gradient of siloxane concentration. A larger percentage of siloxane is at the surface of the polymer than would be expected for the weight percent incorporated. This enrichment of the surface has been seen previously in siloxane-containing polyimide and other polymers.^{2,117,122-127} The lower surface free energy of the PDMS block drives it toward the surface of the phase-separated polymer.

4.1.2 Contact Angle Measurements and Calculations

Contact angle measurements were done on the polyimide control and the two (3.6 K) PDMS containing copolymers. Diiodomethane contact angles were only measured on the polyimide. Contact angles were also calculated for the polyimide using an additive method.¹²⁸ (No additive increment for the molar volume of an imide linkage was available for the calculation, so the molar volume of an amide linkage was substituted as a best approximation.) All values

Table 3. Weight percent PDMS at and near copolymer surfaces as determined from x-ray photoelectron spectroscopy.

Copolymer	Take-off angle		
	<u>15°</u>	<u>45°</u>	<u>90°</u>
10 wt% (3.6K) PDMS	76	51	45
30 wt% (3.6K) PDMS	100	97	85
30 wt% (1.5K) PDMS	76	61	48

Table 4. Measured and calculated contact angles. Standard deviations determined from experiments on a minimum of four droplets.

	H ₂ O	HCONH ₂ [‡]	CH ₂ I ₂ ^{‡‡}
Polyimide Control	75 ± 2	59 ± 2	41 ± 3
Polyimide Control*	78*	58*	39*
10 wt% (3.6K) PDMS	99 ± 3	92 ± 3	nd**
30 wt% (3.6K) PDMS	103 ± 3	96 ± 5	nd**

[‡] Formamide

^{‡‡} Diiodomethane or Methylene Iodide

* calculated values

** not determined

are listed in Table 4. The contact angles for the siloxane-containing polymers are higher than those of the polyimide, suggesting the presence of non-polar siloxane at the surface. The water contact angles on the copolymers are a little lower than the reported water contact angle value of 110° for pure PDMS.¹²⁹ The calculated contact angles of the liquids on the polyimide are in good agreement with the measured contact angles.

The solid surface free energy of the polyimide was estimated using the experimentally determined contact angles and the polar and dispersive components of the surface tensions of the utilized liquids. According to Owens and Wendt,¹³⁰ the contact angle of a liquid on a solid surface can be related to the polar and dispersive components of the surface free energies of the liquid and the solid in the following manner:

$$\frac{\gamma_l}{2}(1 + \cos \theta) = \sqrt{\gamma_s^d} \sqrt{\gamma_l^d} + \sqrt{\gamma_s^p} \sqrt{\gamma_l^p} \quad (35)$$

where γ_l is the surface tension of the measurement liquid and γ_l^p and γ_l^d are the polar and dispersive components of the liquid surface tension, which are obtained from the literature.^{128,129} The values of total, dispersive and polar liquid surface energies used in the calculations are listed in Table 5. Theta is the contact angle. If contact angles are determined for two different liquids, then there are two equations for two unknowns and the polar, γ_s^p , and dispersive, γ_s^d , components of the solid surface free energy are solvable. The dispersive component of the polyimide surface was determined by solving the above equation for the three combination pairs of the liquids formamide,

Table 5. Listing (in units of mJ/m^2) of surface tensions and dispersive and polar components of the surface tensions for the liquids used to determine contact angles against sample polymer films.^{128,130}

	H ₂ O	HCONH ₂	CH ₂ I ₂
γ_1	72.8	58.2	50.8
γ_1^d	21.8	39.5	49.5
γ_1^p	51	19	1.3

Table 6. Listing of the dispersive components of the solid surface free energy of the polyimide control as determined from the different pairs of liquids.

	γ_s^d
H ₂ O & CH ₂ I ₂	34.9
H ₂ O & HCONH ₂	22.4
CH ₂ I ₂ & HCONH ₂	37.3

diiodomethane and water. The values obtained for each pair are listed in Table 6. The variation can be due to a couple of factors, one of which is the validity of the dispersive and polar components of the liquids. This theory assumes that polar forces across the interface can be described adequately by a geometric mean term, which may not always be a good assumption due to the directionality of polar forces. Formamide also has rather a large error associated with the separated components of surface tension.¹²⁸ The best estimate is probably that given by the diiodomethane and water pair, which gives a solid dispersive component of 34.9 mJ/m².

4.2 GEL PERMEATION CHROMATOGRAPHY

Gel permeation chromatography was performed on the above polymers using NMP as the chromatographic solvent. Both the polyimide control and the BTDA-Bis P-30-wt% (1.5 K) PDMS copolymer were completely soluble in the solvent. The 10- and 30-weight-percent (3.6 K) PDMS copolymer solutions were, however, slightly cloudy and had to be filtered prior to the GPC experiment, which may have had an effect on the results. The GPC viscosity chromatograms of all the polymers are shown in Figure 10. These reveal no evidence of homopolymer contamination in the copolymers; the small peaks to the right are "solvent peaks." The intrinsic viscosity of the polyimide homopolymer was found to be 0.54 dL/g, indicating a high molecular weight was attained during polymerization. The number average molecular weight was determined to be 2.46×10^4 g/mol and the polydispersity was 2.5. An exact molecular weight determination of randomly segmented copolymers by GPC is perhaps less reliable due to a lack of predictable correlation between a multi-component

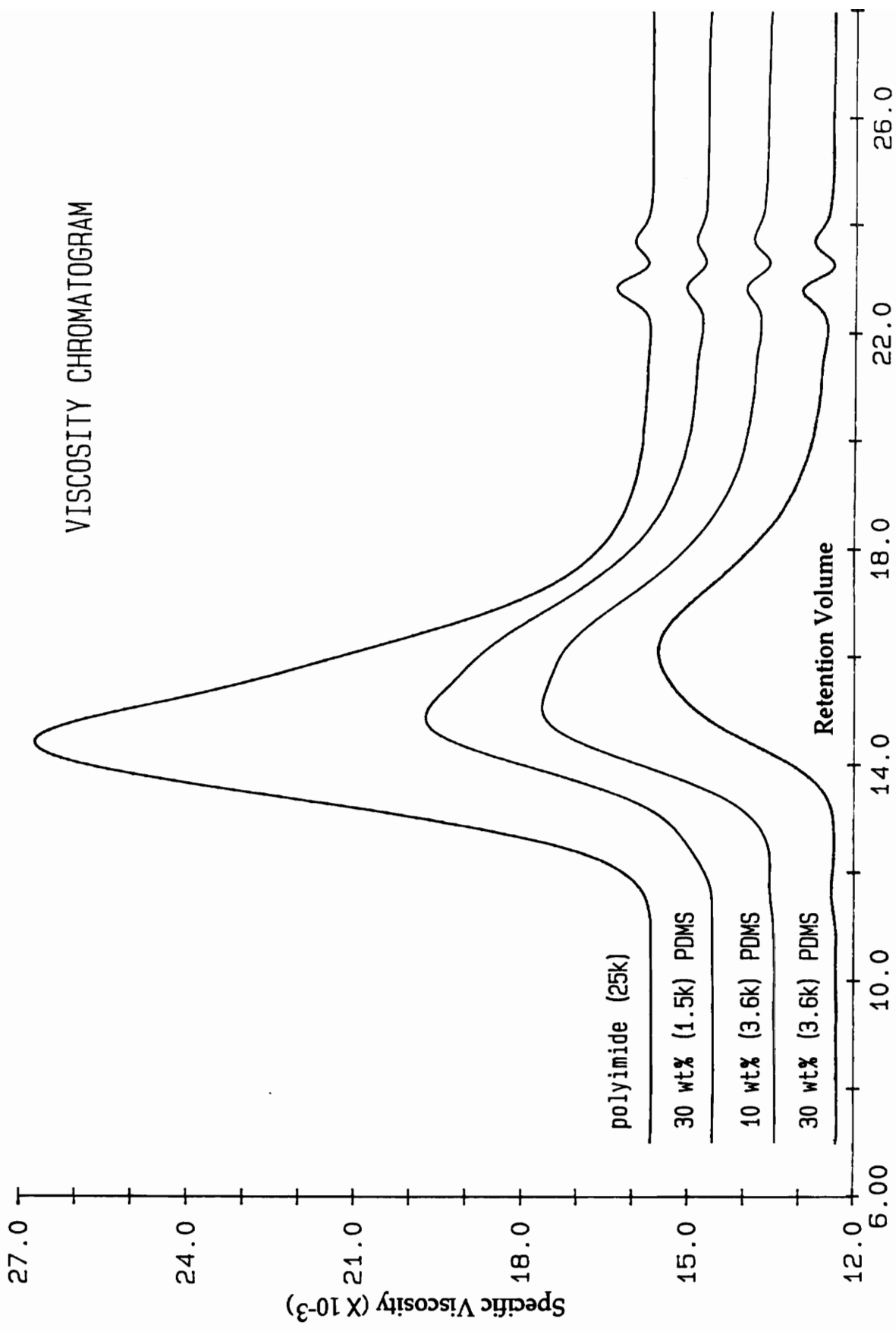


Figure 10. GPC elution traces for polyimide and the siloxane-containing copolymers.

chain's molecular weight and its hydrodynamic volume in a given solvent. GPC is size exclusion chromatography which separates on the basis of the size of the solvated polymer molecule. The intrinsic viscosities of the 10- and 30-weight-percent (3.6 K) PDMS and 30-weight-percent (1.5 K) PDMS copolymers were 0.28, 0.20, and 0.31 dL/g, respectively. The reduction in intrinsic viscosity and the increase in the retention volume of the copolymers compared to the homopolymer may in part be due to the flexibility of the siloxane segments allowing for a more compact hydrodynamic volume.

4.3 BULK CHARACTERIZATION

4.3.1 Thermal Gravimetric Analysis

Thermal gravimetric analysis was performed on the films prepared for the sorption experiments. The films used had been cast from solvent, dried and quenched from well above the glass transition temperature, T_g , as described in the Experimental. The TGA traces for the polymers are shown in Figure 11. No appreciable weight loss occurred near the polymer glass transition temperatures, indicating solvent removal. Initial weight loss is less than one percent and occurs below 100°C, which suggests the loss of adsorbed surface water. This was confirmed using the 30-weight-percent (3.6 K) PDMS copolymer, which was taken to 275°C in the TGA and held for about a half hour. Upon re-exposure of the sample in the TGA pan to the lab atmosphere for 20 minutes, the water was re-adsorbed. Upon re-ramping the copolymer to past 275°C, the loss followed the previous trace. This is shown in Figure 12.

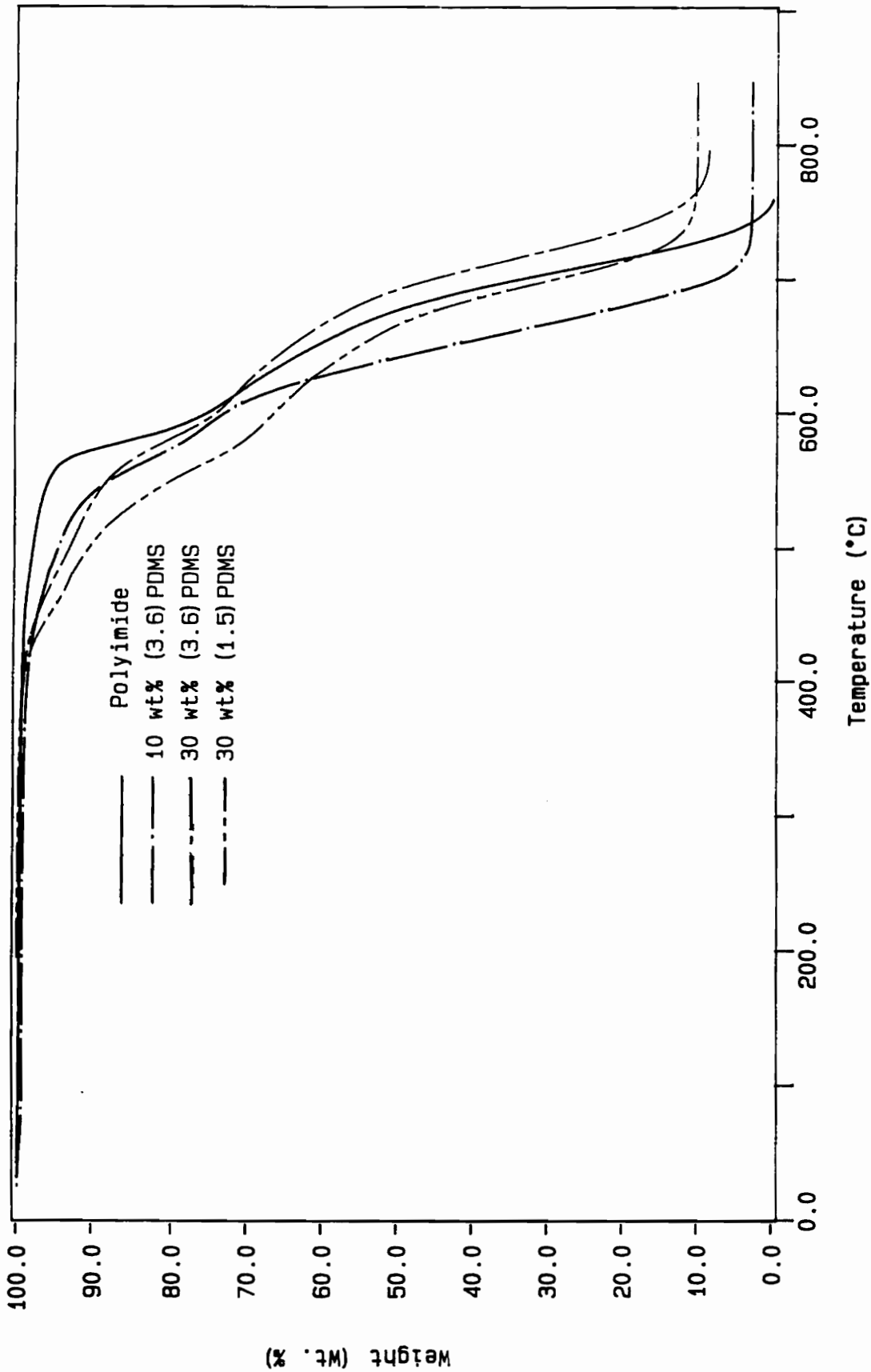


Figure 11. TGA weight percent loss in air of polyimide and polyimidesiloxane copolymers.

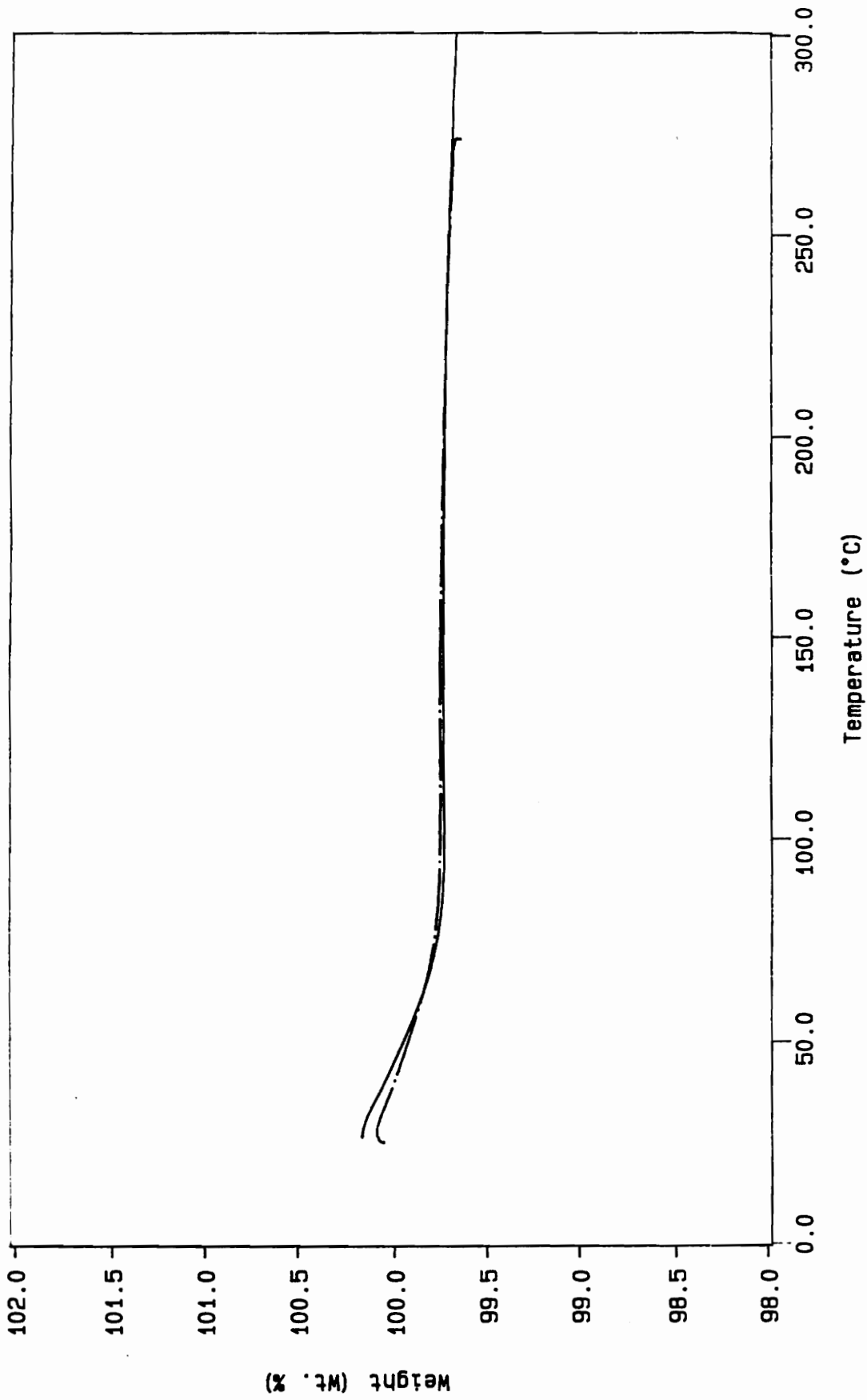


Figure 12 30wt%(3.6K)PDMS TGA in air, run twice with intermediate ambient humidity exposure.

4.3.2 Dynamic Mechanical Thermal Analysis

Dynamic mechanical thermal analysis of the films prepared for the sorption experiment revealed more than one transition temperature evident in the drop of the storage modulus. (Figures 13, 14, 15) This confirmed the existence of microphase separation in the copolymers. A statistically random copolymer exhibits a single glass transition which falls between the two components' homopolymer T_g s. A block copolymer will exhibit two T_g s near the homopolymers' T_g s, if it microphase separates.¹³¹ Microphase separation is generally dependent on a combination of three factors: the dissimilarity of the chemical structures of the components, the molecular weight of the blocks, and the crystallizability of the components. The multi-block copolymers used in this study were expected to exhibit microphase separation. The chemical structures of the imide-block and the siloxane-block are extremely different. The solubility parameters are also not close. The parameter, δ , for the polyimide homopolymer was calculated to be approximately $13.1 \text{ (cal/cm}^3)^{1/2}$ using Van Krevelen's listing of Fedor's table of additive properties of cohesive energy and molar volume.¹²⁸ Polydimethylsiloxane's solubility parameter has been reported in the range $7.3\text{--}7.5 \text{ (cal/cm}^3)^{1/2}$. (Reference 131, pp. 406 and 420.) Such chemical dissimilarity promotes separation even when lengths of PDMS are relatively short. Domain formation of size 30 \AA has been reported for BTDA-DDS-20 wt% (2.0 K) PDMS copolymers, where DDS stands for 3,3'-diaminodiphenylsulfone.¹³² So it is not surprising that the polyimidesiloxanes in this study have the characteristics of microphase separation. In addition to the two transitions near the homopolymer values, there appears a third transition

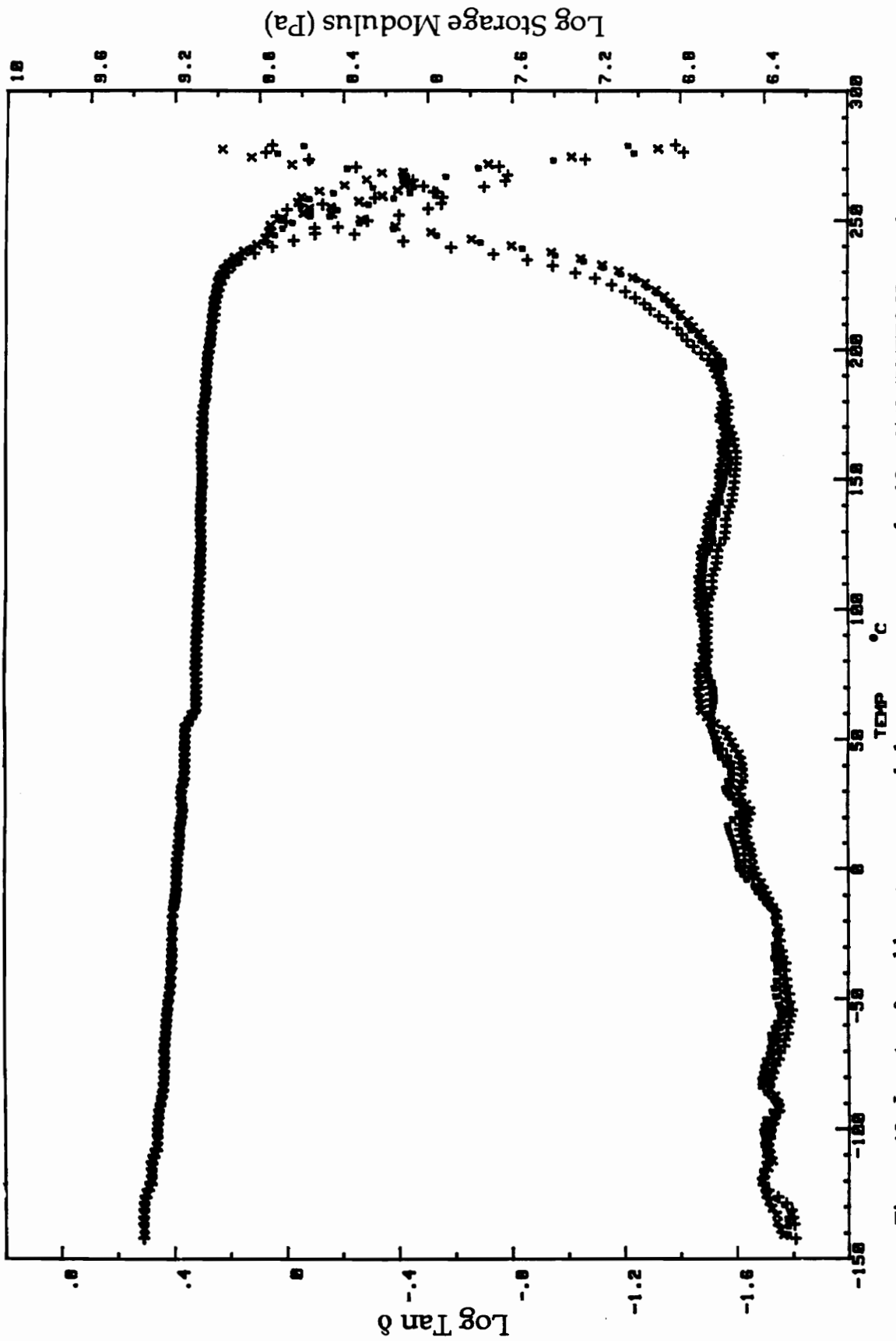


Figure 13. Log tan δ and log storage modulus vs. temperature for 10wt%(3.6K)PDMS copolymer.

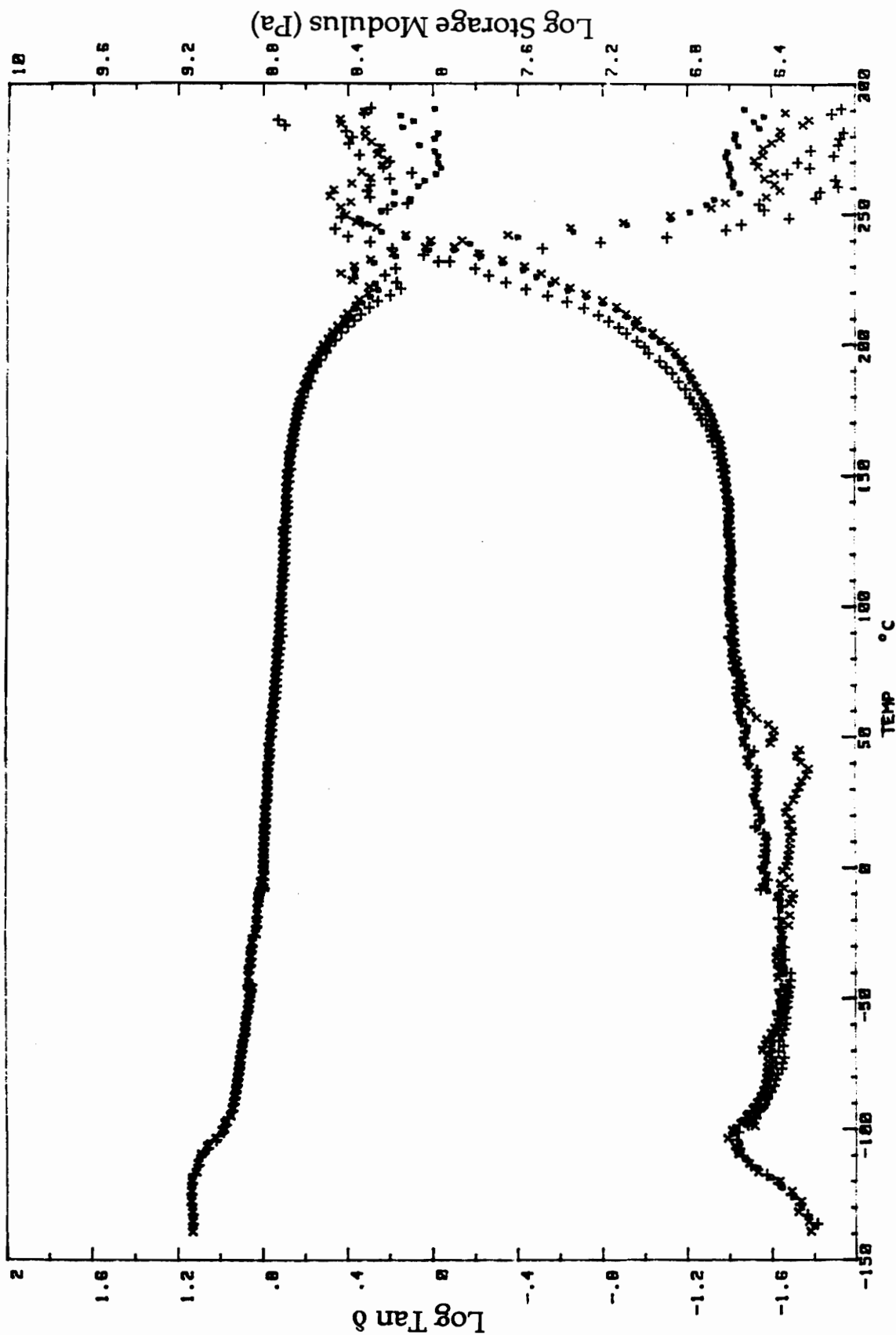


Figure 14. Log tan δ and log storage modulus vs. temperature for 30wt%(3.6K)PDMS copolymer.

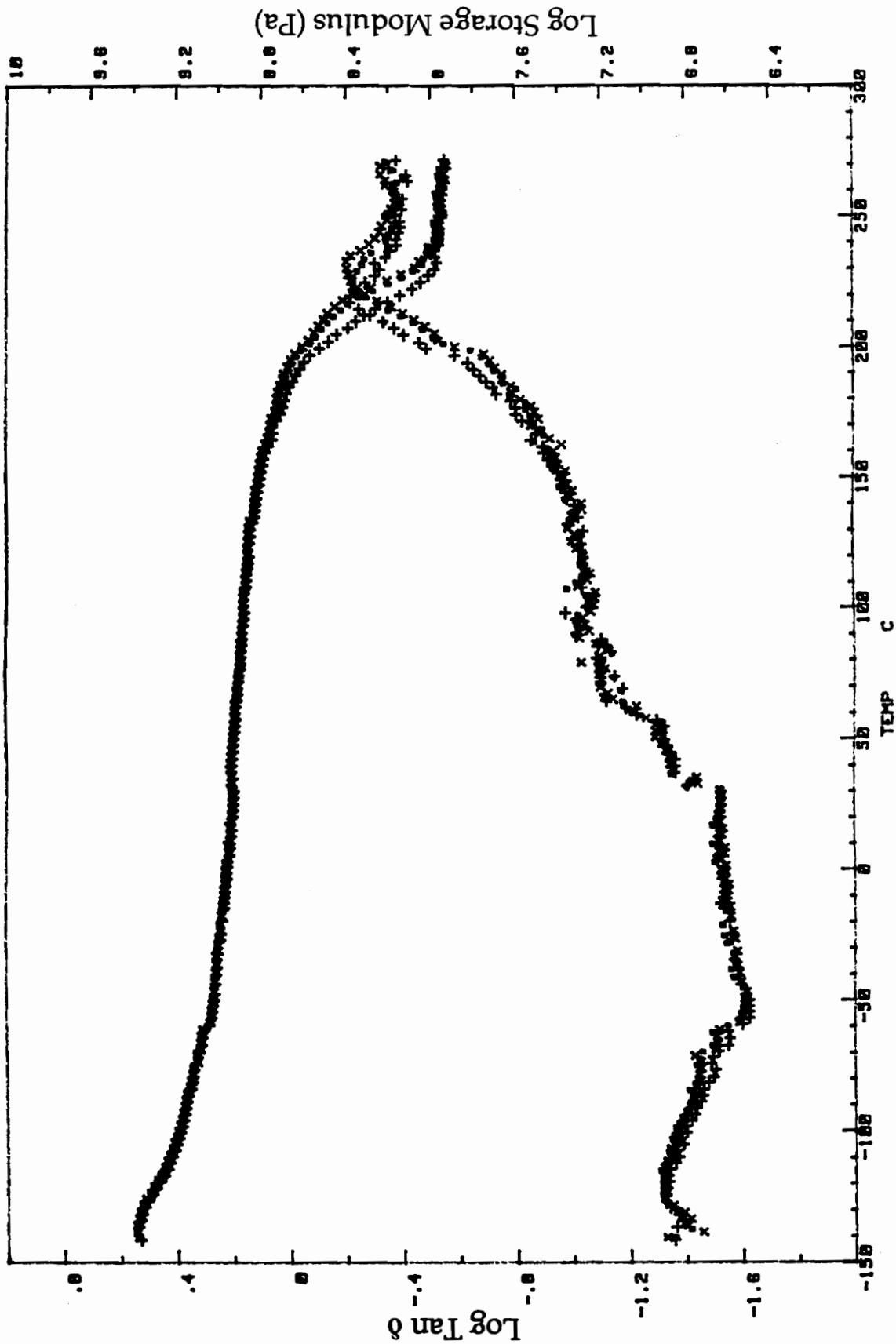


Figure 15. Log tan δ and log storage modulus vs. temperature for 30wt%(1.5K)PDMS copolymer.

between the other two, especially prominent in the $\tan \delta$ (damping) trace for the 30-weight-percent (1.5 K) PDMS copolymer. This can indicate some partial microphase separation where the interface between the domains is diffuse.¹³³ The (1.5 K) copolymer has shorter siloxane blocks. Incorporating a given weight percent of siloxane into a copolymer using shorter blocks requires that a larger number of covalent bonds be made connecting dissimilar blocks. The larger is the number of covalent links between the two blocks, the more difficult it becomes to place these bonds at a "sharp" interface between the two domains. These bonds are a structural contribution toward entropy or disorder and cause a diffuse interface.

4.3.3 Differential Scanning Calorimetry

It was difficult to detect the low temperature siloxane glass transition by differential scanning calorimetry of these copolymers. Upper glass transition temperatures corresponding to the imide block were determined by DSC and are listed in Table 7. The T_g s of the microphase-separated domains will not be affected by changes in composition as long as block lengths are of sufficient molecular weight.¹³¹ The T_g s of the copolymers in this study obviously show a dependence on composition. This involves a molecular weight dependence of the T_g which can be compared to the dependence of homopolymer T_g s on molecular weight below a plateau or entanglement weight. This dependency has been observed for poly(bisphenol A carbonate-dimethylsiloxane) microphase-separated multi-block copolymers.¹³⁴ The polycarbonate T_g depended on the molecular weight or length of its component block; the T_g decreased with decreasing block length. The siloxane segments were considered to be so flexible

Table 7. Upper glass transition temperatures (in °C) determined by DSC of polymer films cast from chloroform and methylene chloride. Methylene chloride cast films were dried at $\approx 215^\circ\text{C}$ in vacuum oven. Chloroform films were vacuum oven dried, quenched from above T_g , and had been previously water vapor sorbed/desorbed.

	CH_2Cl_2	CHCl_3
Polyimide Control	263	260
10 wt% (3.6K) PDMS	246	244
30 wt% (3.6K) PDMS	228	228
30 wt% (1.5K) PDMS	220	na*

*not applicable

that they did not constrain the polycarbonate chains so that the carbonate component could imitate homopolymer properties. The decrease in upper T_g for increasing siloxane content is therefore likely to be due to a decrease in the number average molecular weight of the polyimide block--similar to the polycarbonate-siloxane copolymers. For the (3.6 K) PDMS containing copolymers, the increase from 10 to 30 weight percent must entail the incorporation of more PDMS blocks on average into a given multi-block copolymer chain. The average length of the imide block must decrease, and the T_g decreases as well. The T_g of the 30-weight-percent (1.5 K) PDMS copolymer is decreased relative to the T_g of the 30-weight-percent (3.6 K) PDMS copolymer. A greater number of PDMS segments of weight 1.5 K must be in the chain to reach a 30-weight-percent incorporation, thus further decreasing the probable imide block length.

5. INVERSE GAS CHROMATOGRAPHY SURFACE ENERGETICS

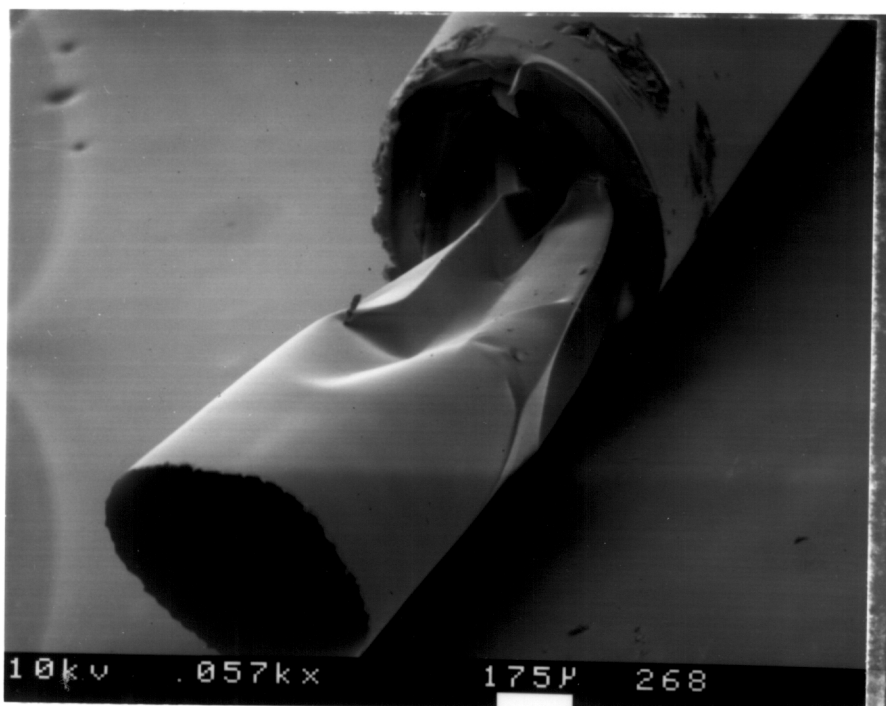
5.1 COMMENTS

Inverse Gas Chromatography was utilized to examine the interaction of water vapor with the solid polymer and copolymer surfaces by determining the free energies of specific interaction, ΔG_{sp}° . Dispersive components were determined from the interaction with a homologous series of normal alkanes. The results are presented and discussed below. The capillary column quality and the applicability of the infinite-dilution based theory to this research is also briefly addressed.

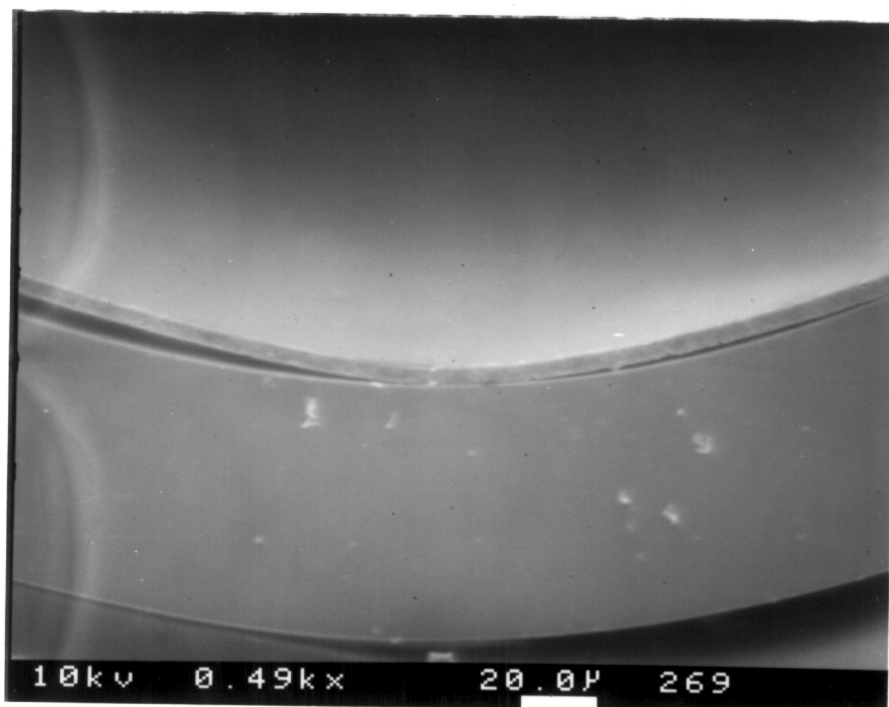
5.2 IGC RESULTS AND DISCUSSION

5.2.1 Capillary Columns

Capillary columns coated by the static coating method with 7.5 ppt polymer solutions had film thicknesses of approximately one micrometer. The 30 ppt polyimide solution gave a column with a film thickness of approximately 4 micrometers. Film thicknesses were estimated using Scanning Electron Microscopy. Figures 16 A&B and 17 A&B are some SEM pictures of the coated columns. The thick film polyimide column had a very uniform coating. The siloxane-containing polymers had non-uniform shallow dimples or patches which suggested phase-separation. The thin-film columns exhibited to varying degrees a film deformity consisting of a series of circumferential ridges along the length of the annular film. This is shown in Figure 17 B. A discussion of the

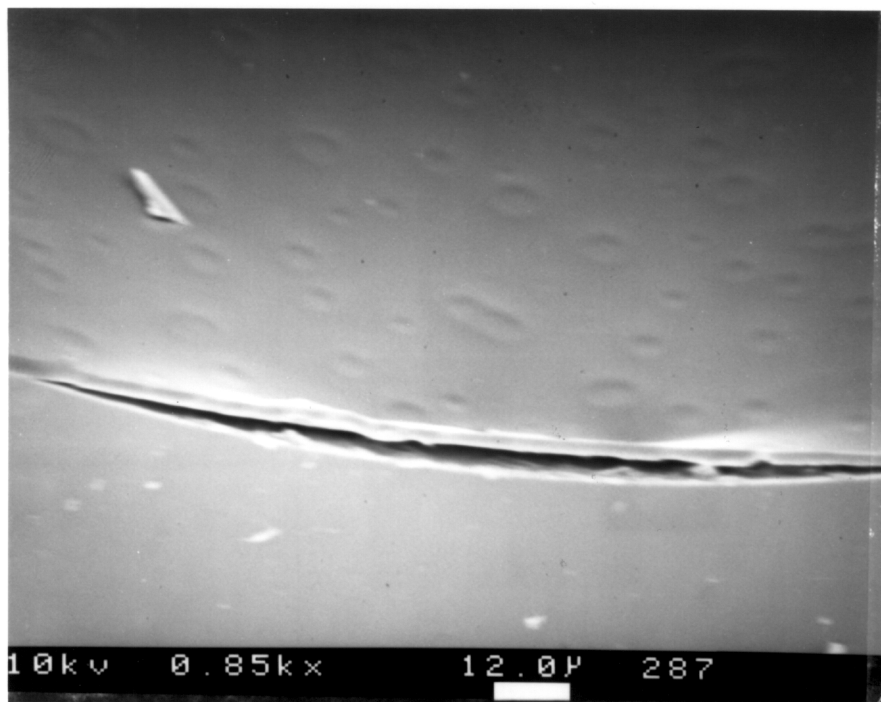


A

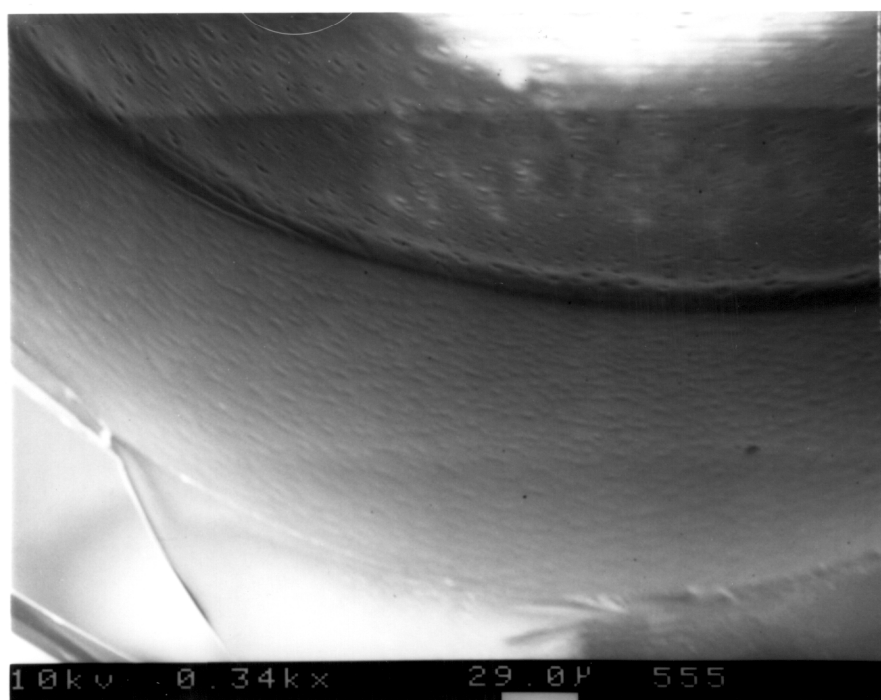


B

Figure 16. SEM pictures of the polyimide control capillary column. A) Film protruding from cut column; B) Film edge from clean cut; thickness $\approx 4 \mu\text{m}$.



A



B

Figure 16. SEM pictures of copolymer capillary columns. A) 10-wt%-PDMS film edge from clean cut ; B) line deformity in 30-wt%-PDMS column film.

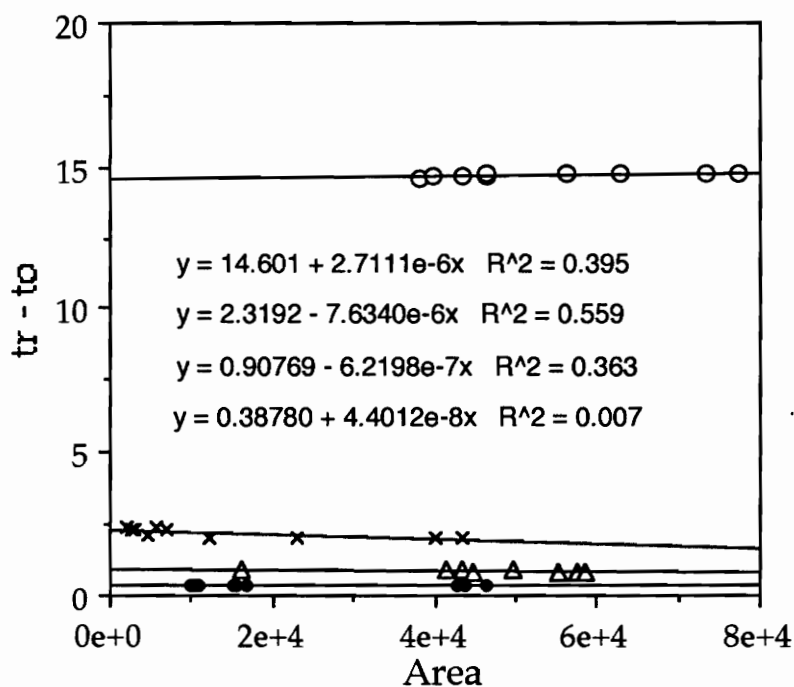
possible cause of this effect is given in Appendix A. In summary, the deformity was believed to be primarily due to an inability of the double water bath to sufficiently control the temperature in the immediate vicinity of the retreating meniscus of the more dilute coating solutions. Although the films would be too irregular for an effective capillary column diffusion coefficient determination, they were considered to be adequate for the surface studies done here.

5.2.2 Surface Energetics Study

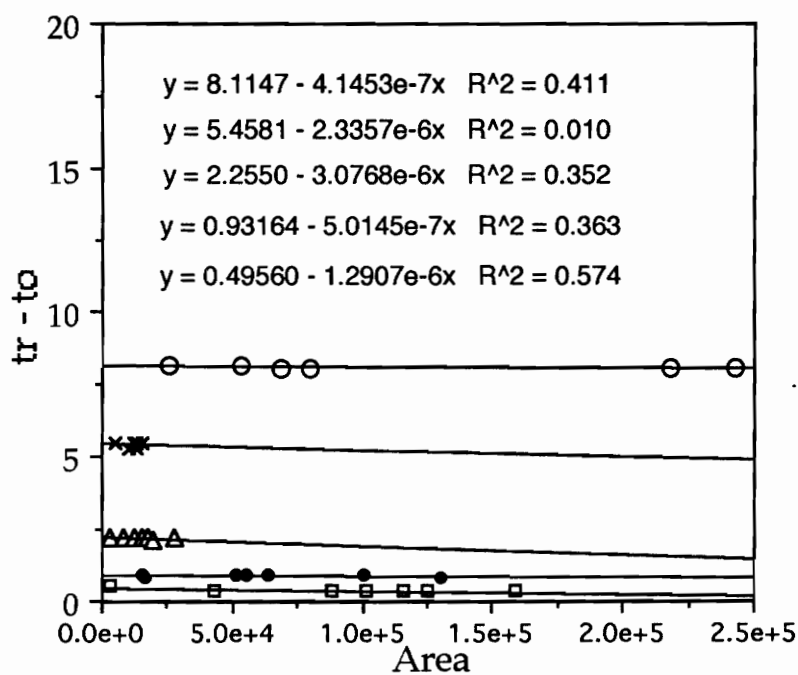
IGC surface studies were conducted using three different columns. One column was a polyimide control column. The other two columns were the 10-weight-percent (3.6 K) PDMS containing copolymer and the 30-weight-percent (3.6 K) PDMS containing copolymer columns. Experiments were done in a temperature range of 30 to 50°C which is well below the upper glass transitions of all the polymers studied. The water and n-alkane probes used were non-solvents for the polymers. It was therefore expected that surface adsorption was the predominant or only retention mechanism under these conditions. Although readily acceptable for the polyimide homopolymer column, this assumption of predominant surface adsorption might be called into question for the copolymers due to the subambient T_g of the siloxane in the copolymers. Previous IGC research on polycarbonate-siloxane copolymers¹³⁵ using n-decane as a probe at temperatures below the upper glass transition included the discovery that the probe lost much of its access into the copolymer bulk at higher weight percents of polycarbonate. A dramatic drop in specific retention volume of the polycarbonate-siloxane columns was found upon decreasing the weight percent PDMS from 36% to 32%, indicating the higher T_g polycarbonate had become the

dominant phase and that surface adsorption predominated. It was therefore concluded that the assumption of a predominance of surface adsorption was valid since the studied copolymers contained weight percents of siloxane less than 36%. The probes did not penetrate into the true bulk of the copolymers. However, if the surface is considered to be more shallow than the width of the first molecular layer, then it cannot be said for certain whether the probes did not penetrate into the siloxane-rich surface of the copolymers.

Maximum injected amounts were estimated to be in a range of approximately 1 to 3 micrograms (μg) using the ideal gas equation and various injection conditions involving capillary split ratio and headspace sampler factors such as the gas sampling valve volume, the sample-vial volume and temperature. Rough estimates employing the approximated maximum amounts place the minimum injected amounts in the tenths of micrograms. These injection amounts were just inside and above the range of injection amounts recommended by Conder and Young³² for infinite dilution surface analysis. The water vapor peaks showed little asymmetry and were considered practically gaussian. The n-alkane peaks, however, did show some tailing, which decreased as the study temperature increased. Higher column temperatures apparently allowed the partitioning process to come closer to achieving equilibrium. Retention times were corrected for dead volume and were extrapolated to infinite dilution values using from six to ten injections for each probe at each study temperature. Examples of these extrapolations are given in Figure 18 A&B. Retention times were found to be generally independent of the amount injected, although a slight dependence was seen for the higher n-alkanes at the lower



A



B

Figure 18. Extrapolation of corrected retention times to infinite dilution for A) polyimide at 50°C and B) 30wt%(3.6K)PDMS copolymer at 40°C. Intercept values are used in further calculations. Probes: C₉ (□), C₁₀ (●), C₁₁ (Δ), C₁₂ (x) and water (o).

temperatures. The most reliable data for the infinite dilution based theory was therefore considered to be that from the study at 50 °C.

The physical properties of the probes required by the theory were either estimated or obtained from the literature. The dispersive components of the liquid surface free energies (γ_l^d) of the probes were obtained from Kaelble¹³⁶ and Jasper.¹³⁷ The surface area of a probe molecule, a , was estimated for the n-alkanes by an extrapolation of the n-alkane surface area data given by Schultz and Lavielle.²⁵ Figure 19 shows the polynomial extrapolation of the literature values and Table 8 lists the values. The surface area of the molecular probe water was estimated to be 13.9 Å² using Van der Waals radii and bond lengths. This estimated value compares relatively well to the value of 12.5 Å² reported by McClellan and Harnsberger¹³⁸ as the area per adsorbed water molecule averaged from several values obtained from experiments reported in the literature. Values in the literature range from approximately 11 to 21 Å².^{138,139} The estimated values for the experimental probes should be sufficient for a valid relative comparison between the polymer systems.

The surface energetics plot obtained for the polyimide homopolymer at 50 °C is shown in Figure 20. The open circle represents the water data. The dispersive reference line was obtained by injecting the n-alkanes decane, undecane, and dodecane. The difference between the ordinates of the water data point and the point directly below it on the dispersive reference line represents the free energy of specific surface interaction. Similar surface energetics studies were conducted on the 10- and 30-weight-percent siloxane copolymers. The 30-weight-percent study at 40 °C, which involved the injection of nonane as a fourth n-alkane, is shown in Figure 21.

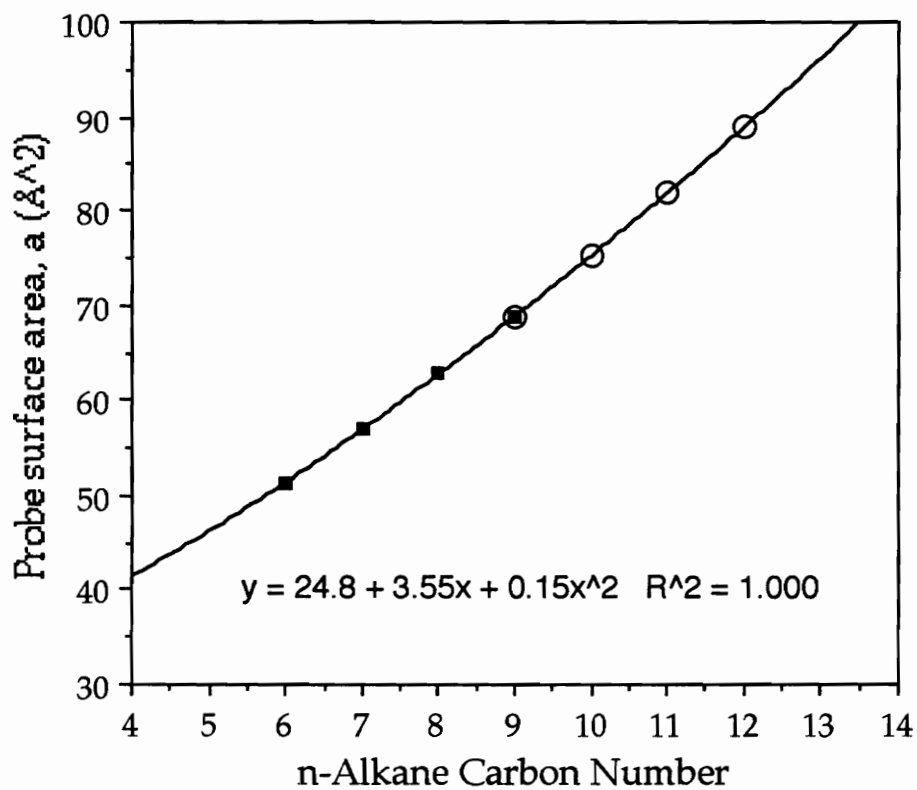


Figure 19. Polynomial extrapolation of n-alkane molecular probe surface areas from literature data.²⁵ Literature values (■); Experimentally utilized values (○).

Table 8. Comparison of literature²⁵ and polynomially-extrapolated molecular surface areas, a , (in \AA^2) of n-alkane probes.

n-alkane	Literature	Polynomial
C ₆	51.5	51.5
C ₇	57	57
C ₈	62.8	62.8
C ₉	68.9	68.9
C ₁₀	np*	75.3
C ₁₁	np	82
C ₁₂	np	89

* not provided²⁵

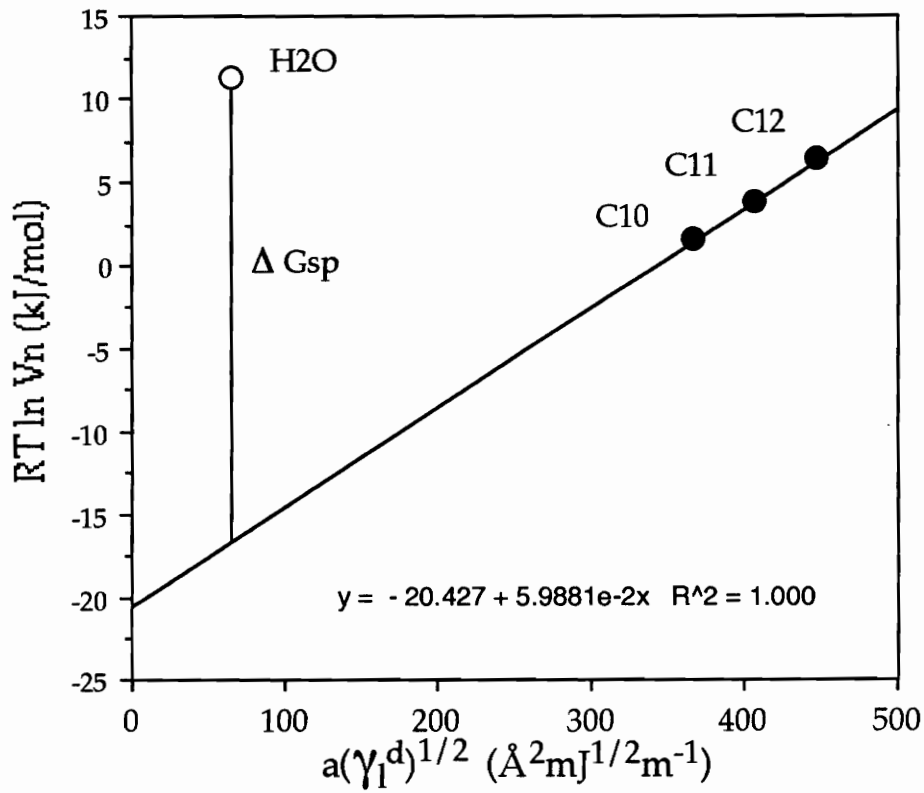


Figure 20. IGC Surface Energetics Plot for polyimide control at 50°C. ΔG_{sp} is the difference in the ordinate values at the top and bottom of the line.

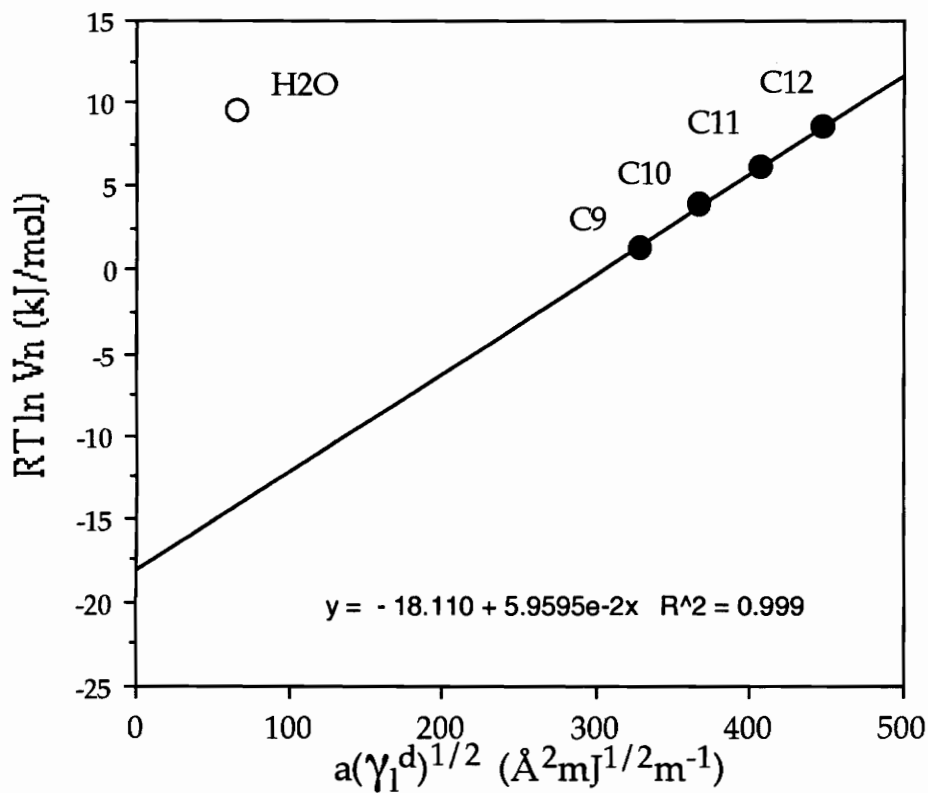


Figure 21. IGC Surface Energetics Plot for 30wt%(3.6K)PDMS copolymer at 40°C. Good correlation of the nonane point on the dispersive reference line reinforces the acceptability of the extrapolated surface area values of the higher n-alkanes.

The free energies of H₂O specific surface interaction obtained from the surface energetics studies on the three polymers at the various temperatures are given in Table 9. All the values are slightly above the range of bond energies expected for permanent dipole-dipole interactions such as hydrogen bonds excluding fluorine (10-26 kJ/mol) and other dipole-dipole interactions excluding hydrogen bonds (4-21 kJ/mol).¹ It is interesting to note that although the calculated surface area for the water probe allows for a valid comparison between systems, it is still a somewhat arbitrary choice. Its value directly influences the values obtained for the free energies of specific interaction. The use of a smaller reported value of the water probe surface area would have increased the values of the free energy of specific interaction, whereas the use of a slightly larger reported area would have placed the results more comfortably into the expected range for hydrogen bonds.

The 10-percent increase in siloxane from the polyimide control to the 10-weight-percent copolymer resulted in an approximately 4 kJ/mol decrease in the free energy of H₂O specific surface interaction at 50 °C. The hydrophobic and flexible poly(dimethylsiloxane) has a lower surface free energy that drives it to migrate to the surface of the copolymer, which causes the reduction in water interaction.¹²⁹ The surface study at 50 °C conducted using the 30-weight-percent siloxane copolymer shows a further 0.8 kJ/mol decrease in the water specific interaction. This decrease is not significant given the precision of these experiments. Decreases in the interaction free energy with increasing siloxane content are also seen at the lower study temperatures. The accuracy of these

Table 9. Free energies of specific surface interaction of water vapor with the polymer surfaces at various experimental temperatures.

	$(\Delta G^{\circ}_{sp}$ in kJ/mol)		
	<u>50°C</u>	<u>40°C</u>	<u>30°C</u>
Polyimide Control	27.9 ± 0.9	26.6 ± 1.3	26.7 ± 1.2
10 wt% (3.6K)PDMS	23.7 ± 0.8	25.2 ± 1.0	23.9 ± 1.4*
30 wt% (3.6K)PDMS	22.9 ± 1.2	23.7 ± 0.8	22.9 ± 1.2

*Actual Study Temperature: 35 °C

Table 10. Dispersive component of the solid surface free energy of polymer surfaces as determined from slope of IGC dispersive reference line at 50°C.

	$(\gamma_s^d$ in mJ/m ²)
Polyimide Control	24.7 ± 2.1
10 wt% (3.6K) PDMS	20.6 ± 1.7
30 wt% (3.6K) PDMS	21.1 ± 2.6

values, however, is considered to be less than that of the 50 °C study for reasons stated above.

The dispersive components of the solid surface free energy determined for the three polymers in the 50°C study are listed in Table 10. The values for the two siloxane-containing copolymers are indistinguishable given the error associated with the measurement. As previously noted, the copolymers are expected to have a surface dominated by the PDMS component and so should have surface characteristics very similar to a PDMS homopolymer. The dispersive component of the solid surface free energy of PDMS has been reported to be 21.7 mJ/m² by Owens and Wendt.¹³⁰ The measured dispersive components of 20.6 and 21.1 mJ/m² are equal within error to this value.

One might also reasonably expect the value of the dispersive component of the solid surface free energy of the polyimide control to be higher than that for a methyl-dominated PDMS-type surface. It was found to be higher, as expected. However, a comparison of the IGC-obtained value with the value obtained by calculations involving contact angle measurements (of distilled water and diiodomethane) indicate that the IGC value is too low. The dispersive component obtained by contact angle measurements using water and formamide is much closer but there is often a large error associated with formamide contact angles.

5.3 IGC SURFACE SUMMARY

It has been shown by an inverse gas chromatographic surface energetics study that the incorporation of siloxane segments into the polyimide decreases the specific interaction of water vapor with the polymer surface by at least

4 kJ/mol. This indicates that the surface does have some role to play in the water resistance. The further increase in the amount of siloxane to 30-weight-percent has not been shown to reduce significantly the specific interaction or increase the water resistance compared to the 10-weight-percent copolymer. This suggests that only 10-weight-percent siloxane (or less) is needed to maximize the surface contribution to the water resistance.

The dispersive components of the surface free energy of the siloxane-containing copolymers were equal within error to the dispersive component of the solid surface free energy of poly(dimethylsiloxane) reported as 21.7 mJ/m² in the literature. The dispersive components determined by IGC for the 10- and 30-weight-percent siloxane-containing copolymers were 20.6 and 21.1 mJ/m², respectively. This is in good agreement with the concept of a siloxane-rich surface of the copolymers.

6. GRAVIMETRIC SORPTION BULK DIFFUSION

6.1 COMMENTS

Diffusion coefficients were determined for the polyimide and three copolymers from Fickian reduced sorption plots of the gravimetric sorption of water vapor. The results are discussed below with particular attention given to small initial deviations from Fickian sorption. The results are interpreted in terms of free volume theories of diffusion and possible morphological influences. Explanations are given for the choice of the method for film preparation. The fundamental corrections of the data collected from the sorption apparatus are also described and discussed.

6.2 DIFFUSION RESULTS AND DISCUSSION

6.2.1 Sorption Films

The need for some sort of continuity in the sample preparation of the polymers for both the diffusion and surface studies drove the search for a method of polymer film preparation involving casting from methylene chloride, the solvent used in the capillary column coating. The method described in the Experimental Section was found to be fairly successful for the siloxane-containing copolymers when methylene chloride was used. The (1.5 K) PDMS copolymer gave good homogeneous films. However, the films of the (3.6 K) PDMS containing copolymers had a noticeable layered-inhomogeneity. The down-side of the cast film was shiny while the air-side was dull or matte. This

may have been due to a solvent preference for one type of polymer block or it may have been due to a high rate of evaporation causing some porosity in the air surface layer. This type of extremely apparent inhomogeneity was undesirable since in sorption diffusion experiments it is assumed that there is no non-random gradient in composition or structure and that the two faces presented to the sorbing species are the same. Casting an acceptable flat film of the polyimide control from methylene chloride was also very difficult. Chloroform, however, was found to give a successful film for the polyimide. When used for the (3.6 K) PDMS copolymers, it also gave films that had no layered inhomogeneity. It was suspected that chloroform's slower rate of evaporation was the influencing factor.

6.2.2 Bulk Sorption Study

6.2.2.1 Introduction

The sorption of water vapor into free-standing polymer films was determined by following the mass increase of each film as it was rapidly exposed to an actual environment of approximately 55 percent relative humidity. Sorption experiments were performed on five films. There were two polyimide control films, one quenched film and one film aged at $T_g - 5^\circ\text{C}$. There was one film each of the 10-weight-percent and 30-weight-percent (3.6 K) PDMS and 30-weight-percent (1.5 K) PDMS copolymers. For each set of conditions, two sorption/desorption cycles were done in the sample chamber on all films except one. Secondary sorption cycles were done without an intermediate thermal treatment. The 10- and 30-weight-percent (3.6 K) PDMS copolymer films were initially quenched and two sorption/desorption cycles were conducted on each. These films were then taken above T_g , in order to attempt to "erase" any

structural memory of sorption, and then the films were aged at $T_g - 5^\circ\text{C}$. The films were then sorbed and desorbed twice. The 30-weight-percent (1.5 K) PDMS copolymer film was quenched from well above T_g and sorbed and desorbed only once. All films were cast from chloroform, except the 30-weight-percent (1.5 K) PDMS copolymer, which was cast from methylene chloride.

6.2.2.2 *Data Collection and Correction*

Prior to sorption, each sample film was dried overnight to constant weight in the sample chamber in a flow of dry, zero-percent relative humidity air. Data on the relative humidity (at the oven temperature) of the air flow and the weight gain of the film during the experiment were collected each minute. In all calculations, the last data point collected before humid air entered the sample chamber was considered to be the point of time zero. There was a possible associated error of 15 seconds due to the manual switching of the dry/humid air flows. (This is a minimal error compared to film thickness error, however. Film thicknesses and associated errors are listed in Table 11.) An example of a data trace of the raw data of humidity increase and weight gain (or mass uptake) is shown in Figure 22. The data is from the first sorption of the quenched polyimide control. Note that the humidity takes a minimum of two minutes to become close to its final maximum but that it is stable at maximum.

The mass uptake raw data was corrected for possible adsorption of water vapor onto the components of the old thermogravimetric analyzer's balance, for example the hook wire that holds the sample. To accomplish this, a blank run of an empty sample chamber was done using the same overall conditions as the sample runs. Scatter in the data was made more apparent by the very small gain

Table 11. Average and standard deviation of thickness of films used in sorption experiments. Values determined from a minimum of ten measurements.

<u>Film</u>	<u>Thickness (mm)</u>
Polyimide Quenched	0.191 ± 0.018
Polyimide Aged	0.163 ± 0.035
10 wt% (3.6K) PDMS	0.128 ± 0.004
30 wt% (3.6K) PDMS	0.130 ± 0.009
30 wt% (1.5K) PDMS	0.139 ± 0.007

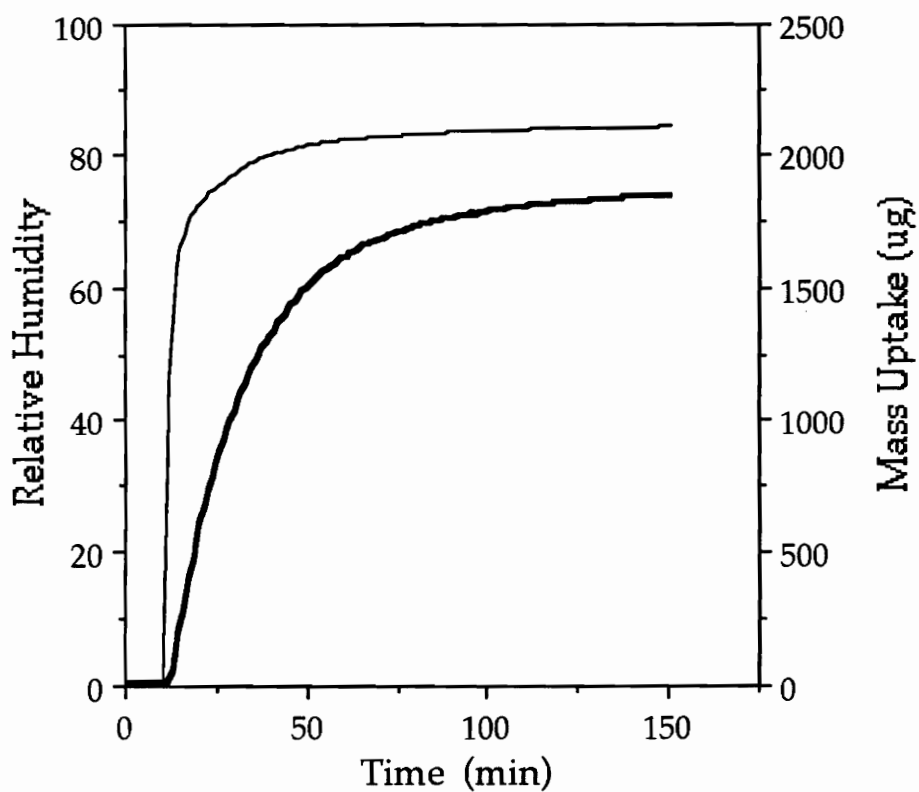


Figure 22. Plot of raw data of mass uptake of water vapor in micrograms and relative humidity for polyimide control sorption experiment. Thin line is humidity increase; thick line is the weight gain of water.

in weight, which was less than 60 micrograms at maximum. The scattered points were fitted to an overall "curve" by means of fitting groups of points to separate curves using the best fit curve regression of Cricket Graph 1.3.2. This is illustrated in Figure 23. To achieve as true an overall curve as possible, the groups of points used often overlapped. The final curve, a collection of several discontinuous curve sections, is given in Figure 24. This raw blank sorption curve was subtracted from all sample sorption runs in order to correct for mass uptake not directly related to sorption in the film. Figure 25 is an example of the results of the correction for the first sorption of the aged polyimide sample film.

6.2.2.3 *Corrected Results and Discussion*

After the weight gain data of the sorption runs were corrected by the blank run, the mass uptake at infinite (long) times, M_{∞} , was determined as the average of the measured mass uptake data points after equilibrium was reached. The fractional uptake was determined as the mass uptake at a given time, M_t , divided by the mass uptake at infinite time. This was plotted against the square root of the time in seconds divided by the film thickness to give reduced sorption plots. Figure 26 is the reduced sorption plot for the first sorption of the quenched polyimide. All of the sorption plots are similar in shape to the polyimide plot. The sorption has the Fickian characteristics of being linear up to 0.6 fractional uptake when plotted against the square root of time. It is also concave to the abscissa above 0.6 fractional uptake and reaches an uneventful equilibrium. All of the sorption plots have similar Fickian characteristics. Figures 27 and 28 give the first sorption cycle curves for the quenched films and the aged films, respectively.

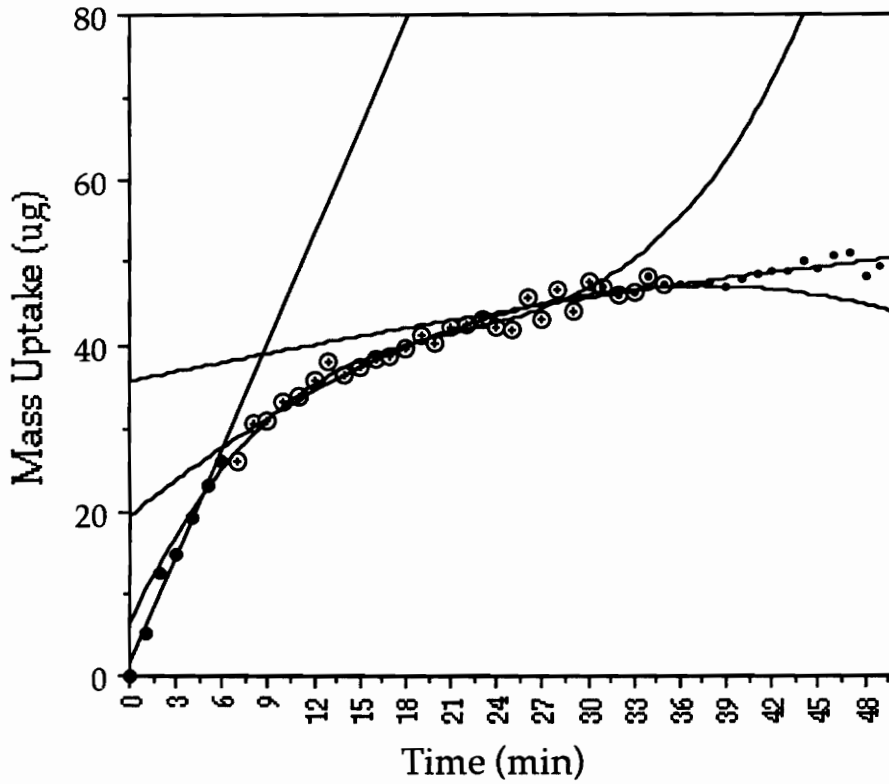


Figure 23. Curve fitting of blank sorption run in order to obtain a smooth curve for subtraction. The straight line represents the initial segment of filled circles (●); a third order polynomial (+) represents the second segment of points; the second order polynomial (o) represents the third segment of points; another third order polynomial represents a fourth segment of filled square points (■) until long times.

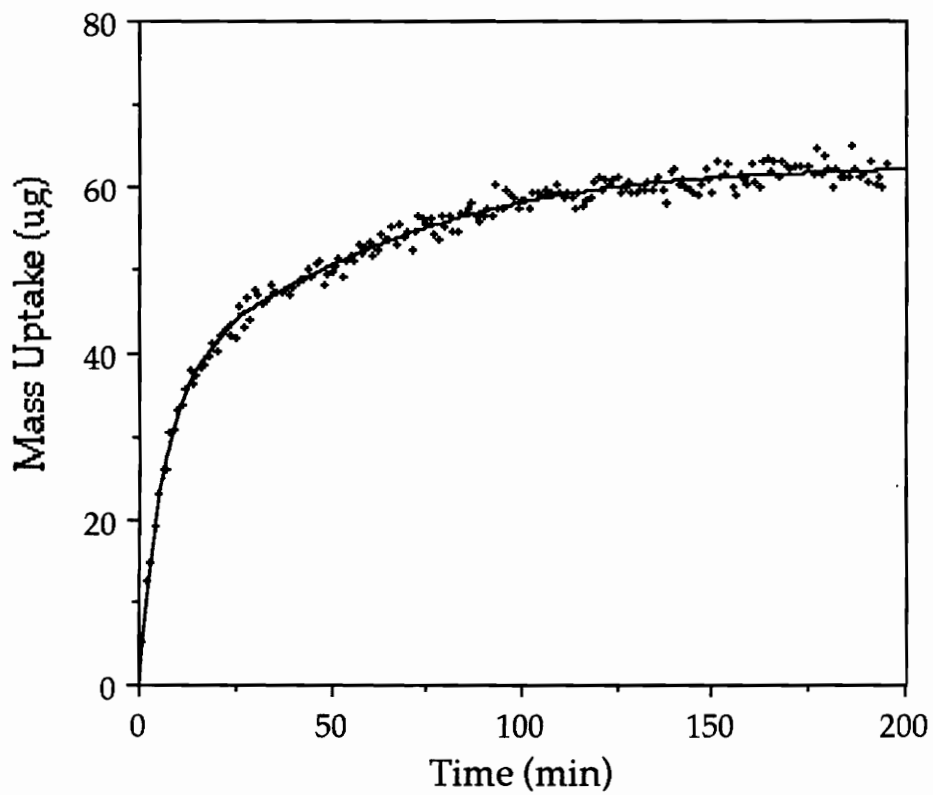


Figure 24. Final smoothed curve of blank sorption run in comparison with the raw blank uptake data.

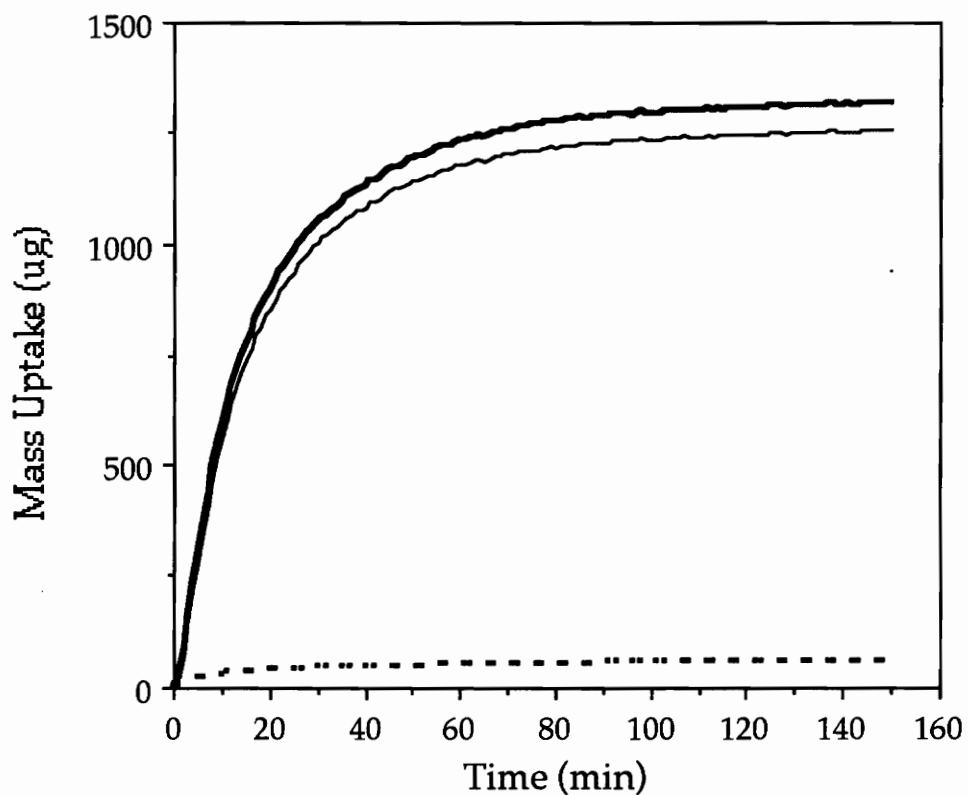


Figure 25. Example of the subtraction of the blank run sorption curve from the raw uptake data of the first sorption cycle of the aged polyimide control film. The broken curve is the blank sorption run; the thick line is the raw aged PI uptake data; the thin line is the corrected raw data.

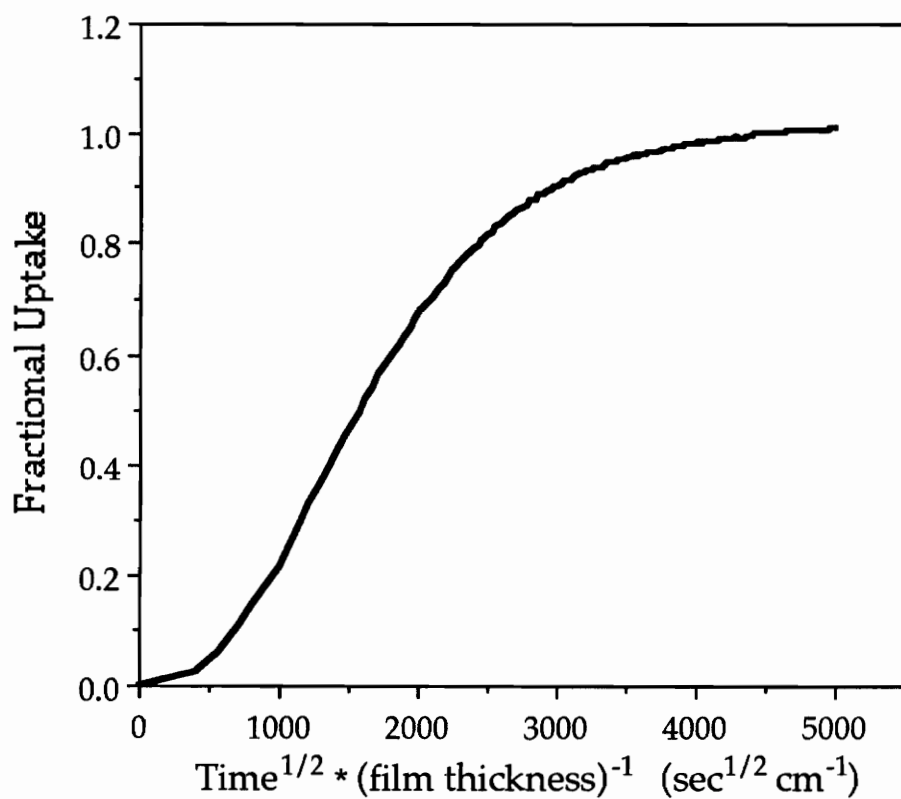


Figure 26. Reduced sorption plot for quenched polyimide film.

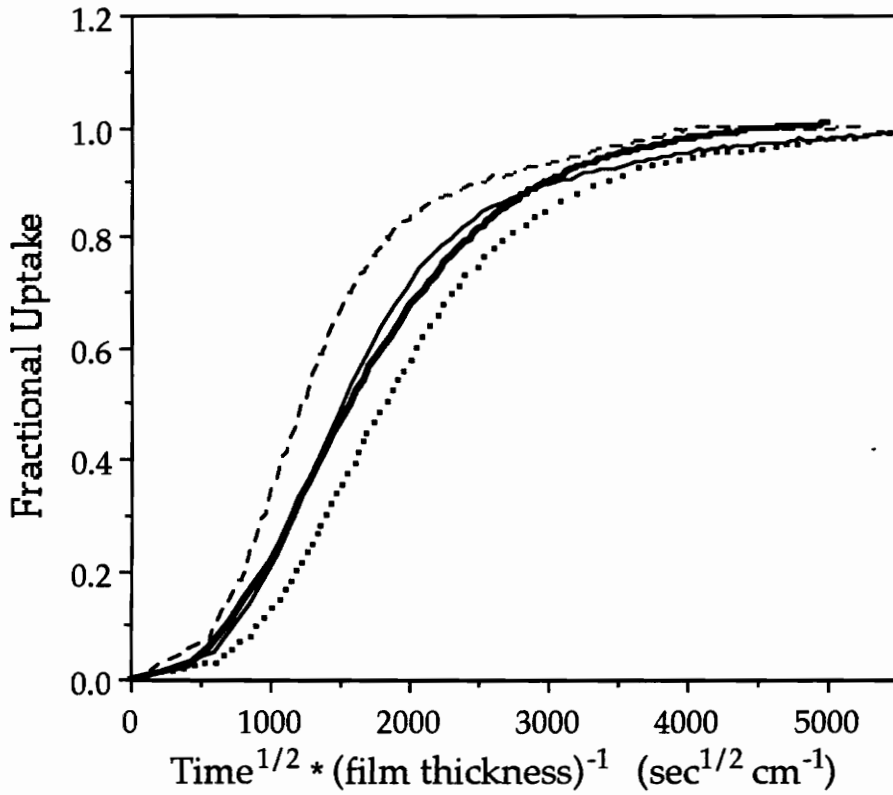


Figure 27. Compilation of reduced sorption plots for first sorption cycle of quenched films. Curves: polyimide = thick solid line; 10-wt%-(3.6 K) PDMS copolymer = thick dotted line; 30-wt%-(3.6 K) PDMS copolymer = thin solid line; 30-wt%-(1.5 K) PDMS copolymer = thin dashed line.

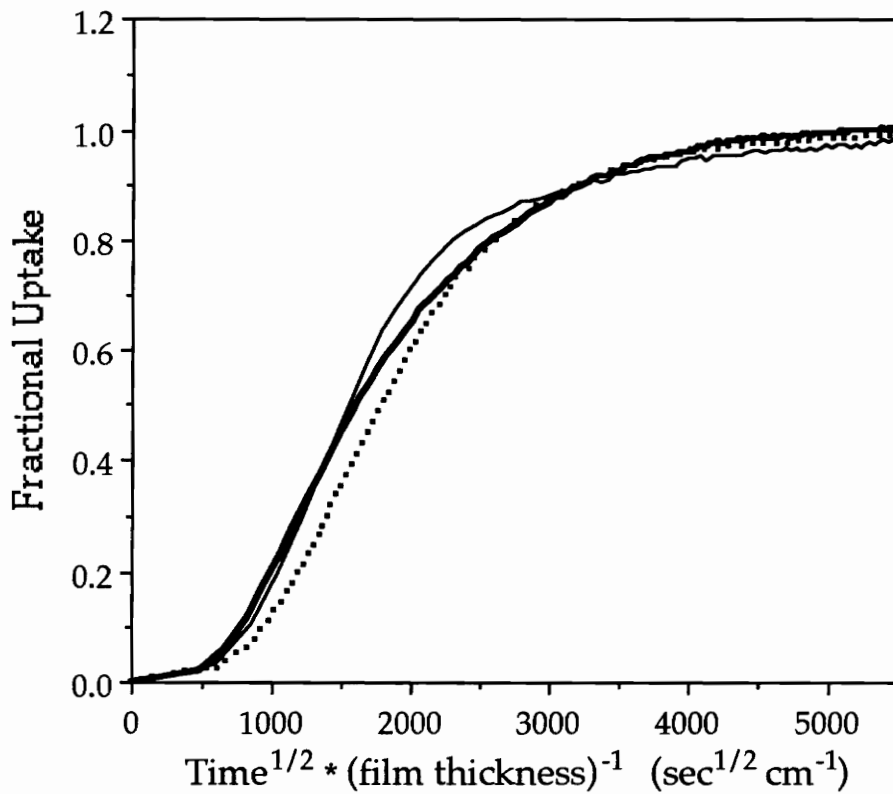


Figure 28. Compilation of reduced sorption plots for first sorption cycle of T_g - 5°C aged films. Curves: polyimide = thick solid line; 10-wt%-(3.6 K) PDMS copolymer = thick dotted line; 30-wt%-(3.6 K) PDMS copolymer = thin solid line.

In all the reduced sorption data plotted in Figures 27 and 28, there is a slight deviation from the initial linearity expected for Fickian sorption. This is limited to the first two data points of the sorption curve and is believed to be related to the initial lag time in the humidity increase. Included in this deviation from initial linearity is a shift along the abscissa away from the origin, which again may be the result of the initial two minutes of the sorption occurring at too low humidities. Jou, et.al.,^{101,103} has recently published curves which have characteristics remarkably similar to those presented here. These were reduced sorption plots of the sorption of NMP vapor into PMDA-ODA polyimide films¹⁰³ and the sorption of water into three polyimide films.¹⁰¹ (A short summary of these papers is given in the Literature Review.) The initial deviation to the otherwise Fickian sorption curves was noted as an "induction period" and not explained in detail. The NMP/PMDA-ODA sorption induction periods tended to increase as film thickness decreased, indicating perhaps a dependence on film thickness exaggerated by the reduced sorption plot. The water/ polyimide studies,¹⁰¹ however, revealed no clear correlation between induction times and film thickness. The longest induction period occurred with the BPDA-PDA samples, which the authors considered the most hydrophobic of the studied polyimides. In the present research, the longest "induction period" apparently belongs to the 10-wt%-PDMS(3.6K) siloxane-containing copolymer. It would be premature to conclude that this is the manifestation of an extra resistance to water. There may be experimental artifacts at work; the induction periods appear less severe for the water/ polyimide study,¹⁰¹ in which the films were immersed, than for the NMP vapor¹⁰³ or the (present) water vapor sorption

studies. The polyimide films studied by Jou, et.al., were not free-standing but were cast and then bulk-imidized on silicon wafers. The coated films were also much thinner than the films used in the present water sorption study. Whether the "induction period" in this work can be related to some sort of initial resistance to water cannot be determined effectively unless several film thicknesses are utilized and the vapor exposure rate can be made "instantaneous."

The initial linear slope of the reduced sorption curves is directly proportional to the diffusion coefficient. The equation was used to calculate the diffusion coefficient from the slope was:

$$D = \frac{\pi}{16} (\text{slope})^2 \quad (36)$$

which follows directly from the equations at the end of the Fickian diffusion Theory section. The slope utilized was that of the line of the reduced plot data up to 0.6 fractional uptake. Figure 29 gives a pictorial example of the fit of such a line to the reduced sorption curve for the quenched polyimide. For all experiments, the squared correlation coefficient, R^2 , was between 0.998 and 1.000, indicating very good correlation. The diffusion coefficients obtained from all sorption cycles are listed in Table 12. Errors were calculated by standard error propagation rules. Only the error in the determination of the film thickness was propagated, since it is by far the largest contributing error.

The diffusion coefficients are of the order of magnitude of 10^{-8} cm²/sec. This is faster than most of the diffusion coefficients reported for polyimides in the literature ($\approx 10^{-9}$ cm²/sec). This increase in diffusion coefficient may be due to several possibilities. Polyimides in the literature are often bulk-imidized and

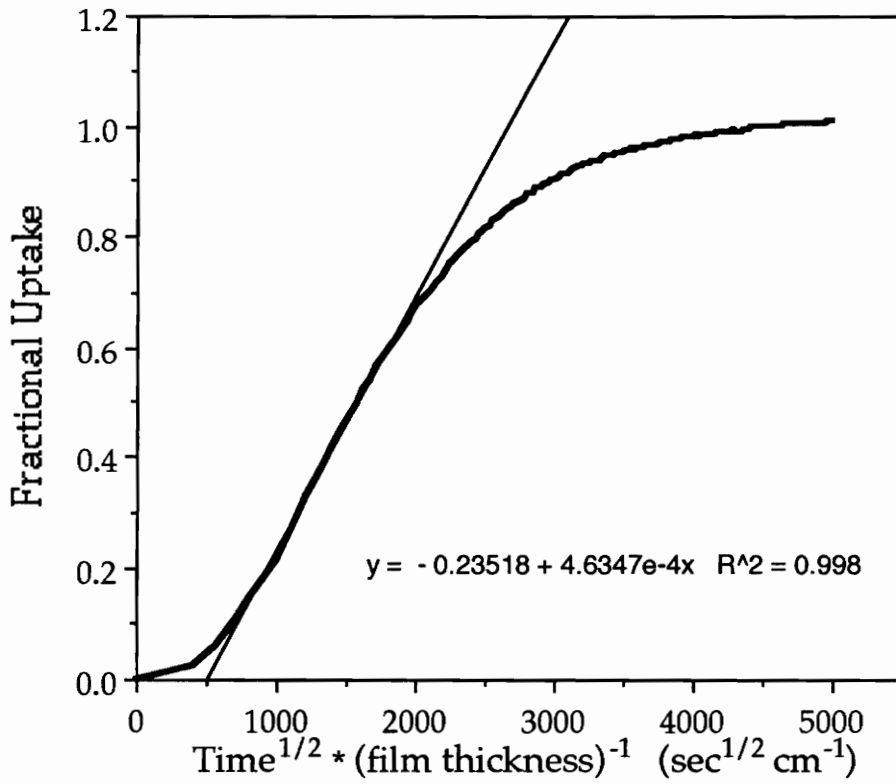


Figure 29. Reduced sorption plot for quenched polyimide film with regression line representing the initial 60% of uptake, excluding initial deviation.

Table 12. Diffusion coefficients determined from the first and second sorption cycles of the gravimetric sorption experiments.

$$D \times 10^8 \text{ (cm}^2 \text{ sec}^{-1}\text{)}$$

First Sorption Cycle:

	<u>Quenched</u>	<u>Aged</u>
Polyimide Control	4.2 ± 0.8	4.5 ± 1.9
10 wt% (3.6K) PDMS	4.2 ± 0.2	4.8 ± 0.3
30 wt% (3.6K) PDMS	6.1 ± 0.9	6.9 ± 1.0
30 wt% (1.5K) PDMS	10.0 ± 1.0	nd*

Second Sorption Cycle:

	<u>Quenched</u>	<u>Aged</u>
Polyimide Control	3.9 ± 0.7	4.2 ± 1.8
10 wt% (3.6K) PDMS	3.7 ± 0.2	4.5 ± 0.2
30 wt% (3.6K) PDMS	6.3 ± 0.9	6.7 ± 0.9
30 wt% (1.5K) PDMS	nd	nd

*not determined

may have some cross-linking which would reduce the "openness" of the resulting polymer compared to the solution imidized polymers studied here. The Bis P component of the imide structure may allow for greater flexibility than some of the more commonly studied polyimides. The polyimide studied here may also have had small amounts of low molecular weight impurities or a larger number of chain ends compared to literature polyimides which would have increased free volume and influenced diffusion. TGA experiments indicated polymers without solvent impurity. However, the DSC-determined glass transition temperature of the chloroform-cast polyimide sorption film was depressed 3°C compared to that of the methylene chloride cast film, indicating perhaps the presence of a small amount plasticizing solvent.

Although there appears to be a slight decrease in diffusion coefficient in many cases for the second sorption cycle, all but one of the sorption cycle pairs are the same within error. A comparison of the results of the quenched and aged films for both the first and second sorption cycles reveals, if errors are ignored, a slight apparent increase in diffusion coefficients. For the 3.6 K PDMS copolymers, it might be suggested that this is the result of previous sorption cycles opening the structure, but the aged polyimide film, which shows the same trend, had not been previously sorbed. Aging just below T_g for 24 hours may have caused subtle structural changes. In any case the quenched and aged values for these conditions are generally not significantly different given the error involved.

The most significant results from these sorption experiments are contained in the comparison of the diffusion coefficients of the different polymers studied. This discussion will focus on the values determined for the primary sorption

study of the quenched samples only. The diffusion coefficients of the polyimide control and the 10-weight-percent (3.6 K) PDMS copolymer are the same within error. The diffusion coefficient of the 30-weight-percent (3.6 K) PDMS copolymer increases to 1.5 times that of the 10-weight-percent (3.6 K) PDMS copolymer and is significantly different. Although perhaps not strictly comparable, since the film was cast from methylene chloride, the diffusion rate in the 30-weight-percent (1.5 K) PDMS copolymer was much faster than the other polymers: 1.6 times faster than the 30-weight-percent (3.6 K) PDMS copolymer and 2.4 times faster than the polyimide and the 10-weight-percent (3.6 K) PDMS copolymer. It is apparent from this trend that the incorporation of PDMS into the polyimide tends to increase the ease of diffusion of a penetrant, in this case water vapor. This is not terribly surprising if viewed in terms of a free volume phenomenology of diffusion.

6.2.2.4 Free Volume Interpretations

Free volume theories were discussed in more detail (and with references) in the previous Theory section and only a simplistic version of the free volume approach will be used here. The WLF equation has often been used in free volume based diffusion theories and in it is the assumption of a linear increase in fractional free volume given by the equation:

$$f = f_g + \alpha_f(T - T_g) \quad (22)$$

where f_g , the fractional free volume at the glass transition temperature is similar for all polymers. The fractional free volume increases at temperatures above the

glass transition proportional to a thermal expansion coefficient of the free volume. A simplistic explanation for the increase in diffusion coefficient with incorporation of siloxane is contained in this equation. The glass transition temperature of the polyimide homopolymer film was 260°C. The T_g of poly(dimethylsiloxane) is approximately -127°C.¹⁴⁰ The temperature of the sorption experiments was just above room temperature so the polyimide is below its T_g . Polyimide fractional free volume is fixed at the T_g value of f_g . This assumes no physical aging. The fractional free volume of PDMS at a temperature well above its T_g is much greater than that of the polyimide. The incorporation of siloxane into the polyimide therefore increases the available free volume for diffusion. A similar conclusion is possible if one considers the extreme flexibility of PDMS compared to the polyimide. (Flexibility is, of course, intimately related to chain chemical structure and the glass transition. The diffusion coefficient of water in a silicone has been reported to be $3.5 \times 10^{-5} \text{ cm}^2/\text{sec}$ near room temperature.⁶³)

The increase in free volume due to the incorporation of the flexible, low T_g siloxane can be used as a general explanation for the increase in the rate of diffusion as determined by experiment. However, the actual trends observed are better explained in terms of an understanding of the bulk morphology of the microphase-separated copolymers. The added siloxane segments increase the local free volume of the phase-separated systems. If the local increase in free volume becomes more probable, or in other words is more uniformly distributed throughout the polymer, then the probability of hole formation is increased and the movement of the diffusing species is made easier. The diffusion coefficient will thus increase. In the case of the 10-weight-percent (3.6 K) PDMS copolymer,

it is expected that the siloxane domains are dispersed in a continuous phase of polyimide. The polyimide phase is perhaps of high enough molecular weight to have small-scale motion properties similar to that of the polyimide homopolymer. The number of localities of free volume increase is small since the copolymer is only 10 weight percent PDMS and 90 weight percent polyimide. The probability of a diffusant encountering local increase free volume is increased slightly, but perhaps this cannot be capitalized upon due to the limited diffusion in the surrounding polyimide phase. The diffusion coefficient does not therefore increase noticeably.

In the other siloxane-containing polymers, the diffusion coefficient does increase. The greater incorporation of siloxane allows for perhaps a greater number of siloxane domains distributed throughout the polymer--thus increasing the hole formation probability and the diffusion coefficient. A comparison of the diffusion coefficients of the two 30-weight-percent PDMS copolymers indicates that the decrease in siloxane segment length causes an increase in diffusion. This can again be due to an increase in the probability of increased local free volume for hole formation. The increase in the number of covalent bonds between the two dissimilar blocks when the PDMS segments are shorter likely makes complete phase-separation more difficult. The structural linkages are a built-in contribution to entropy which forces the imide segments to be more closely associated with the flexible siloxane. This distributes free volume more evenly and increases local hole probability. However, it is too simplistic to attribute this effect just to some increase in the number and distribution of siloxane domains. Perhaps the best explanation of the diffusion increase is given by an examination of the upper glass transition temperatures of

the copolymers. The T_g s decrease, which indicates that the polyimide blocks were lower in molecular weight. Similar trends are found in homopolymers and are correlated to an increase in homopolymer free volume due to an increase in chain ends. In the copolymers, the available free volume in the polyimide phase itself becomes influenced by the decrease in molecular weight of the blocks. This is perhaps especially true since the imide blocks are not restrained by the attached, flexible siloxane segments.

6.3 SORPTION BULK DIFFUSION SUMMARY

Diffusion coefficients were determined by a gravimetric sorption technique in order to examine the possible resistance of poly(imidesiloxane) polymers to the ingress of water. The diffusion coefficients obtained were slightly larger than expected when compared to other values for polyimides, but they were not unreasonable. The incorporation of higher levels of polydimethylsiloxane into the copolymers was found to cause the diffusion coefficients to increase. The flexible, low- T_g siloxane segments were considered to contribute extra free volume in localized regions of the microphase-separated copolymers. The greater distribution of regions of increased free volume, due to various reasons discussed previously, in the two 30-weight-percent PDMS copolymers resulted in a higher probability of the diffusing water encountering "holes," which made diffusion faster.

The diffusion coefficient of the 10-weight-percent (3.6 K) PDMS copolymer was however not significantly different than that of the polyimide control, indicating that perhaps the regions of increased free volume were too localized.

Slower diffusion in the polyimide phase was considered to be a limiting factor. Smaller amounts of siloxane can therefore be incorporated without greatly degrading bulk diffusive resistance to water.

7. CONCLUSION

The surface and bulk properties of polyimidesiloxane copolymers have been characterized in an attempt to determine the important factors in resistance to water ingress. Inverse gas chromatography was used to conduct a surface energetics study on two copolymers of increasing siloxane content and a polyimide homopolymer control. The free energies of specific interaction of water vapor with the polymer surfaces were found to decrease with the incorporation of siloxane into the polyimide. The dispersive components of the solid surface free energy of the siloxane-containing copolymers were equal within error to that of pure poly(dimethylsiloxane), indicating a PDMS-rich, hydrophobic surface. The free energies of specific interaction with water vapor were also not significantly different which suggests that the copolymer surfaces were very similar. The surface composition properties as a function of siloxane incorporation appeared to have reached a maximum level. This suggested there was a minimum weight-percent of siloxane incorporation required to maximize the copolymer's surface water resistance. The minimum weight-percent for the (3.6 K) PDMS system studied here was ten percent (or less), which was favorable since at higher weight-percent siloxane incorporation mechanical properties begin to decrease.

Gravimetric sorption experiments revealed that higher levels of siloxane incorporation cause a definite increase in the rate of water diffusion in the copolymers. The increase in diffusion rate for the 30-wt% siloxane -

containing copolymers was found to be influenced by siloxane segment length and was explained in terms of free volume arguments. Increased diffusion coefficients suggested a decreased resistance to water ingress. The diffusion coefficient of the 10-wt% PDMS copolymer, however, was found not to be increased relative to the polyimide. Such a result was encouraging in that it suggested there can be a balance between the surface and bulk properties of siloxane-containing copolymers such that the hydrophobic surface water resistance can be "maximized" without greatly degrading bulk diffusion properties. The diffusion coefficient of a 10-wt% copolymer with shorter PDMS segments may be increased relative to the homopolymer, however.

The incorporation of siloxane into polyimides has been shown to increase resistance to water due to the hydrophobicity of the siloxane-rich surface. However, higher siloxane content also increased the rate of ingress of water inside the bulk of the polymer, presumably allowing water to speed toward an adhesive bondline and possibly decreasing durability. It appeared from this work that an increased water resistance of the surface can be achieved at lower siloxane concentrations without decreasing bulk mechanical or increasing the bulk diffusive properties to undesirable levels.

8. SUGGESTED FUTURE WORK

These idealized studies were done just on the polymers themselves and did not involve any consideration of the conditions encountered in practical coating or adhesive applications. One specific factor related to the increased hot/wet durability of the polyimidesiloxanes that may warrant further study is the stress distribution in the adhesive layer of the adhesive-adherend joint during the swelling of the polymer upon water sorption. The incorporation of siloxane has been shown to reduce the total equilibrium uptake of water. Water will have decreased solubility in copolymers that have increased hydrophobic character not only at the surface but also throughout the bulk. The equilibrium solubility has already been shown⁷ to be influenced by the siloxane segment length, which indicates a dependence on morphology or distribution of the siloxane throughout the bulk. The less water that can dissolve into a given adhesive, the lower will be the swelling and associated stresses in the joint. The increased adhesive bond durability of these copolymers may be in part due to a reduction of such swelling stresses.

The IGC surface energetics theory used in this thesis is well established and has been utilized by a number of researchers. Lower than expected dispersive components of the solid surface free energy of polar polymers have been reported and attributed to above-ambient temperatures and application of incorrect n-alkane probe surface areas.⁵⁴ The polyimide value in this work was indeed lower than expected. Probe surface areas of n-alkanes^{23,25} have been determined by injection onto nonpolar surfaces. Further studies could be done to

ascertain n-alkane probe areas on polar polymers. It would be interesting to see if the nonpolar n-alkanes adsorb in more compact shapes on the polar surfaces, due to a "dislike" of the polar nature of the surface, or if they are expanded, since the dispersive component of the surface tension of polar polymers is often considerable. The increase or decrease in surface area compared to presently used literature values would be expected to change proportionally with the size of the alkane such that the overall slope of the dispersive reference line is increased. For example with more compact coils, the longest n-alkane's surface area would decrease more relative to the literature value than the shortest n-alkane's surface area even though the proportions would be the same. If this were the case it would increase the slope and therefore the dispersive component of the solid surface free energy.

9. REFERENCES

1. A.J. Kinloch, Chap. 1 in *Durability of Structural Adhesives*, A.J. Kinloch, Ed., Applied Science Publishers, New York (1983).
2. C.A. Arnold, J.D. Summers, Y.P. Chen, R.H. Bott, D. Chen, and J.E. McGrath, *Polymer.*, **30(6)**, 986 (1989).
3. C.J. Lee, 30th Natl. SAMPE Symp., 52 (1985).
4. K.L. Mittal, Ed., *Polyimides*, Vol. 1&2, Plenum Press, New York (1984).
- ⑤ C.A. Arnold, Ph.D. Dissertation, VPI & SU, 1988.
- ⑥ R.H. Bott, Ph.D. Dissertation, VPI & SU, 1988.
- ⑦ J.D. Summers, Ph.D. Dissertation, VPI & SU, 1988.
8. R.H. Bott, J.D. Summers, C.A. Arnold, L.T. Taylor, T.C. Ward, and J.E. McGrath, *J. Adhesion.* **23**, 67 (1987)
9. T. Marzi, U. Schroder, M. Hess and R. Kosfeld, *Mat. Res. Soc. Symp. Proc.*, **170**, 123 (1990).
10. H.M. McNair and E.J. Bonelli, *Basic Gas Chromatography*, Consolidated Printers, Berkeley, (1968).
11. O. Smidsrød and J.E. Guillet, *Macromolecules.* **2(3)**, 272 (1969).
12. A. Lavoie and J.E. Guillet, *Macromolecules.* **2(4)**, 443 (1969).
13. J.-M. Braun, A. Lavoie and J.E. Guillet, *Macromolecules.*, **8(3)**, 311 (1975).
14. J.-M. Braun and J.E. Guillet, *Macromolecules.*, **8(6)**, 882 (1975).
15. D.G. Gray and J.E. Guillet, *Macromolecules.*, **6(2)**, 223 (1973).
16. D. Patterson, Y.B. Tewari, H.P. Schreiber and J.E. Guillet, *Macromolecules.*, **4(3)**, 356 (1971).
17. O. Olabisi, *Macromolecules.*, **8(3)**, 316 (1975).

18. J.M. Braun and J.E. Guillet, *Adv. Polym. Sci.* , **21**, 108 (1976).
19. J.E. Guillet and A.N. Stein, *Macromolecules.*, **3**, 102 (1970).
20. W.J. Orts, M. Romansky and J.E. Guillet, *Macromolecules.*, **25(2)**, 949 (1992).
21. S. Galassi and G. Audisio, *Makromol. Chem.*, **175**, 2975 (1974).
22. J.M. Braun and J.E. Guillet, *Macromolecules.*, **9(2)**, 340 (1976).
23. J. Schultz, L. Lavielle and C. Martin, *J. Adhesion.* **23**, 45 (1987).
24. A.E. Bolvari, M.S. Thesis, VPI & SU, 1988.
25. J. Schultz and L. Lavielle in *Inverse Gas Chromatography*; D.R. Lloyd, H.P. Schreiber and T.C. Ward, Eds.; ACS Symposium Series No. 391; American Chemical Society, Washington, D.C., (1989), p. 185.
26. A.E. Bolvari and T.C. Ward in *Inverse Gas Chromatography*; D.R. Lloyd, H.P. Schreiber and T.C. Ward, Eds.; ACS Symposium Series No. 391; American Chemical Society, Washington, D.C., (1989), p. 217.
27. F.M. Fowkes, *Ind. Eng. Chem.* **56**, 40 (1964).
28. J.S. Aspler in *Pyrolysis and GC in Polymer Analysis*, Vol 29, Chromatographic Science Series, S.A. Liebman and E.J. Levy, Eds.; Marcel Dekker, Inc., New York (1985), p.399.
29. J.E.G. Lipson and J.E. Guillet, *Development in Polymer Characterization-3*; J.V. Dawkins, Ed., Applied Science Pub., London (1982).
30. V.G. Berezkin, V.R. Alishoyev and I.B. Nemirovskaya, Chap. 8 in *Gas Chromatography of Polymers*, Vol. 10, J. Chromatography Library, Elsevier Scientific Publishing Company, New York (1977).
31. R. Vilcu and M. Leca, *Polymer Thermodynamics by Gas Chromatography*, Studies in Polymer Science 4, Elsevier Science Publishing Company, Inc., New York (1990).
32. J.R. Condor and C.L. Young, *Physicochemical Measurement by Gas Chromatography* John Wiley & Sons, New York (1979).

33. D.R. Lloyd, H.P. Schreiber and T.C. Ward, Eds., *Inverse Gas Chromatography*; ACS Symposium Series No. 391; American Chemical Society, Washington, D.C. (1989).
34. A. Voelkel, *Crit. Rev. Anal. Chem.* **22(5)**, 411 (1991).
35. G.J. Courval and D.G. Gray, *Can. J. Chem.*, **54**, 3496 (1976).
36. G.J. Courval and D.G. Gray, *Macromolecules.*, **8(3)**, 326 (1975).
37. Z.Y. Al-Saigh and P. Munk, *Macromolecules.* **17(4)**, 803 (1984).
38. T.W. Card, Z.Y. Al-Saigh and P. Munk, *Macromolecules.* **18(5)**, 1030 (1985).
39. P. Munk, Z.Y. Al-Saigh and T.W. Card, *Macromolecules.* **18(11)**, 2196 (1985).
40. T.W. Card, Z.Y. Al-Saigh and P. Munk, *J. Chromatography*, **301**, 261 (1984).
41. P.A. Koning, Ph.D. Dissertation, VPI & SU, Blacksburg, 1988.
42. J.Y. Wang and G. Charlet, *Macromolecules.*, **22(9)**, 3781 (1989).
43. D.G. Gray and J.E. Guillet, *Macromolecules*, **5(3)**, 316 (1972). QD380M52
44. M.D. Croucher and H.P. Schreiber, *J. Polym. Sci.: Polym. Phys. Ed.*, **17**, 1269 (1979).
45. H.P. Schreiber and M.D. Croucher, *J. Appl. Polym. Sci.*, **25**, 1961 (1980).
46. P. Koning, T.C. Ward, R.D. Allen and J.E. McGrath, *Polym. Prepr., (Am. Chem. Soc., Polym. Chem. Div.)*, **26(1)**, 189 (1985).
47. H.P. Schreiber, M.R. Wertheimer and M. Lambla, *J. Appl. Polym. Sci.*, **27**, 2269 (1982).
48. S.P. Wilkinson, Ph.D. Dissertation, VPI & SU, 1991.
49. S.P. Wilkinson and T.C. Ward, *Int. SAMPE Symp. Exhib.* **35(2, Adv. Mater.: Challenge Next Decade)**, 1180 (1990).
50. L.Lavielle and J. Schultz, *Langmuir*, **7**, 978 (1991).

51. V. Gutmann, *The Donor Acceptor Approach to Molecular Interactions*, Plenum Press (1983).
52. F. Chen, *Macromolecules.*, **21**(6), 1640 (1988).
53. R.S. Drago, G.C. Vogel and T.E. Needham, *J. Am. Chem. Soc.*, **93**, 6014 (1971).
54. U. Panzer and H.P. Schreiber, *Macromolecules.* **25**(14), 3633 (1992).
55. A.V. Kiselev, *J. Chromatography*, **49**, 84 (1970).
56. J. Roles and G. Guiochon, *J. Chromatography*, **591**, 233 (1992).
57. A.C. Tiburcio and J.A. Manson, *J. Appl. Polym. Sci.*, **42**, 427 (1991).
58. J. Jagiello and E. Papirer, *J. Coll. Interface Sci.* **142**(1), 232 (1991).
59. A.H. Windle, in *Polymer Permeability*, J. Comyn, Ed., Elsevier Applied Science, New York (1985).
60. A. Fick, *Ann. Physik*, **94**, 59 (1855); A. Fick, *Ann. Phys. Lpz.*, **170**, 59 (1855).
References from references 62 and 65.
61. J.B. Fourier, *Théorie analytique de la chaleur. Œuvres de Fourier* (1822).
Reference from reference 65.
62. W.R. Vieth, *Diffusion In and Through Polymers*, Hanser Publishers, New York (1991).
63. J. Comyn, in *Durability of Structural Adhesives*, A.J. Kinloch, Ed., Applied Science Publishers, New York (1983).
64. J. Comyn, Chap. 1 in *Polymer Permeability*, J. Comyn, Ed., Elsevier Applied Science, New York (1985). QJ 381 P6117 1985 (recall).
65. J. Crank, *The Mathematics of Diffusion*, Oxford University Press, London (1956).
66. H.S. Carslaw and J.C. Jaeger, *Conduction of Heat in Solids*, 2nd Edn., Clarendon Press, Oxford (1959). Reference from reference 67.

67. C.E. Rogers, in *Polymer Permeability*, J. Comyn, Ed., Elsevier Applied Science, New York (1985).
68. R.M. Felder and G.S. Huvar, in *Methods of Experimental Physics*, 16c, Academic Press, Inc., New York (1980).
69. J. Comyn, Chap. 5 in *Polymer Permeability*, J. Comyn, Ed., Elsevier Applied Science, New York (1985).
70. H. Fujita, *Adv. Polym. Sci.*, **3**, 1 (1961). Reference from reference 63.
71. J. Crank and G.S. Park, Eds., *Diffusion in Polymers*, Academic Press, New York (1968).
72. D. Machin and C.E. Rogers, in *CRC Critical Reviews in Macromolecular Science*, CRC Press, Cleveland (1972) p. 245.
73. V. Stannett, H.B. Hopfenberg and J.H. Petropoulos, in *Macromolecular Science*, 8, C.E.H. Bawn, Ed., University Press, Baltimore (1972).
74. F. Bueche, *Physical Properties of Polymers*, Interscience, New York (1962). Reference from reference 79.
75. C.A. Kumins and T.K. Kwei, in *Diffusion in Polymers*, J. Crank and G.S. Park, Eds., Academic Press, New York (1968).
76. H. Fujita, in *Diffusion in Polymers*, J. Crank and G.S. Park, Eds., Academic Press, New York (1968); H. Fujita, A. Kishimoto and K. Matsumoto, *Trans. Faraday Soc.*, **56**, 424 (1960).
77. M.L. Williams, R.F. Landel and J.D. Ferry, *J. Am. Chem. Soc.*, **77**, 3701 (1955). Reference from reference 71.
78. N.G. McCrum, B.E. Read and G. Williams, *Anelastic and Dielectric Effects in Polymeric Solids*, Dover Publications, Inc., New York (1967).
79. L.G.F. Stuk, *J. Polym. Sci.: Part B: Polym. Phys.*, **28**, 127 (1990).
80. J.S. Vrentas and J.L. Duda, *J. Polym. Sci., Polym. Phys. Ed.*, **15**, 403 (1977).
81. J.S. Vrentas and J.L. Duda, *J. Appl. Polym. Sci.*, **22**, 2325 (1978).
82. J.S. Vrentas, H.T. Liu and J.L. Duda, *J. Appl. Polym. Sci.*, **25**, 1297 (1980).

83. J.L. Duda, J.S. Vrentas, S.T. Ju and H.T. Liu, *A.I.Ch.E. Journal*, **28(2)**, 279 (1982).
84. J.S. Vrentas, J.L. Duda and H.-C. Ling, *Macromolecules*, **21**, 1470 (1988).
85. J.S. Vrentas and C.M. Vrentas, *Macromolecules*, **24**, 2404 (1991).
86. J.S. Vrentas and C.M. Vrentas, *J. Appl. Polym. Sci.*, **45**, 1497 (1992).
87. J.S. Vrentas and C.M. Vrentas, *J. Polym. Sci.: Part B: Polym. Phys.*, **30**, 1005 (1992).
88. K. Ganesh, R. Nagarajan and J.L. Duda, *Ind. Eng. Chem. Res.*, **31**, 746 (1992).
89. D.R. Lefebvre, Ph.D. Dissertation, VPI & SU, 1988.
90. D.R. Lefebvre, D.A. Dillard and T.C. Ward, *J. Adhesion*, **27**, 1 (1989).
91. J.J. Imaz, J.L. Rodriguez, A. Rubio and I. Mondragon, *J. Mater. Sci. Lett.*, **10**, 662 (1991). TA 401 J 675 Econ
92. C.-C.M. Ma and S.-W. Yur, *Polym. Eng. Sci.*, **31**, 34 (1991). TP 986 A1 S 573 2
93. S. Laoubi and J.M. Vergnaud, *Eur. Polym. J.*, **27(12)**, 1425 (1991). QD 201 P6E Econ
94. S.J. John, A.J. Kinloch and F.L. Matthews, *Composites*, **22(2)**, 121 (1991). TA 418.9 C 63
95. C. Bastioli, I. Guanella and G. Romano, *Polym. Compos.*, **11(1)**, 1 (1990).
96. A.E. Lozano, J. De Abajo, J.G. De La Campa and J. Preston, *J. Polym. Sci.: Part A: Polym. Chem.*, **30**, 1327 (1992). QD 471 J 642 Econ
97. M. Fukuda, M. Ochi, M. Miyagawa and H. Kawai, *Textile Res. J.*, **61(11)**, 668 (1991). TS 1300 T 43 Econ
98. I. Auerbach and M.L. Carnicom, *J. Appl. Polym. Sci.*, **42**, 2417 (1991). TP 156 P6 J6 Econ
99. S.Z. Li, Y.S. Pak, K. Adamic and S.G. Greenbaum, *J. Electrochem. Soc.*, **139(3)**, 662 (1992). TP 250 E 542 Econ *
100. R.Y.M. Huang and X. Feng, *Sep. Sci. Technol.*, **27(12)**, 1583 (1992).

101. J.-H. Jou, R. Huang, P.-T. Huang and W.-P. Shen, *J. Appl. Polym. Sci.*, **43**, 857 (1991). *
102. W.P. Pawlowski, M.I. Jacobson, M.E. Teixeira and K.G. Sakorafos, *Mat. Res. Soc. Symp. Proc.*, **167**, 147 (1990).
103. J.-H. Jou, Y.-L. Chang and C.-H. Liu, *Macromolecules*, **25(20)**, 5186 (1992). *
104. K. Tanaka, M. Okano, H. Toshino, H. Kita and K.-I. Okamoto, *J. Polym. Sci.: Part B: Polym. Phys.*, **30**, 907 (1992). See ...
105. K. Toi, T. Ito, T. Shirakawa and I. Ikemoto, *J. Polym. Sci.: Part B: Polym. Phys.*, **30**, 549 (1992).
106. J.-H. Jou and P.-T. Huang, *Polymer*, **33(6)**, 1218 (1992).
107. T.C. Gsell, E.M. Pearce and T.K. Kwei, *Polymer*, **32(9)**, 1663 (1991).
108. B.T. Swinyard, P.S. Sahoo, J.A. Barrie and R. Ash, *J. Appl. Polym. Sci.*, **41**, 2479 (1990).
109. A. Golovoy, M.-F. Cheung, M. Zinbo and H.K. Plummer, *Polym.-Plast. Technol. Eng.*, **30(7)**, 635 (1991).
110. L.P. Razumovskii, V.G. Zaikov, T.V. Druzhinina, M.O. Lyshevskaya and L.S. Gal'braikh, *Intern. J. Polymeric Mater.*, **16**, 213 (1992). ; L.P. Razumovskii, V.G. Zaikov, T.V. Druzhinina, M.O. Lyshevskaya and L.S. Gal'braikh, *Eur. Polym. J.*, **28(2)**, 203 (1992). (same paper).
111. L.Y. Shieh and N. A. Peppas, *J. Appl. Polym. Sci.*, **42**, 1579 (1991).
112. P.E.M. Allen, D.J. Fennel and D.R.G. Williams, *Eur. Polym. J.*, **28(4)**, 347(1992).
113. S. Petrik, F Hadobas, L Simek and M. Bohdanecky, *Eur. Polym. J.*, **28(1)**, 15 (1992).
114. S. Petrik, M. Bohdanecky, F Hadobas, and L Simek, *J. Appl. Polym. Sci.*, **42**, 1759 (1991).
115. N.S. Schneider, J.L. Illinger and F.E. Karasz, *Polym. Prepr., Am. Chem. Soc., Div. Polym. Chem.*, **33(2)**, 497 (1992).

116. D.H. Rein, R.F. Baddour and R.E. Cohen, *J. Appl. Polym. Sci.*, **45**, 1223 (1992).
117. C.A. Arnold, J.D. Summers and J.E. McGrath, *Polym. Eng. Sci.*, **29(20)**, 1413 (1989).
118. J.E. McGrath, P.M. Sormani, C.S. Elsbernd and S.Kilic, *Macromol. Chem. Macromol. Symp.*, **6**, 67 (1986).
119. C.S. Elsbernd, M. Spinu, V.J. Krukonis, P.M. Gallagher, D.K. Mohanty and J.E. McGrath, Chap. 8 in *Silicon-Based Polymer Science*, J.M. Zeigler and F.W.G. Fearon, Eds., Advances in Chemistry Series No. 224, American Chemical Society, Washington (1990).
120. C.A. Pawlisch, Ph.D. Dissertation, Univ. of Mass., 1985.
121. R.C. Weast, M.J. Astle and W.H. Beyer, Eds., *CRC Handbook of Chemistry and Physics*, 66th edition, CRC Press, Inc., Boca Raton, Florida (1985). definition: p. F-99; values for X: pp. D190 and E37.
122. C.A. Arnold, Y.P. Chen, D.H. Chen, M.E. Rogers and J.E. McGrath, *Mat. Res. Soc. Symp. Proc.*, **154**, 149 (1989).
123. D.W. Dwight, J.E. McGrath, G. Lawson, N. Patel and G. York, in *Multiphase Macromolecular Systems*, B.M. Culbertson, Ed., Plenum Publishing Corporation (1989).
124. N.M. Patel, D.W. Dwight, J.L. Hedrick, D.C. Webster and J.E. McGrath, *Macromolecules*, **21(9)**, 2689 (1988).
125. R.L. Schmitt, J.A. Gardella, Jr., J.H. Magill, L.S. Salvati, Jr., and R.L. Chin, *Macromolecules*, **18(12)**, 2675 (1985).
126. R.L. Schmitt, J.A. Gardella, Jr. and L.S. Salvati, Jr., *Macromolecules*, **19(3)**, 648 (1986).
127. S.D. Smith, J.M. DeSimone, H. Huang, G. York, D.W. Dwight, G.L. Wilkes and J.E. McGrath, *Macromolecules*, **25(10)**, 2575 (1992).
128. D.W. Van Krevelen and P.J. Hoftyzer, *Properties of Polymers: Their Estimation and Correlation with Chemical Structure*, Elsevier Scientific Publishing Company, New York (1976).

129. M.J. Owen, Chap. 40 in *Silicon-Based Polymer Science*, J.M. Zeigler and F.W. Gordon Fearon, Eds.; Adv. Chem. Ser. No. 224; American Chemical Society, Washington (1990).
130. D.K. Owens and R.C. Wendt, *J. Appl. Polym. Sci.*, **13**, 1741 (1969).
131. A. Noshay and J.E. McGrath, *Block Copolymers: Overview and Critical Survey*, Academic Press, New York (1977).
132. J.D. Summers, C.S. Elsbernd, P.M. Sormani, P.J.A. Brandt, C.A. Arnold, I. Yilgor, J.S. Riffle, S. Kilic and J.E. McGrath, Chap. 14 in *Inorganic and Organometallic Polymers*, M. Zeldin, K.J. Wynne and H.R. Allcock, Eds., American Chemical Society, Washington (1988).
133. J.V. Dawkins, Chap. 8A in *Block Copolymers*, D.C. Allport and W.H. Janes, Eds., Applied Science Publishers LTD, London (1973).
134. R.P. Kambour, in *Block Polymers*, S.L. Aggarwal, Ed., (1970); *J. Polym. Sci., Part B*, **7(8)**, 573 (1969); *Polym. Preprints, Am. Chem. Soc., Div. Polym. Chem.*, **10(2)**, 885 (1969). References from reference 131.
135. T.C. Ward, D.P. Sheehy, J.S. Riffle and J.E. McGrath, *Macromolecules*, **14(6)**, 1791 (1981).
136. D.H. Kaeble, P.J. Dynes and E.H. Cirlin, *J. Adhesion.*, **6**, 23 (1974).
137. J.J. Jasper, *J. Phys. Chem. Ref. Data.*, **1(4)**, 914 (1972).
138. A.L. McClellan and H.F. Harnsberger, *J. Coll. Interface Sci.*, **23**, 577 (1967).
139. S.J. Gregg and K.S.W. Sing, *Adsorption, Surface Area and Porosity*, 2nd ed., Academic Press, New York (1982), pp. 262-282.
140. J. Brandup and E.H. Immergut, Eds., *Polymer Handbook*, 3rd ed., John Wiley & Sons, New York (1989), p. VI-241.

APPENDIX A: Capillary Column Non-uniformity Discussion

Attempts to make thick film copolymer columns were met with failure and extremely non-uniform spongy films, but thin film columns were successfully made although they exhibited peculiar characteristics. For all four co-polymer thin-film columns, the evaporation process involved a strange phenomena that was not observed with the control columns. This involved a visible jumping of the meniscus in small increments toward the capped end--not the continuous withdrawal observed in the control column evaporations. The jumping was not erratic but was instead smooth and regular. The jump distance was largest (≈ 1 mm) at the beginning of the column and became progressively smaller until the jump size reached a nearly uniform length. SEM studies of the thin-film co-polymer columns revealed fairly uniform films that had absolutely no spongy character at all. Each jump appeared to have left a narrow and flat ridge that wound around the inside circumference of the column like one twist in a squished helix. Otherwise, the film was smooth and uniform and showed small, shallow dimples which suggested phase-separated domains.

That the jump effect was not observed during the homopolymer coating processes suggested at first that it was related to the heterogeneous nature of the co-polymers. However, a later inspection of the thin film polyimide column revealed fine lines about the circumference which were fairly evenly spaced throughout the length of the column. Again, no non-uniformities were found in the thicker film polyimide column. It is thought therefore that the lines may be the result during the coating process of a localized temperature change at the

retreating meniscus due to the evaporation of the solvent. The temperature change perhaps perturbs the meniscus position slightly. The less concentrated polymer solutions evaporate faster (coating rate is faster) than the 30 ppt polyimide solution, so it is believed that the water bath is unable to stabilize the local temperature fluctuation rapidly enough to prevent the film perturbation. The possible relationship between solution concentration, local temperature changes and the film non-uniformities was also indicated in the observation that the thin-film polyimide column lines were evenly spaced and the spacing of the copolymer columns' lines gradually decreased until reaching a nearly uniform length near the capped end. The copolymer columns were filled with the polymer solution at summertime lab temperatures of approximately 26°C but had to be equilibrated at temperatures of 17-20°C in order to get them to coat. This unavoidable temperature change caused the solution in the column to reduce its volume with the solution/ air meniscus at the open end retreating 20-30 cm toward the capped end. This may have caused a slight concentration gradient in the solution in the column, which may have resulted in the perturbation jump rate to decrease toward the capped end. Obviously this is not a complete explanation and a full understanding will not be had unless further studies are done. If it is fundamentally related to poor temperature control at the location of the retreating meniscus, then an improved bath system will solve the problem.

APPENDIX B: Thermodynamic and Experimental Diffusion Coefficient Relation

The chemical potential can be defined in the following manner.

$$\mu_i = \left(\frac{\delta G_i}{\delta n_i} \right)_{T,P} = \mu_i^\theta + RT \ln a_i$$

where G_i is the Gibbs free energy, μ_i^θ is a constant (reference) and a_i is the activity of component i in the system. The activity is related to the concentration by the activity coefficient, γ :

$$a_i = \gamma_i C_i$$

The thermodynamic diffusion coefficient, \mathcal{D} , relates the flux to the chemical potential gradient, however the experimental diffusion coefficient, D , derived from Fick's law relates the flux to the concentration gradient. Since the flux J will be the same, the relation between the thermodynamic and the experimental diffusion coefficients can be found as follows:

$$J = -\mathcal{D} \left(\frac{\delta \mu}{\delta x} \right) = -D \left(\frac{\delta c}{\delta x} \right)$$

$$D = \mathcal{D} \left(\frac{\delta \mu}{\delta c} \right)$$

Given the definition of the chemical potential above, the change in chemical potential with respect to the change in concentration can be written:

$$\frac{\delta\mu}{\delta c} = \frac{\delta(RT \ln a)}{\delta c} = \frac{RT \delta(\ln a)}{\delta c}$$

With the implementation of a devious math trick based on the definition of the differentiation of a natural logarithm, one is able by substitution to obtain the following relation between the two diffusion coefficients.

$$\delta(\ln c) = \frac{1}{c} \delta c$$

$$\frac{\delta\mu}{\delta c} = \frac{RT}{c} \frac{\delta(\ln a)}{\delta(\ln c)}$$

$$\mathcal{D} = \frac{D_c}{RT} \frac{\delta(\ln c)}{\delta(\ln a)}$$

If the system is thermodynamically ideal, then $\delta(\ln c)/\delta(\ln a) = 1$. The activity might be viewed as a "concentration term" corrected for deviation from ideality. Activities or activity coefficients that are negative can cause diffusion to occur against an increasing concentration gradient. Thermodynamic diffusion coefficients are often used in the study of the temperature and concentration dependence of the diffusion coefficient.

APPENDIX C: Error Propagation

As in all cases of error propagation, the resulting propagated error is often an underestimate due to underestimation of contributing errors and also to exclusion of unknown errors. All errors calculated here are errors in precision.

Where possible, standard error propagation methods were used. For addition, subtraction, multiplication and division and all such combinations thereof, the following basic equations were used.

$$(a \pm \delta a) + (b \pm \delta b) = a + b \pm \sqrt{(\delta a)^2 + (\delta b)^2}$$

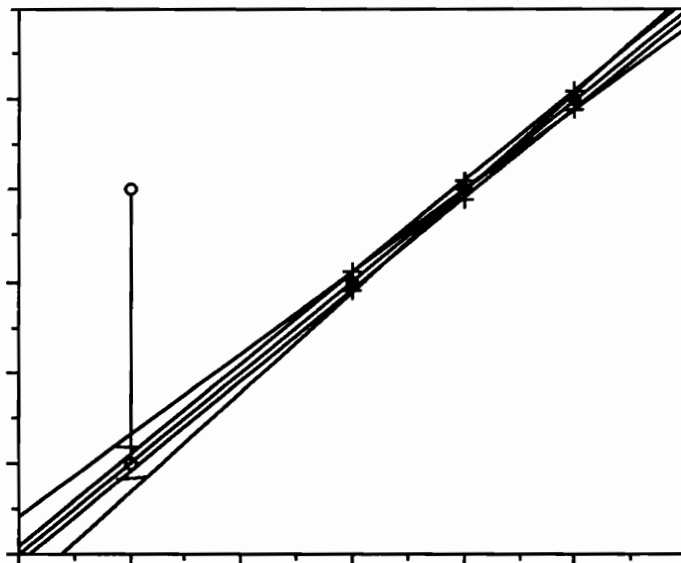
$$(a \pm \delta a)^n (b \pm \delta b)^m = ab \pm ab \sqrt{\frac{n^2(\delta a)^2}{a^2} + \frac{m^2(\delta b)^2}{b^2}}$$

These were obtained from Dr. P.E. Field's Physical Chemistry Laboratory Class Notebook used at VPI&SU in Physical Chemistry labs during at least 1986-88. The propagation of error in the diffusion coefficients was determined solely from the error in film thickness using these equations.

Propagation of error in the determination of the free energies of specific interaction of water vapor and the dispersive components of the solid surface energies for the IGC experiments was more involved. Extrapolation of corrected retention times to infinite dilution involved linear regression. The error in the intercept (as well as the slope) of a regression line can be determined from standard equations, which can be found in any good statistics book, for example,

Probability and Statistics for Engineers and Scientists, 3rd ed., by Ronald E. Walpole and Raymond H. Myers, MacMillan Publishing Corp. 1985. The error in the infinite dilution intercept value of the corrected retention time was propagated with the other knowable errors using the two above equations. Knowable errors included errors in flowmeter gradations, measured average flowrate and error in precision of barometric (outlet) pressure. Errors were taken as 1/2 the smallest measurable increment unless they were known to be larger. The error in the y-coordinate of each probe data point plotted in the surface energetics plots was successfully propagated in this manner.

The error in the ΔG_{sp}° is a simple error associated with subtraction of the y-coordinates of the water data point and the corresponding point of the dispersive reference line. To determine the error in the reference line point, the errors associated with the n-alkane data points need to be propagated through the linear regression. Normal regression analysis does not take into account errors in the regressed points. No standard statistical method to do this was found to be readily available in accessible statistics books. Therefore a method was devised and a computer program written to do the task. The method is described below and the program printout follows. The method assumes the errors in the x-coordinates are negligible; in fact one cannot correctly propagate " δx " errors with this method because it is based on normal regression which requires x to be the independent variable. For this research known errors in the abscissa were small.



Given "n" normal alkane points with their respective errors " $\pm \delta y$ ", take three possibilities for the y-value of a each normal alkane point to be:

- 1) $y + \delta y$
- 2) y
- 3) $y - \delta y$

There are 3^n possible combinations of the n points. Do a linear regression on each possible combination to obtain 3^n linear equations. (The above illustration only shows 4 combinations plus the original line.) Obtain the corresponding reference y-coordinate and the slope of each regression line. The average of the 3^n values will be within 3/1000 % of the value obtained for the linear regression of the original set of points. The best estimate of the standard deviation (BESD) of the 3^n values will be the propagated error. Further error propagation simply involves the initial two rules stated above.

```
CLS
REM CALCULATION OF ERROR IN WATER DISPERSIVE-REFERENCE-LINE-
REM POINT AND IN SLOPE OF THE DISPERSIVE REFERENCE LINE
```

```
REM Program written by Joyce M. Kaltenecker-Commerçon and Pascal
REM Commerçon in February-March 1992. Final documentation 5.25.92.
REM Dr. T.C. Ward's Labs, at VPI&SU, Blacksburg, VA 24061.
REM Written in Microsoft Basic 2.00 for MacIntosh
```

```
REM Program calculates the Error in the water dispersive reference
REM Y point and in the dispersive reference line slope.
```

```
PRINT "Enter the number of points in the dispersive reference line."
PRINT "No less than two points may be entered; more than 6 points entered"
PRINT "will cause the program to run extremely slowly, if at all."
INPUT N
T=3^N
DIM A(N,T),X(N),Y(N),D(N)
```

```
REM Generation of the sign array--This part of the code was written
REM by Pascal Commerçon. It creates an N by 3^N array full of the
REM possible combinations of +1, -1, 0. It will be used later to create
REM the sets of possible combinations of y+dy, y-dy, y. These sets are
REM referred to as skewed y sets. The total number of combinations is
REM given by the variable T.
```

```
FOR I=1 TO N
P=3^(I-1)-1
FOR K=0 TO P
L=K*3^(N-I+1)
M=3^(N-I)
FOR J=L+1 TO L+M
A(I,J)=1
NEXT J
FOR J=L+1+M TO L+2*M
A(I,J)=0
NEXT J
FOR J=L+2*M+1 TO L+3*M
A(I,J)=-1
NEXT J
NEXT K
NEXT I
```

```
REM Print sign array on the screen in order to check if it is working
REM properly.
```

```
FOR I=1 TO N
  FOR J=1 TO T
    PRINT A(I,J);
  NEXT J
  PRINT
NEXT I
```

```
REM Enter the data x and y and y-deviation (dy) values, where x is
REM a*sqrtgamma (or the molecular probe surface area multiplied by
REM the square root of the dispersive component of the probe liquid surface
REM tension) and y is  $RT\ln V_n$  (or  $[8.314 \cdot 10^{-3} \text{ kJ/molK}^{-1}] \cdot \text{temperature in Kelvin} \cdot \text{natural logarithm of the net retention volume}$ ) and y-deviation
REM or dy is the error in  $RT\ln V_n$ . These values are calculated separately
REM from this program. This author's values are listed in lab notebook #3.
```

```
FOR Z=1 TO N
INPUT "Enter x,y,dy";X(Z),Y(Z),D(Z)
NEXT Z
```

```
REM *****
REM This section of code does the following things: 1) Calculates the
REM "J"-th set of skewed y's; 2) Performs a linear regression on the
REM J-th set of skewed y's to determine the best fit slope and intercept
REM for the set; 3) Places the calculated slope and intercept into two arrays;
REM 4) Calculates the y-value corresponding to the reference point for water
REM on the dispersive reference line from the slope and intercept, and puts
REM the value in an array; 5) Moves on to the "J+1"-th set of skewed y's and
REM repeats the cycle. Values are placed in arrays for later determination
REM of the averages and best estimates of the standard deviations for
REM the total set of combinations.
```

```
DIM YWR(T),NY(4),SLOPE(T),INTRCP(T)
```

```
FOR J =1 TO T
```

```
REM Calculation of J-th set of skewed y's which is put into array NY
  FOR I=1 TO N
    NY(I)=Y(I)+A(I,J)*D(I)
  NEXT I
```

```

REM Linear regression to find slope and intercept for skewed set's "line"
  REM Summation of x*y's
    SUMXY=0
    FOR I=1 TO N
      SUMXY=SUMXY+X(I)*NY(I)
    NEXT I
  REM Summation of x's
    SUMX=0
    FOR I=1 TO N
      SUMX=SUMX+X(I)
    NEXT I
  REM Summation of skewed y's
    SUMY=0
    FOR I=1 TO N
      SUMY=SUMY+NY(I)
    NEXT I
  REM Summation of (x^2)'s
    SUMXSQ=0
    FOR I=1 TO N
      SUMXSQ=SUMXSQ+X(I)^2
    NEXT I
  REM Calculation of the denominator of the regression equations
    DNM=N*SUMXSQ-SUMX^2

  REM Calculation of slope and intercept and placement of the values
  REM in arrays so that the averages and standard deviations may be
  REM later calculated
    SLOPE(J)=(N*SUMXY-SUMX*SUMY)/DNM
    INTRCP(J)=(SUMXSQ*SUMY-SUMX*SUMXY)/DNM

  REM Calculation of water reference point y for the set using
  REM x= 64.94644 and placement in array YWR for later determination
  REM of the average and standard deviation of values from all possible
  REM combinations.
    YWR(J)=SLOPE(J)*64.94644+INTRCP(J)

  PRINT SLOPE(J),INTRCP(J),YWR(J)

NEXT J
REM *****

```

```
REM Calculation of the average water reference point (ywr) and the
REM average slope and intercept of the dispersive reference line using
REM the values previously placed in the arrays.
```

```
SUM=0
```

```
SUM1=0
```

```
SUM2=0
```

```
FOR J=1 TO T
```

```
    SUM=SUM+YWR(J)
```

```
    SUM1=SUM1+SLOPE(J)
```

```
    SUM2=SUM2+INTRCP(J)
```

```
NEXT J
```

```
AVE=SUM/T
```

```
AVE1=SUM1/T
```

```
AVE2=SUM2/T
```

```
REM Calculation of the BESD (best estimate of the standard deviation)
REM for ywr & slope. Formula for the BESD is the same as the standard
REM deviation equation given on p. 189 in Walpole and Myers
REM "Probability for Engineers and Scientists"
```

```
SUM=0
```

```
SUM1=0
```

```
FOR J=1 TO T
```

```
    SUM=SUM+(AVE-YWR(J))^2
```

```
    SUM1=SUM1+(AVE1-SLOPE(J))^2
```

```
NEXT J
```

```
BESD=SQR(SUM/(T-1))
```

```
SLBESD=SQR(SUM1/(T-1))
```

```
REM Print results to computer screen [LPRINT prints to a printer]
```

```
PRINT "average reference line ordinate (ywr) corresponding to water ";AVE
```

```
PRINT "ywr BESD or standard deviation";BESD
```

```
PRINT "average Slope in dispersive reference line";AVE1
```

```
PRINT "Slope BESD or standard deviation";SLBESD
```

```
PRINT "average Intercept";AVE2
```

```
REM Calculation of the YWR error for 95% confidence interval via p. 222
```

```
REM in Walpole & Myers using the t-table in the back of the book for
```

```
REM t-values
```

```
IF N<>2 THEN THREE
```

```
    REM for N=2 points or T=9
```

```
    ERR95=2.306*BESD/SQR(T)
```

```
    ERR99=3.355*BESD/SQR(T)
```

THREE:

IF N<>3 GOTO FOUROMO

REM for N=3 points or T=27

ERR95=2.056*BESD/SQR(T)

ERR99=2.779*BESD/SQR(T)

FOUROMO:

IF N<4 GOTO FINPRT

REM FOR N>3 points (4 OR more) OR t=infinite value in t-table

ERR95=1.96*BESD/SQR(T)

ERR99=2.576*BESD/SQR(T)

FINPRT:

REM Final Printing of Confidence Interval values

PRINT "YWR Error for 95% C.I.";ERR95

PRINT "YWR Error for 99% C.I.";ERR99

END

VITAE

Joyce Marie Kaltenecker-Commerçon was born to John M. and Mary L. Kaltenecker in Parkersburg, West Virginia on September 25, 1965. After graduating as co-valedictorian from Parkersburg Catholic High School in 1983, she enrolled at Virginia Polytechnic Institute and State University, Blacksburg, Virginia, where she graduated summa cum laude with a Bachelor of Science in Chemistry in 1988. While an undergraduate, she participated in the VPI & SU cooperative education program by working at Baker Instruments Corporation in Winchester, Virginia. She was a recipient of some academic and financial aid scholarships and was invited to join Phi Beta Kappa during her junior year. She remained at VPI & SU as a graduate student in order to study polymer (and surface) physical chemistry. She was associated with the Center for Adhesive and Sealant Science and the NSF STC for High Performance Polymeric Adhesives and Composites and was the recipient of four Adhesive and Sealant Council Fellowships. She presented several posters and also two papers at national meetings of The Adhesion Society and The American Chemical Society. It was during her graduate years that she met Pascal Commerçon, whom she married in a civil ceremony in Chevagny-les-Chevrières, France, on August 24, and in a religious ceremony in Parkersburg, West Virginia, on August 31, 1991.

